THESIS REPORT

Surface temperature reduction in urban areas- Case of Kochi, India

Abstract

GIS based analysis

Gopikrishna VS

S302170

Politecnico di Torino

Master's Degree in

TERRITORIAL, URBAN, ENVIRONMENTAL, AND LANDSCAPE PLANNING

Curriculum: Planning for the Global Urban Agenda

Academic Year: 2023/2024

Surface temperature reduction in urban areas: Case of Kochi, India

Supervisors:

Tutor: Prof. Tiepolo Maurizio

Co- Tutor: Prof. Guilio Tonolo Fabio

Candidate:

Gopikrishna Venugopal Sreelatha (s302170)

Acknowledgment

I am immensely grateful to God Almighty for granting me the strength, health, and opportunity to complete this thesis.

I would like to express my deepest appreciation to my distinguished supervisor, Professor Tiepolo Maurizio. His generous acceptance of my thesis topic, coupled with his steadfast support, guidance, and invaluable suggestions, have been instrumental in every stage of this work. His encouragement and insightful advice have inspired and motivated me throughout this journey. It has been a privilege to work under his mentorship, which has been crucial for the successful completion of this thesis.

My heartfelt thanks also go to my co-supervisor, Professor Guilio Tonolo Fabio, for his unwavering support and insightful feedback. His dedication to providing access to resources and his valuable technical guidance in remote sensing have played a significant role in shaping this research.

I am deeply grateful to my mentor from my undergraduate studies, Professor Chithra Pradeep Kumar, for her continuous guidance and encouragement throughout this academic journey.

I extend my gratitude to Mr. Sreekanth Oorathan, Town Planning Officer at the Greater Cochin Development Authority, for his valuable counsel, and to the officials of the Kochi Municipal Corporation, Government of Kerala, for their assistance in accessing essential data for this research.

Special thanks are due to Architects Ar. Swathi Sethuram, Ar. Arun Antony Aloscious, Ar. Ann Riya Rajesh, Ar. Aswin Raju, Ar. Akhil Tom Aloscious, Ar. Caris Susan Dayson, Ar. Vaishnavi Sreenivasan, Eng. Lekshmy Thampy Usha, and Ar. Ninitha Saji for their generosity in sharing their expertise.

I am profoundly thankful to everyone who, directly or indirectly, contributed to the completion of this thesis. I am also deeply appreciative of my friends, who have become like family in this foreign land, enriching my life with their support and making it a second home filled with cherished experiences and cultural insights.

A special note of thanks goes to my close friends from various fields, Bony D'Claus, Padmanabhan, Anuroop Das, Manu Biju, and Govind Paniker, for their emotional support and encouragement throughout this process.

Lastly, I owe a deep debt of gratitude to my family for their unwavering support and encouragement. My father, Dr. K. Venugopal, my mother, Dr. P. R. Sreelatha, and my sister, Dr. Gopika Venugopal, who have been my constant source of strength and guidance.

Abstract - English

The literature studies in tropical monsoon cities have analyzed the city as a whole, often resulting in generic recommendations without considering geographical subunits like municipal wards. This lack of localization limits the effectiveness of proposed solutions. Additionally, satellite images used in these studies were retrieved randomly from a season, potentially missing peak Land Surface Temperature (LST) conditions necessary for accurate analysis. Kerala, particularly during March to May, faces intense heatwaves due to natural factors such as the northward movement of the sun and surrounding oceanic humidity, leading to high temperatures and prolonged heatwaves. Cochin, a rapidly urbanizing city in Kerala, faces similar challenges with elevated surface temperatures impacting public health.

This thesis aims to comprehensively investigate LST in a tropical monsoon city, Kochi, using Geographic Information Systems (GIS), remote sensing data, and statistical methods. The objectives include analyzing spatial variations in LST across urban wards and identifying LST hotspots during the warmest days of the year, as well as determining LST drivers in the city.

The literature study focuses on geographical conditions of Kochi, where the tropical monsoon climate causes significant seasonal temperature variations. Literature reviews on research articles on different cities in tropical monsoon climatic zone emphasize the importance of retrieving both daytime and nighttime images for comprehensive temperature analysis. Some literature study articles consider demographic factors, high-density roads, and green spaces, proposing specific solutions for urban heat mitigation. The literature study infers to retrieve Landsat data from peak temperature days and validates remote sensing data with ground truth measurements.

The thesis is organized into sections including introduction, literature review, methodology, analysis, findings, and conclusions. It uses statistical method to pinpoint the warmest day of the year in Kochi, and uses remote sensing for analyzing LST, NDBI, NDVI, and other parameters to identify LST drivers. The ward-wise analysis ensures precise, localized recommendations for planners and decision makers.

Findings reveal that green cover negatively impacts LST, while built-up areas, roads, and industrial activities increase it. Ward-specific recommendations offer more compatible solutions for urban planning.

Conclusions indicate that ward-wise LST analysis provides valuable insights for strategic planning, emphasizing the importance of increasing green spaces, modifying road materials, and introducing green roofs, to reduce LST and enhance thermal comfort in Kochi. These findings contribute to urban planning and public health strategies, particularly in the context of rising temperatures and climate change.

Abstract - Italian

Gli studi sulla letteratura nelle città con clima monsonico tropicale hanno analizzato la città nel suo insieme, spesso risultando in raccomandazioni generiche senza considerare le subunità geografiche come i quartieri municipali. Questa mancanza di localizzazione limita l'efficacia delle soluzioni proposte. Inoltre, le immagini satellitari utilizzate in questi studi sono state recuperate casualmente da una stagione, potenzialmente mancando le condizioni di picco della Temperatura della Superficie Terrestre (LST) necessarie per un'analisi accurata. Il Kerala, in particolare da marzo a maggio, affronta intense ondate di calore dovute a fattori naturali come il movimento verso nord del sole e l'umidità oceanica circostante, portando a temperature elevate e prolungate ondate di calore. Cochin, una città in rapida urbanizzazione in Kerala, affronta sfide simili con temperature superficiali elevate che influenzano la salute pubblica.

Questa tesi mira a investigare in modo completo la LST in una città con clima monsonico tropicale, Kochi, utilizzando Sistemi di Informazione Geografica (GIS), dati di telerilevamento e metodi statistici. Gli obiettivi includono l'analisi delle variazioni spaziali della LST nei quartieri urbani e l'identificazione dei punti caldi della LST durante i giorni più caldi dell'anno, nonché la determinazione dei fattori che influenzano la LST nella città.

Lo studio della letteratura si concentra sulle condizioni geografiche di Kochi, dove il clima monsonico tropicale causa significative variazioni stagionali della temperatura. Le revisioni della letteratura su articoli di ricerca su diverse città nella zona climatica monsonica tropicale enfatizzano l'importanza di recuperare immagini sia diurne che notturne per un'analisi completa della temperatura. Alcuni articoli di studio della letteratura considerano fattori demografici, strade ad alta densità e spazi verdi, proponendo soluzioni specifiche per la mitigazione del calore urbano. Lo studio della letteratura suggerisce di recuperare dati Landsat dai giorni di temperatura di picco e di validare i dati di telerilevamento con misurazioni di verità a terra.

La tesi è organizzata in sezioni che includono introduzione, revisione della letteratura, metodologia, analisi, risultati e conclusioni. Utilizza un metodo statistico per identificare il giorno più caldo dell'anno a Kochi e utilizza il telerilevamento per analizzare LST, NDBI,

NDVI e altri parametri per identificare i fattori che influenzano la LST. L'analisi per quartiere assicura raccomandazioni precise e localizzate per i pianificatori e i decisori.

I risultati rivelano che la copertura verde influisce negativamente sulla LST, mentre le aree edificate, le strade e le attività industriali la aumentano. Le raccomandazioni specifiche per quartiere offrono soluzioni più compatibili per la pianificazione urbana.

Le conclusioni indicano che l'analisi della LST per quartiere fornisce preziose intuizioni per la pianificazione strategica, enfatizzando l'importanza di aumentare gli spazi verdi, modificare i materiali stradali e introdurre tetti verdi per ridurre la LST e migliorare il comfort termico a Kochi. Questi risultati contribuiscono alla pianificazione urbana e alle strategie di salute pubblica, in particolare nel contesto dell'aumento delle temperature e dei cambiamenti climatici.

Abbreviations

LST	Land Surface Temperature
GIS	Geographic Information Systems
NDBI	Normalized Difference Built-up Index
NDVI	Normalized Difference Vegetation Index
UHI	Urban Heat Island
LST R	Land Surface Temperature Reduction
CDP	City Development Plan
KMC	Kochi Municipal Corporation
IMD	India Meteorological Department
LC	Land Cover
LULC	Land Use Land Cover
Am zone	Tropical Monsoon Climate
Landsat -TM	Landsat Thematic Mapper
NIR	Near-Infrared
BSI	Built-up Area Index
MNDWI	Modified Normalized Difference Water Index
SWIR	Shortwave Infrared
NBS	Nature-Based Solutions
ANN	Artificial Neural Network
DSP	Data Supply Portal
R – Value	Pearsons's coefficient
TOA	Top of Atmosphere
GCDA	Greater Cochin Development Authority

Table of Contents

List of Figures

List of Tables

List of Annexure

1.Introduction

Urban areas worldwide are experiencing escalating surface temperatures, leading to the emergence of urban heat islands (UHIs) and exacerbating heat-related health risks, energy consumption, and environmental degradation. (IPCC, 2014) (Menon et al., 2010)

Being located near the Equator, the tropical monsoon climate experiences warm temperatures throughout the year. This would provide higher health risks not just for humans but also for the flora and fauna in those zones. (Beck et al., 2020)

Research on temperature in tropical monsoon climates is crucial for understanding the dynamics of heat distribution, particularly in regions prone to high humidity and intense rainfall. Land surface temperature (LST) is the preferred parameter for studying this issue because it is measured over the entire area of interest and not just at a few points, as air temperature is captured by meteorological stations or along transects by temperature sensors and data loggers installed on vehicles. (Tiepolo et al., 2023)

LST is detected from satellite sensors capturing emissivity, surface albedo, and atmospheric conditions being crucial for accurate estimation. (Weng et al., 2011)

The estimation of LST patterns and drivers should guide adaptation to urban heat.

The literature on LST in tropical monsoon cities has three recurrent objectives:

- To analyze the spatial LST pattern and intensity.
- To analyze the landcover change for a period ranging from 10-30 years.
- To analyze the relationship between LST and LC composition and configuration.

Most of the literature studies refer to LST as the ones recorded by Landsat TM. The key metrics used to identify determinants of Land Surface Temperature (LST) in most studies include landcover classified as 'Built-up area,' 'Open Space' or 'Barren land,' 'Vegetation,' and 'Waterbodies.' And these metrics were observed to be the key LST drivers.

Land Surface Temperature (LST) Reduction involves strategies like increasing green spaces, using cool roofs and pavements, and enhancing urban tree cover to mitigate the urban island effect through shading and evapotranspiration[1]. (US EPA, 2013)

Among the recurring problems in the literature on LST in tropical monsoon cities is the analysis of the city as a whole, without considering any geographical subunits. Hence the proposals to face urban heat are too generic and not localized. Another frequent problem is the day of retrieval of the satellite images is not taken in the warmest season and hence analysis may not provide the peak LST conditions required for the accurate proposals to face warm spells.

Hypotheses are that: (i) the data/images retrieved from the satellite on the warmest day of the year and (ii) analyzing LST by administrative units such as wards[2], rather than the entire city, will enhance the study's utility for decision-makers in adapting to warm spells.

The objectives of this thesis are:

- To analyze spatial variations in land surface temperatures (LST) across different urban wards and identify LST hotspots within a Tropical monsoon city on the warmest days of the year.
- To figure out the LST drivers.

[1] Evapotranspiration is the sum of all processes by which water moves from the land surface to the atmosphere via evaporation and transpiration. (School, 2018)

[2] The division of municipal wards in Kerala is based on several factors (including population, contagious area, natural boundaries, accessibility, connectivity, political boundaries, existing land use and urban characteristics) to ensure effective local governance and representation (State Election Commission, Delimitation, n.d.) (State Election Commission, https://www.sec.kerala.gov.in). Municipal wards in India are administrative units that serve important functions, majorly related to local governance, administration, and service delivery for the population in the urban local body.

To achieve the above-mentioned objectives, the city of Cochin (the Kochi Municipal Corporation) is selected for the thesis study as the site. Cochin, also known as Kochi, is a major port city on the southwest coast of India, in the state of Kerala, in the Ernakulam district known for its rich history and cultural diversity (Britannica, 2024) (Kochi Municipal Corporation, 2024).

This selection is mainly because of the following aspects:

- Kochi stands out as the most urbanized city in Kerala, characterized by rapid urban development, industrial growth, and a dense population (Corporation, City Development Plan (CDP), 2023).

- The availability of air temperature data of the past decades recorded by the Kochi Radar (IMD - India Meteorological Department) in the Cochin International Airport can enhance the feasibility of the study (Ministry of Earth Sciences, n.d.).

- The city's diverse land cover (LC) types, including dense urban areas, green spaces, and water bodies, offer a comprehensive environment for examining the correlations between different spectral indices like NDVI and NDBI with LST (Corporation, City Development Plan (CDP), 2023).

- The municipal ward-wise division can be used as a minimal geographical unit for the LST analysis and recommendations can be ward-specific.

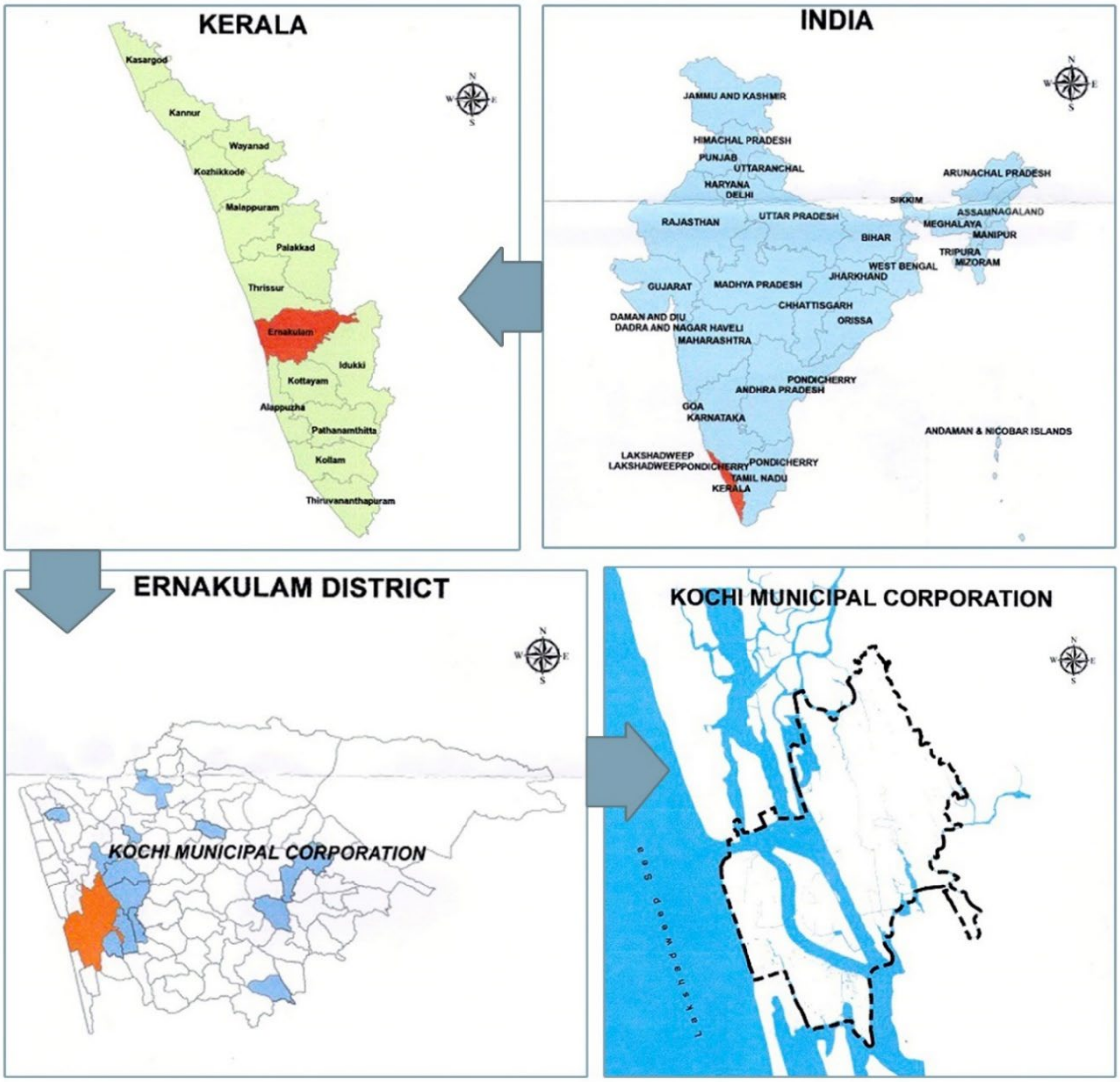

Figure 1: Administrative map of Kochi Municipal Corporation, Ernakulam district, Kerala, India (Source: GCDA)

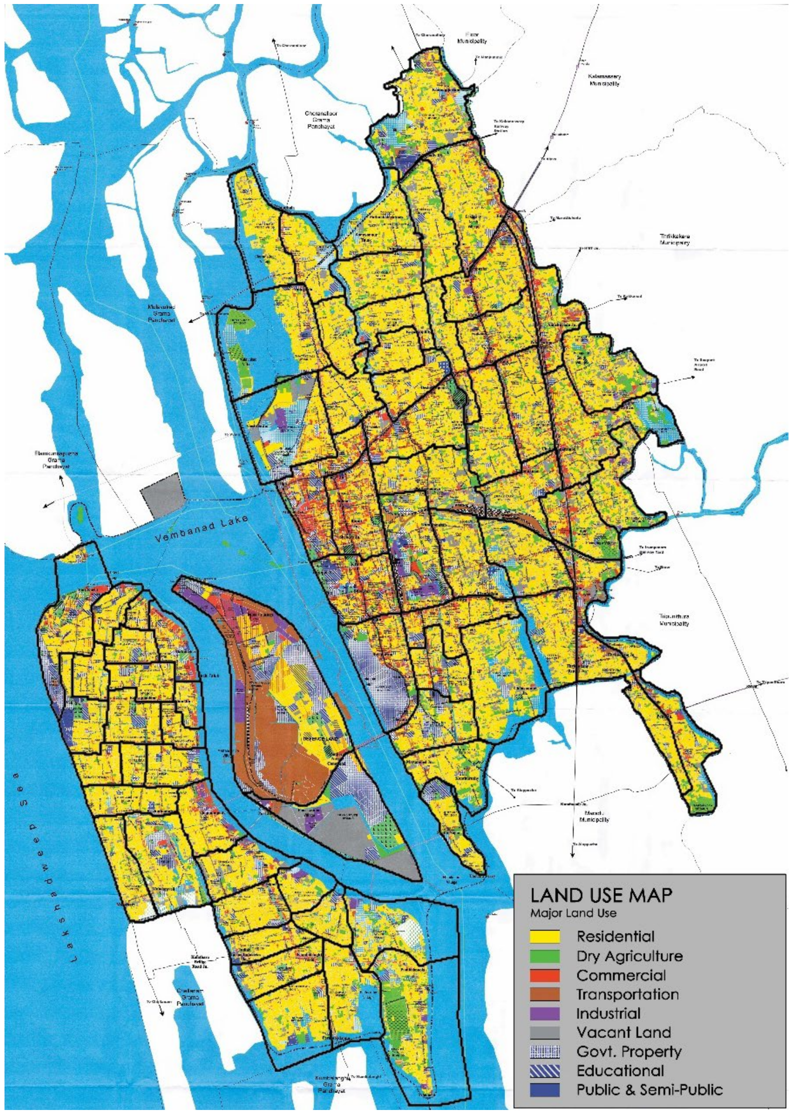

Figure 2: Existing Land use map of Cochin Municipality as of 2022 (Source: GCDA. Modified by Author)

Finding the warmest wards, determinants of LST, and possible heat reduction policies could impact the thermal comfort and health of the residential population in Kochi[3] and

[3] Cochin, a rapidly growing city in Kerala, India, faces similar challenges, with urbanization, land use changes, and climate variability contributing to elevated surface temperatures. This is severely impacting the health of the residential population in the town (Government of Kerala. & StatePlanningBoard., 2017) (Corporation, Kochi Municipal Corporation Annual Report 2018-2019, 2022).

"The increasing temperature can cause heat stroke, sunburn, and heat rashes. In such cases, it is recommended to consult a doctor. Also, using an umbrella while going out can help avoid direct exposure to heat." - Dr K Sakeena, district medical officer in Ernakulam (Editor, 2024)

the comfortability of the tourists which further impacts the tourism sector mainly concentrated near the Fort Kochi (Government of Kerala. & StatePlanningBoard., 2017) (Corporation, Kochi Municipal Corporation Annual Report 2018-2019, 2022).

Therefore, this thesis investigates surface temperature reduction analysis in urban areas of Cochin using Geographic Information Systems (GIS), remote sensing data, and statistical analysis. The analysis will ascertain:

- *How do LSTs vary across different urban wards in Cochin Municipality, and what factors contribute to these temperature variations?*
- *What is the relationship between land use/land cover patterns and surface temperature distribution in Cochin, and how can this relationship inform urban planning and climate adaptation strategies?*
- *To what extent do green spaces and vegetation cover influence surface temperature reduction in urban areas of Cochin?*
- *What measures can be implemented to enhance the effectiveness of current land use planning policies and regulations in mitigating temperature rise in Cochin?*

The findings of this research will provide valuable insights for urban planners, policymakers, and stakeholders to develop evidence-based strategies for enhancing urban livability, environmental quality, and climate resilience in Cochin Municipality on a ward scale.

2. Literature Review

The Koppen climate classification system categorizes the world's climates based on average temperature and precipitation patterns.

The tropical monsoon climate (Am zone), prevalent in regions near the equator, features pronounced seasonal variations in precipitation driven by monsoon winds. These regions experience heavy rainfall and high humidity during the wet season (May to September) and significantly reduced rainfall during the dry season (October to April). This cyclical pattern impacts local environments, agriculture, and urban planning, requiring adaptive strategies for water management and flood mitigation. Understanding the tropical monsoon climate is crucial for developing resilient infrastructure and effective urban planning, especially in rapidly urbanizing areas like Kochi (Peel et al., 2007).

Figure 3: Tropical Monsoon & Tropical Savannah Climatic Zone (Source: (Geodiode, 2011))

It has become essential to figure out the LST hotspots in urban areas and propose solutions to cope with the current global heat rise. Using LST in the analysis of heat rise offers precise, spatially resolved temperature data, allowing for the identification of hotspots and the assessment of heat distribution across different urban areas. (Nandi & Dede, 2022)

Literature reviews based on pertinent publications are crucial to get a thorough grasp of the research focused on the study of Land Surface Temperature (LST) and land use changes in cities within the Tropical Monsoon climatic zone. Examining previous academic publications in this area can offer insightful information about many study facets, such as approaches, conclusions, and ramifications.

The urban heat island effect, which describes the phenomena where cities experience greater temperatures than surrounding rural areas, is one of the major themes that may emerge from the literature. Studies may also look at how changes in land use, such as deforestation, urbanization, and the growth of built-up regions, affect local microclimates and LST patterns. (Arnfield, 2003)

By reviewing relevant studies, researchers can better understand how land surface features, urban growth, and climate interact in cities with Am climates. This knowledge helps improve the analysis of land surface temperature and land cover in urban areas by refining research methods, data handling, and interpretation of results.

Several articles were chosen based on the geographical location of cities that fall in tropical monsoon (Am climatic zone) climatic zone characterized by high temperatures, humidity, and distinct wet and dry seasons, focusing on aspects such as urban weather assessment, land surface temperature (LST) analysis, and land use/land cover (LULC) changes. Although some articles have a smaller number of citations, the study objectives and results were novel.

Table 1: Details of the case study articles used for Literature study (Source: Author)

Sl.No.	Name of the city	Country	Author Name	Year	Journal Name	APA #Google Scholar citations
1.	Thiruvananthapuram, Kerala	India	R S Anupriya & T A Rubeena	2023	**Geology, Ecology, and Landscapes, 2023**: Spatio-temporal urban land surface temperature variations and heat	Anupriya, R. S., & Rubeena, T. A. (2023). Spatio-temporal urban land surface temperature variations and heat stress vulnerability index in Thiruvananthapuram city of Kerala, India.

					stress vulnerability index in Thiruvananthapuram city of Kerala, India	Geology, Ecology, and Landscapes, 1-17. Cited by 1
2.	Kurunegala	Sri Lanka	Manjula Ranagalage, Sujith S. Ratnayake, DMSLB Dissanayake, Lalit Kumar, Hasula Wickremasinghe, Jagathdeva Vidanagama, Hanna Cho, Susantha Udagedara, Keshav Kumar Jha, Matamyo Simwanda, Darius Phiri, ENC Perera & Priyantha Muthunayake	2020	**International Journal of Geo-Information**: Spatiotemporal Variation of Urban Heat Islands for Implementing Nature-Based Solutions: A Case Study of Kurunegala, Sri Lanka	Ranagalage, M., Ratnayake, S. S., Dissanayake, D. M. S. L. B., Kumar, L., Wickremasinghe, H., Vidanagama, J., ... & Muthunayake, P. (2020). Spatiotemporal variation of urban heat islands for implementing nature-based solutions: A case study of Kurunegala, Sri Lanka. ISPRS International Journal of Geo-Information, 9(7), 461. Cited by 30
3.	Chittagong	Bangladesh	Shahriar Abdullah, Dhrubo Barua, Sk. Md. Abubakar Abdullah, Yasin Wahid Rabby	2022	**Earth Systems and Environment (2022) 6:221–235**: Investigating the Impact of Land Use/Land Cover Change on Present and Future Land Surface Temperature (LST) of Chittagong, Bangladesh	Abdullah, S., Barua, D., Abdullah, S. M. A., & Rabby, Y. W. (2022). Investigating the impact of land use/land cover change on present and future land surface temperature (LST) of Chittagong, Bangladesh. Earth Systems and Environment, 6(1), 221-235. Cited by 25
4.	Hat Yai	Thailand	Poonyanuch Ruthirako, Rotcganatch Darnsawasdi, Wichien Chathupote	2014	**WALAILAK JOURNAL**: Intensity and Pattern of Land Surface Temperature in Hat Yai City, Thailand	Ruthirako, P., Darnsawasdi, R., & Chatupote, W. (2015). Intensity and pattern of land surface temperature in Hat Yai City, Thailand. Walailak Journal of Science and Technology

						(WJST), 12(1), 83-94. Cited by 10
5.	Manila	Philippines	King Joshua Almadrones-Reyes, Nikki Heherson A. Dagamac	2022	**GeoJournal (2023) 88:1415–1426**: Land-use/land cover change and land surface temperature in Metropolitan Manila, Philippines using landsat imagery	Almadrones-Reyes, K. J., & Dagamac, N. H. A. (2023). Land-use/land cover change and land surface temperature in Metropolitan Manila, Philippines using landsat imagery. GeoJournal, 88(2), 1415-1426. Cited by 4
6.	Mumbai	India	Mehebub Sahana, Shyamal Dutta & Haroon Sajjad	2018	**International Journal of Urban Sciences**: Assessing land transformation and its relation with land surface temperature in Mumbai city, India using geospatial techniques	Sahana, M., Dutta, S., & Sajjad, H. (2019). Assessing land transformation and its relation with land surface temperature in Mumbai city, India using geospatial techniques. International Journal of Urban Sciences, 23(2), 205-225. Cited by 68
7.	Pune	India	Kashyap Jyoti Gohain, Pir Mohammad, Ajanta Goswami	2019	**Quaternary International 575-576 (2021) 259–269:** Assessing the impact of land use land cover changes on land surface temperature over Pune city, India	Aithal, B. H., & MC, C. (2019). Assessing land surface temperature and land use change through spatio-temporal analysis: a case study of select major cities of India. Arabian Journal of Geosciences, 12, 1-16. Cited by 116
8.	Kolhapur	India	Patil Prashant Tanaji, Chougule Vidya Ajit, Dhumal Satyavan Vishnu	2021	**Disaster Advances Vol. 14 (4) April (2021):** Urban weather assessment using LST, NDBI and NDVI of Kolhapur city, Maharashtra	Tanaji, P. P., Ajit, C. V., & Vishnu, D. S. Urban weather assessment using LST, NDBI and NDVI of Kolhapur city, Maharashtra. Cited by nil

Out of 8 articles chosen for study, 4 of them are coastal cities. This geographical resemblance facilitates comparative analyses, providing a basis for understanding common patterns and dynamics in environmental, climatic, and socio-economic aspects across these coastal cities. These selections, sourced from Google Scholar, aimed to explore the relationship between LST variations, urban expansion, and environmental impacts in rapidly developing regions. Keywords used for search engines were 'LST', 'Land Surface Temperature', 'UHI', 'Urban Heat Island', 'tropical monsoon climate'.

By examining LST patterns, spectral indices, and urban heat island (UHI) formation, the studies provided insights into sustainable urban planning strategies and nature-based solutions to mitigate heat stress and enhance urban sustainability.

All the articles had some common underlying objectives:

- To analyze the spatial LST pattern and intensity.
- To analyze the landcover change for a time span ranging from 10-30 years.
- To analyze the relationship between LST and LC composition and configuration.

The research conducted in Trivandrum was specifically focused on developing a Heat Stress Vulnerability Index, which involved integrating the impacts of Urban Heat Island (UHI) with demographic distribution data (Anupriya & Rubeena, 2023). Similarly, studies carried out in Kurunegala and Hat Yai City were directed towards formulating mitigation strategies and urban planning measures to address the challenges posed by UHI in the context of future urban development (Ranagalage et al., 2020) (Ruthirako et al., 2015). Additionally, the study conducted in Chittagong aimed at constructing a predictive model for forecasting Land Surface Temperature (LST) patterns, with a focus on anticipating urban climate conditions for planning purposes up to the year 2050. These initiatives collectively underscore the importance of proactive measures in tackling the adverse effects of UHI and urban climate dynamics on sustainable urban development.

Most of the studies relied on Landsat 5 TM satellite imagery as their primary input data (the thermal radiation information in the form of Thermal Infrared bands) in order to generate LST maps, particularly for analyses conducted for periods before 2015. However, more recent time-period investigations utilized Landsat 8 satellite images, which offer improved resolution (of 15 m for band 8) compared to Landsat 5 imagery (maximum resolution of 30 m). While Landsat 8 images boast higher resolution, they also offer lower-resolution options, allowing for flexibility in data selection based on the specific requirements of each study (Maxwell, 2013).

The research endeavors spanned over a considerable period, typically ranging between 20 to 30 years, during which data were collected at intervals of 10 to 15 years for most studies. However, the Hat Yai City and Kolhapur study notably lacked temporal comparative analysis and detailed assessment of land cover changes due to the absence of adequate data intervals as they investigated only Landsat images of only one time period (Ruthirako et al., 2015; Tanaji et al., 2021). Conversely, the Chittagong and Pune study adopted a more comprehensive approach, scrutinizing seasonal variations by acquiring data from three distinct seasons (Autumn, Summer, and Winter) across the three different years selected for analysis (Abdullah et al., 2022; Gohain et al., 2021). Additionally, all the articles uniformly utilized daytime images for analysis, with the majority sourced from the early morning period, ensuring consistency in data collection methodologies across various studies.

Except for the Kurunegala study, the rest of them used a minimum unit of analysis of 30m as it was the maximum resolution they could avail.

The Landsat images will have to be converted into GIS for determining the land cover/ land use classes. The metrics used for LST determinants identification in most studies are 'Built-up area', 'Open Space' / 'Barren land', 'Vegetation', and 'Waterbodies'. This is done by converting the Landsat image into spectral radiance and then to spectral indices whose values range from -1 to 1. All the studies mainly used normalized difference vegetation index (NDVI) and normalized difference built-up index (NDBI).

NASA established the Landsat program in 1972, and it consists of satellites that take multispectral images of the Earth's surface. Utilized on Landsat 4 and Landsat 5, the Landsat Thematic Mapper (TM) sensors gather high-resolution images over seven spectral bands, spanning visible to thermal infrared wavelengths. For many years, these satellites have been essential for observing changes in land cover, land use, and environmental dynamics. This has aided geological, agricultural, forestry, and urban planning applications. (Irons et al., 2012)

Normalized Difference Vegetation Index (NDVI) is a numerical indicator used in remote sensing to assess the density and health of vegetation in a given area. It is calculated using near-infrared (NIR) and red-light wavelengths captured by satellite sensors. The formula for NDVI is (NIR - Red) / (NIR + Red), where higher NDVI values indicate denser and healthier vegetation cover.

Normalized Difference Built-up Index (NDBI) is a spectral index used in remote sensing to quantify the extent and density of built-up or urban areas within a landscape. It is computed from the near-infrared (NIR) and shortwave infrared (SWIR) bands of satellite imagery. The formula for NDBI is (SWIR - NIR) / (SWIR + NIR), where higher NDBI values correspond to greater built-up area density. (Jensen, 2009)

The Pune study classified the vegetation space more specifically into 'shrub land', 'agriculture land', 'fallow land', and 'vegetation' (Gohain et al., 2021). The Mumbai study also specifically classified land cover based on moisture content as 'wetland', 'other water bodies', and 'open land'. For these analyses, spectral indices like Normalized Difference Moisture Index (NDMI), Built-up Area Index (BSI), and Modified Normalized Difference Water Index (MNDWI) had to be considered for those studies (Sahana et al., 2019).

Normalized Difference Moisture Index (NDMI) is a spectral index commonly used in remote sensing to assess vegetation moisture content and water body distribution within a given area. It is calculated using near-infrared (NIR) and shortwave infrared (SWIR) bands of satellite imagery. The formula for NDMI is (NIR - SWIR) / (NIR + SWIR), where higher NDMI values typically indicate areas with higher vegetation moisture content.

Modified Normalized Difference Water Index (MNDWI) is a spectral index used in remote sensing to detect and delineate open water bodies within a landscape. It is computed using green and shortwave infrared (SWIR) bands of satellite imagery. The formula for MNDWI is (Green - SWIR) / (Green + SWIR), where higher MNDWI values are associated with the presence of water bodies. (Xu, 2006)

The Built-up Area Index represents the proportion of a specific area that is covered by built-up or urban infrastructure, such as buildings, roads, and other man-made structures, relative to the total land area. (Zhang et al., 2003)

LST and Urban Heat Island are found to have peaked in Built-up areas than the other spaces. These areas are characterized by infrastructure such as buildings, roads, and pavements. This peak temperature is often a result of the combined effects of the urban heat island (UHI) phenomenon, anthropogenic heat sources, low vegetation cover, and heat-retaining materials like asphalt and concrete. (Voogt & Oke, 2003)

The Land Surface Temperature (LST) maps, created using Landsat data for various cities, are analyzed in GIS along with spectral indices to understand the link between LST and Land Use/Land Cover (LULC) features. The studies show a strong positive correlation between LST and the Normalized Difference Built-up Index (NDBI) with correlation coefficients exceeding 0.665, indicating that LST increases with more built-up areas. Conversely, there is a negative correlation between LST and the Normalized Difference Vegetation Index (NDVI) with correlation coefficients falling below -0.503, meaning vegetation helps lower LST and reduces the Urban Heat Island (UHI) effect. These findings highlight the impact of land cover, especially built-up areas and vegetation, on local temperature patterns in urban areas.

The correlation analysis between Land Surface Temperature (LST) and Modified Normalized Difference Water Index (MNDWI) in the Chittagong and Mumbai studies yielded contrasting results: while the former showed a negative correlation, the latter exhibited a positive one (Abdullah et al., 2022; Sahana et al., 2019). This discrepancy suggests that the presence of a water body does not always lead to a decrease in LST within the region, highlighting the complexity of factors influencing temperature dynamics. Additionally, the observed negative correlation between LST and Normalized Difference Moisture Index (NDMI) warrants further investigation, emphasizing the importance of considering moisture content in understanding LST variations. These findings underscore the need for comprehensive analyses to elucidate the nuanced relationships between LST and spectral indices, informing more accurate assessments of urban heat dynamics and mitigation strategies.

Table 2: Summary for minimum and maximum values of NDBI, NDVI, and LST of all study areas in the selected literature study articles. (Source: Author)

City	NDBI Minimum Value	NDBI Maximum Value	NDVI Minimum Value	NDVI Maximum Value	LST Minimum Value	LST Maximum Value
Trivandrum, India	-0.414	0.640	-0.2	0.5	19.01	39.49
Kurunegala, Sri Lanka					23	32.0
Chittagong, Bangladesh					21.49	31.87
Hat Yai, Thailand					15.79	33.69
Manila, Philippines	-0.43	0.72	-0.71	0.6	17.13	42.64
Mumbai, India	-0.48	0.8	-0.5	0.8	18	46
Pune, India					12.8	50.5
Kolhapur, India	-0.28	0.47	-0.23	0.62	24.09	44.64

Table 3: Summary for correlation values of NDBI, NDVI, MNDWI, NDMI, and BSI with LST of all study areas in the selected literature study articles. (Source: Author)

City	Correlation of LST with NDBI	Correlation of LST with NDVI	Correlation of LST with MNDWI	Correlation of LST with NDMI	Correlation of LST with BSI	Correlation of LST with Demography
Trivandrum, India	r = 0.665 (2022)	r = -0.503 (2022)				Positive
Kurunegala, Sri Lanka	r (FIS) = 0.97 (2019)	r (FGS) = -0.91 (2019)				
Chittagong, Bangladesh	Positive	Negative	Negative		Positive	
Hat Yai, Thailand	r = 0.705	r = -0.505				
Manila, Philippines	Strong positive	Negative				
Mumbai, India	Positive		Positive	Negative		
Pune, India						
Kolhapur, India	0.998	-0.954				

None of the case studies use political boundaries like municipal wards as a minimum geographical unit to assess LST, instead, they all analyzed the city as a whole without inner boundaries.

Another observation found in the Pune city study was that the change in the percentage of LST over different land use land cover classes was greater in the winter season as compared to the summer season during all three decades. The latent heat process of humidity and soil moisture could be the reason for reducing LST over different land cover classes, especially in the winter season. Maximum cooling intensity has been found during the winter season over the study area.

The literature proposes various measures to mitigate the Urban Heat Island (UHI) effect, with increasing green space in urban areas emerging as the most common suggestion. This recommendation aligns with findings indicating a negative correlation between Land Surface Temperature (LST) and Normalized Difference Vegetation Index (NDVI), which quantifies the amount of green space in the region.

The Kurunegala and Manila studies propose replacing grey infrastructure with green infrastructure and green buildings to reduce surface temperatures and mitigate the UHI effect. Enhancing parks, gardens, and urban forests promotes evapotranspiration and provides shade, integrating nature-based solutions into urban planning to improve environmental resilience and quality of life. (Almadrones-Reyes & Dagamac, 2023; Ranagalage et al., 2020)

Chittagong and Mumbai studies recommend protecting natural resources such as rivers, lakes, and ecosystems like Mumbai's Mangrove forests to maintain ecological balance, enhance biodiversity, and mitigate UHI effects. These natural features contribute to local climate regulation through evaporative cooling and coastal protection. (Abdullah et al., 2022; Sahana et al., 2019)

The Manila study also suggests using alternative building materials with higher reflectivity and lower thermal conductivity to reduce heat absorption in urban structures

(Almadrones-Reyes & Dagamac, 2023). Additionally, three studies emphasize public involvement in decision-making and strategy planning, highlighting the importance of community engagement and awareness in implementing effective UHI mitigation measures and promoting sustainable urban development.

Table 4: Summary of solutions/ recommendation for tackling the LST all study areas in the selected literature study articles. (Source: Author)

	Sustainable Urban Development Strategies	**Increase green spaces**	**Green-Blue Space management**	**Vertical development**	**Green and environment-friendly buildings at all its stages**	**Green Walls/ green walls**	**Grey infrastructure to green infra using natural and seminatural system**	**Low impact development Strategies**	**Protect Natural resources and ecosystem**	**People participation**	**Alternative Materials**	**Urban Green corridor and urban agriculture**
Trivandrum, India	✓	✓								✓		
Kurunegala, Sri Lanka		✓	✓	✓	✓	✓	✓	✓		✓		
Chittagong, Bangladesh	✓								✓	✓		
Hat Yai, Thailand		✓										
Manila, Philippines	✓	✓				✓	✓		✓		✓	
Mumbai, India	✓								✓			
Pune, India												

Kolhapur, India		✓										✓
TOTAL FREQUENCY	**4**	5	**1**	**1**	**1**	**2**	**2**	**1**	**3**	**3**	**1**	1

Several fields remain to be investigated in the study of Land Surface Temperature (LST) and Urban Heat Island (UHI) effects. Long-term monitoring of land use and cover changes is essential for understanding urban environmental dynamics. The Chittagong study highlights the need for more research on the link between biophysical variables and LST. Time series spatiotemporal remote sensing data can assess the evolution of UHI effects and land use changes, aiding decision-making (Abdullah et al., 2022).

The Hat Yai study suggests using higher-resolution satellite data and expanding research to diverse urban settings for better insights into land use, LST, and UHI relationships (Ruthirako et al., 2015). Investigating Nature-Based Solutions (NBS) for UHI mitigation holds promise for addressing urban heat challenges. Understanding the relationship between LST and various land cover types is crucial to see how different landscapes influence UHI dynamics.

The Mumbai study proposes using microwave remote sensing data to improve LST assessments (Sahana et al., 2019). The Pune study calls for more research on factors impacting LST, such as air temperature and elevation (Gohain et al., 2021). Finally, studying heatwave vulnerability in coastal cities is vital for developing targeted adaptation and resilience strategies for vulnerable communities. These areas are important for advancing our understanding of LST and UHI effects in urban environments.

Table 5: Summary of fields that remain to be investigated in the selected literature study articles. (Source: Author)

City	**Fields that remain to be investigated**
Trivandrum, India	• Long term monitoring of LU/LC changes and UHI effects. • Utilization of time series spatiotemporal remote sensing data. • Assessment of UHI effects and land use dynamics using Landsat data. • Study of varying LU/LC patterns on a spatio-temporal scale. • Investigation of landscape modifications using accurate time series data and remote sensing.
Kurunegala, Sri Lanka	• Investigating the impact of Nature-Based Solutions (NBS) on Urban Heat Island (UHI) mitigation. • Exploring the effectiveness of urban green-blue space management in reducing UHI effects. • Studying the relationship between land surface temperature (LST) and different land cover types. • Assessing the potential of green infrastructure like green walls in buildings for UHI mitigation.
Chittagong, Bangladesh	• Spatial distribution of heatwave vulnerability in coastal cities • Modification of normalized difference water index (NDWI) for enhancing open water features • Impacts of spatial clustering of urban land cover on land surface temperature • Effects of landscape composition and patterns on land surface temperature • Remote sensing of forest change using artificial neural networks
Hat Yai, Thailand	• Studying the relationship between urban greening and the thermal environment. • Analyzing urban heat island patterns using Landsat TM data and ASTER data. • Characterizing early successional forest patterns in western Oregon using multi-temporal Landsat data. • Further research on the relationship between land use and the urban heat island effect in Mexicali, B.C., Mexico.

Manila, Philippines	• Effects of atmospheric boundary layer turbulence, wind speed, and stability on wind farm-induced temperature changes. • Change detection methods and accuracy assessment for land use land cover. • Impact of urban green spaces on the urban thermal environment and its seasonal variations.
Mumbai, India	• Continued study on the urban heat island effect and the impact of urban growth on LST variations in different regions. • Exploration of advanced remote sensing methods, such as microwave data, to enhance the accuracy of LST retrieval. • Further research on the relationship between different land cover changes and their effects on Land Surface Temperature (LST).
Pune, India	• Further investigation into the impact of land use and land cover changes on climate change. • Study of the specific factors contributing to urban heat island development. • Analysis of the relationship between land surface temperature variations and different land cover classes.
Kolhapur, India	• Relationship between NDVI and NDBI • Impact of land surface temperature (LST) on urban heat island phenomena • Planning strategies for controlling urban heat pockets

The studies identified several limitations impacting the comprehensiveness and reliability of their findings.

- In Trivandrum, reliance on daytime data and a spatial resolution of 30m restricted the ability to capture nighttime temperature variations and fine-scale thermal dynamics crucial for understanding UHI effects (Anupriya & Rubeena, 2023).
- The Kurunegala study highlighted the absence of specific Nature-Based Solutions (NBS) data, hindering detailed analysis of their effectiveness in mitigating UHI effects and underlining the need for comprehensive data to assess the impact of green infrastructure on urban thermal dynamics (Ranagalage et al., 2020).

- In Chittagong, the lack of multi-seasonal data analysis and advanced artificial neural network (ANN) algorithms for land use/land cover classification potentially overlooked seasonal variations in UHI effects and land surface temperature dynamics (Abdullah et al., 2022).
- The Hat Yai city study faced constraints such as reliance on Landsat TM data, which may have impacted the accuracy of LST measurements, especially in complex urban environments. The focus on a specific region limited the generalizability of findings to other urban areas with different characteristics, compounded by mismatches in data comparisons and a lack of temporal change interpretation due to the analysis of only one time period (Abdullah et al., 2022).
- The Manila study considered only two time periods for analysis, restricting the exploration of urban land cover dynamics over a broader temporal scale and potentially limiting the understanding of long-term trends in UHI effects and land surface temperature patterns (Almadrones-Reyes & Dagamac, 2023).
- The Mumbai city study faced constraints due to the use of Landsat data, which restricted the temporal frequency of analysis and was affected by cloud coverage issues, impacting the accuracy of LST results (Sahana et al., 2019).
- The Pune study acknowledged potential limitations in the resolution and interpretation of satellite data, emphasizing the importance of careful consideration and validation of remote sensing data in UHI research to ensure robust and meaningful results (Gohain et al., 2021).

All the studies selected provided recommendations and solutions on a general level rather than on a ward level, which will make it more complex for the authorities to use those proposals.

Another major limitation observed in the studies (except Chittagong and Pune studies) was that the time and date of the Landsat images were random with the least cloud coverage or with the ones data was available for in the last century (i.e., Landsat images retrieved in days of 20th century when the frequency of recording the images was less). As a result, the LST values analyzed in those studies need not be the highest values observed in those years.

Some important aspects of the literature study can be noted. Retrieving both daytime and nighttime images is crucial, as daytime images provide maximum temperature data while nighttime images yield minimum temperature results, offering a comprehensive view of temperature dynamics.

The Landsat data/images retrieved for the study should have maximum LST observed/recorded in the year. This is for having a more accurate analysis on LST and UHI as peak values are used for the study.

Ground truth validation is essential for confirming the authenticity of remote sensing data and ensuring the reliability of study results. Seasonal variations can be examined to understand changing climate and temperature trends over time, while also considering spatial demographic factors' influence on UHI trends. Furthermore, investigating the impact of high-density roads on UHI and proposing mitigation strategies can also be a field of research. Additionally, understanding the relationship between land moisture content, water bodies, and UHI, through derived spectral indices such as NDVI, NDBI, NDMI, and MNDWI, can provide valuable insights into UHI dynamics in Cochin.

The municipal wards of Cochin can be used as a minimal investigation geographical unit for LST analysis as these ward boundary division was based on a general land use characteristics of the zones with consideration to political boundaries and demographic characteristics. A ward-wise comparative analysis can provide a greater and precise understanding about LST in each ward which can smoothen the formation of planning guidelines for the planners. Finally, incorporating green spaces into urban planning can significantly alleviate UHI effects, emphasizing the importance of nature-based solutions in mitigating urban heat challenges in Cochin.

3. Case Study Presentation

Kerala (a state in south India) has been experiencing intense heatwaves, particularly during the months of March to May leading to record-breaking temperatures and prolonged heatwave durations. These extreme conditions are attributed to several natural factors, including the northward movement of the sun and the presence of a large body of ocean water surrounding Kerala, which increases atmospheric humidity and contributes to intense ultraviolet radiation.

The prevailing El Niño phenomenon in the Pacific Ocean has further exacerbated the heatwave conditions by altering global circulation patterns and restricting cloud formation.

Human-induced factors such as global warming and increased urbanization (being an increasingly significant global concern) have also intensified the severity of heatwaves, with urban heat island effects significantly elevating temperatures in densely populated areas (S, 2024).

Cochin city is located in Ernakulam District, between 76 ° 14' and 76° 21' East longitude and 9° 52' and 10° 1' North Latitude. The Corporation (KMC) has a harbor, railway junction, international airport, the Naval Base, and various industries in its command area and its peripheries (Kochi Municipal Corporation, 2024).

The Cochin Municipality with a total area of 85.48 sq. km. is considered for the study which contains 74 municipal wards ranging from an area of 0.21 sq. km to 5.44 sq. km. per ward (Figure 4). This division is based on political boundaries, population density, homogeneity of the urban fabric, and land use regulations making local governance more convenient (Corporation, City Development Plan (CDP), 2023). The population of the Municipality is 6,26,551 people with ward-wise population ranging from 4,414 to 1,4723 as of Census 2023 data.

Ward 29 (industrial area, naval base, and port) and 30 (Mostly vacant land) comprise the Willington Island which is the largest artificial island in India. Wards 1, 5, 6, 9, 11, 55, 56, 61, 62, 63, 65, 66, 67 and the strip along the National Highway 47 contribute the majority of commercial activities in the Municipality (Figure 2) (Corporation, City Development Plan (CDP), 2023).

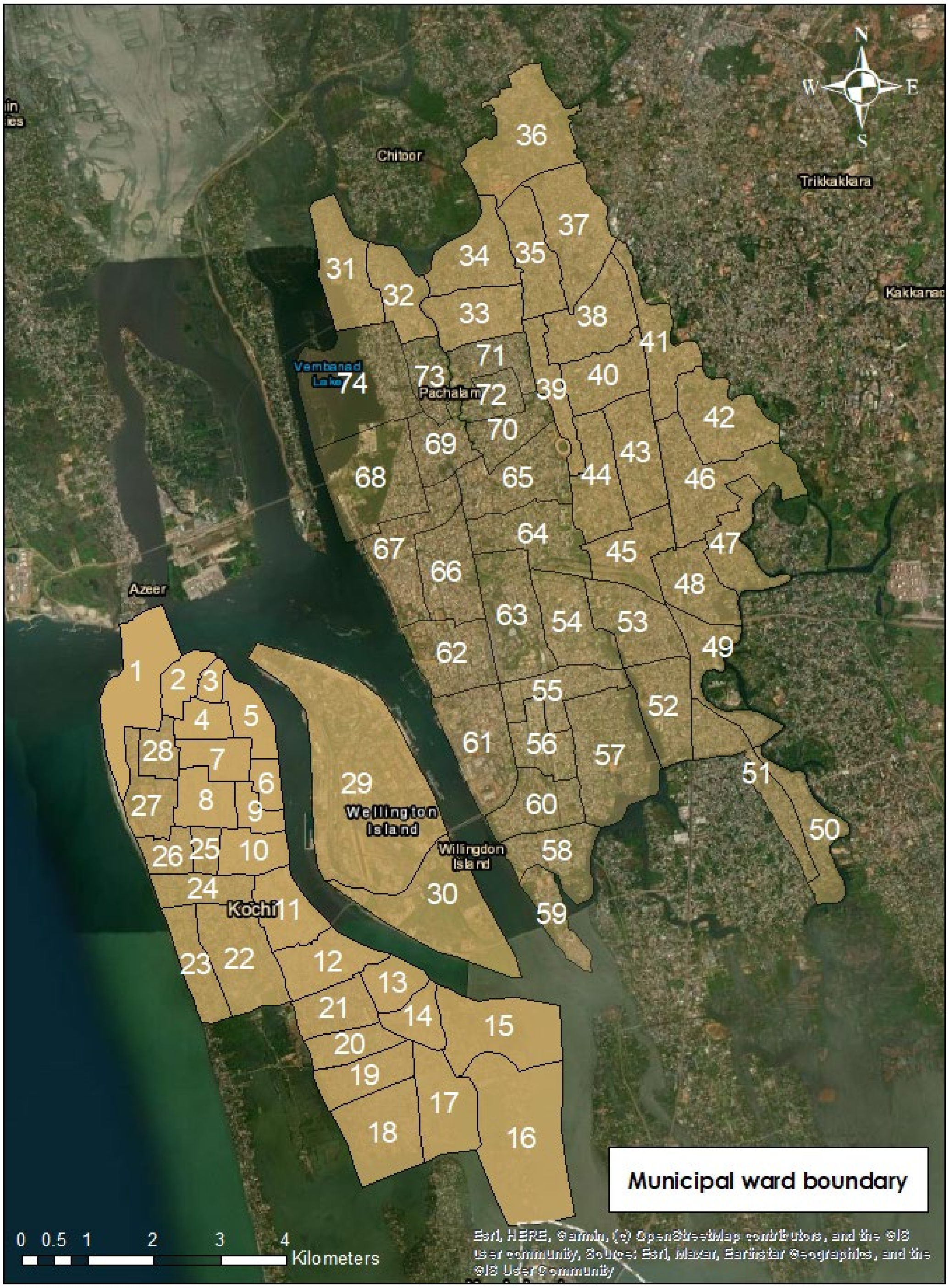

Figure 4: Map of the Administrative boundary of Kochi Municipality with ward-wise division (Source: GCDA. Modified by Author)

Under the Koppen climate classification, cochin falls under the category of tropical monsoon climate (designated as Am). Due to its proximity to the equator and its coastal position, Kochi sees minimal fluctuations in temperature throughout the year, coupled with moderate to high levels of humidity. The annual temperature typically ranges between 23 and 31 °C (73 and 88 °F), with the highest recorded temperature being 36.5 °C (97.7 °F) and the lowest recorded temperature at 16.3 °C (61.3 °F). During the period from June to September, heavy rainfall occurs as Kochi is situated on the windward side of the Western Ghats, influenced by the southwest monsoon. Subsequently, from October to December, Kochi experiences lighter but still significant rainfall due to the northeast monsoon, as it is located on the leeward side. The average annual rainfall measures 3,014.9 mm (118.70 in), distributed over an average of 124 rainy days per year (Table 6) (koeppen-geiger).

Table 6: Climate data for Kochi (Kochi Naval Base) 1981 - 2010, extremes 1951 - 2012 (Source: (Ministry of Earth Sciences, n.d.))

Climate data for Kochi (Kochi Naval Base) 1981–2010, extremes 1951–2012													
Month	**Jan**	**Feb**	**Mar**	**Apr**	**May**	**Jun**	**Jul**	**Aug**	**Sep**	**Oct**	**Nov**	**Dec**	**Year**
Record high °C (°F)	36.4 (97.5)	35.7 (96.3)	36.0 (96.8)	36.5 (97.7)	35.2 (95.4)	34.2 (93.6)	33.1 (91.6)	32.5 (90.5)	34.2 (93.6)	34.6 (94.3)	35.0 (95.0)	35.2 (95.4)	36.5 (97.7)
Mean daily maximum °C (°F)	31.9 (89.4)	32.0 (89.6)	32.6 (90.7)	33.0 (91.4)	32.4 (90.3)	30.3 (86.5)	29.6 (85.3)	29.5 (85.1)	30.2 (86.4)	30.7 (87.3)	31.3 (88.3)	31.9 (89.4)	31.3 (88.3)
Mean daily minimum °C (°F)	23.0 (73.4)	24.2 (75.6)	25.5 (77.9)	25.9 (78.6)	25.7 (78.3)	24.2 (75.6)	23.8 (74.8)	24.0 (75.2)	24.2 (75.6)	24.1 (75.4)	24.1 (75.4)	23.2 (73.8)	24.3 (75.7)
Record low °C (°F)	16.5 (61.7)	16.3 (61.3)	21.6 (70.9)	21.2 (70.2)	21.1 (70.0)	20.4 (68.7)	17.6 (63.7)	20.6 (69.1)	21.1 (70.0)	19.2 (66.6)	19.2 (66.6)	17.7 (63.9)	16.3 (61.3)
Average rainfall mm (inches)	24.3 (0.96)	27.1 (1.07)	45.0 (1.77)	113.1 (4.45)	284.5 (11.20)	700.3 (27.57)	575.5 (22.66)	378.8 (14.91)	310.3 (12.22)	366.6 (14.43)	150.4 (5.92)	39.0 (1.54)	3,014.9 (118.70)
Average rainy days	1.1	1.2	2.6	6.9	11.0	23.0	22.8	19.0	13.4	14.2	7.2	1.8	124.2
Average relative humidity (%) (at 17:30 IST)	61	65	68	70	73	82	83	82	79	77	72	64	73
Average ultraviolet index	11	12	12	12	12	12	12	12	12	12	10	10	12

Cochin's climate, patterns of land use, and environmental features are significantly shaped by its topography and geography. Cochin is a city in southwest India and is a part of the Malabar Coast, a bigger region. The topography and geography of Cochin are described as follows:

- Coastal Location: Cochin's location along the Arabian Sea coast moderates temperatures and adds to the city's high levels of humidity. The closeness to the coast promotes a robust fishing sector and eases marine trade. This led to the formation of the port and industrial area in Cochin.
- Backwaters and Estuaries: Confluences of multiple rivers, like as the Periyar, Muvattupuzha, and Vembanad, provide the complicated network of backwaters, estuaries, and lagoons that make Cochin famous.
- Islands and Peninsulas: Willingdon Island, Fort Kochi, and Mattanchery are just a few of the islands and peninsulas that make up Cochin. These landforms are popular tourist attractions and add to the city's distinctive cultural legacy.
- Land Use and Urbanization: As a result of Cochin's rapid urbanization, the city's residential, commercial, and industrial zones have grown. The city's urban sprawl has impacted biodiversity and land surface temperatures by encroaching on agricultural and natural ecosystems.

It is necessary to comprehend the topography and geography of Cochin to do GIS-based land surface temperature research. These variables affect heat distribution, patterns of land cover, and environmental vulnerabilities; they offer important information for the region's efforts at urban development and climate resilience.

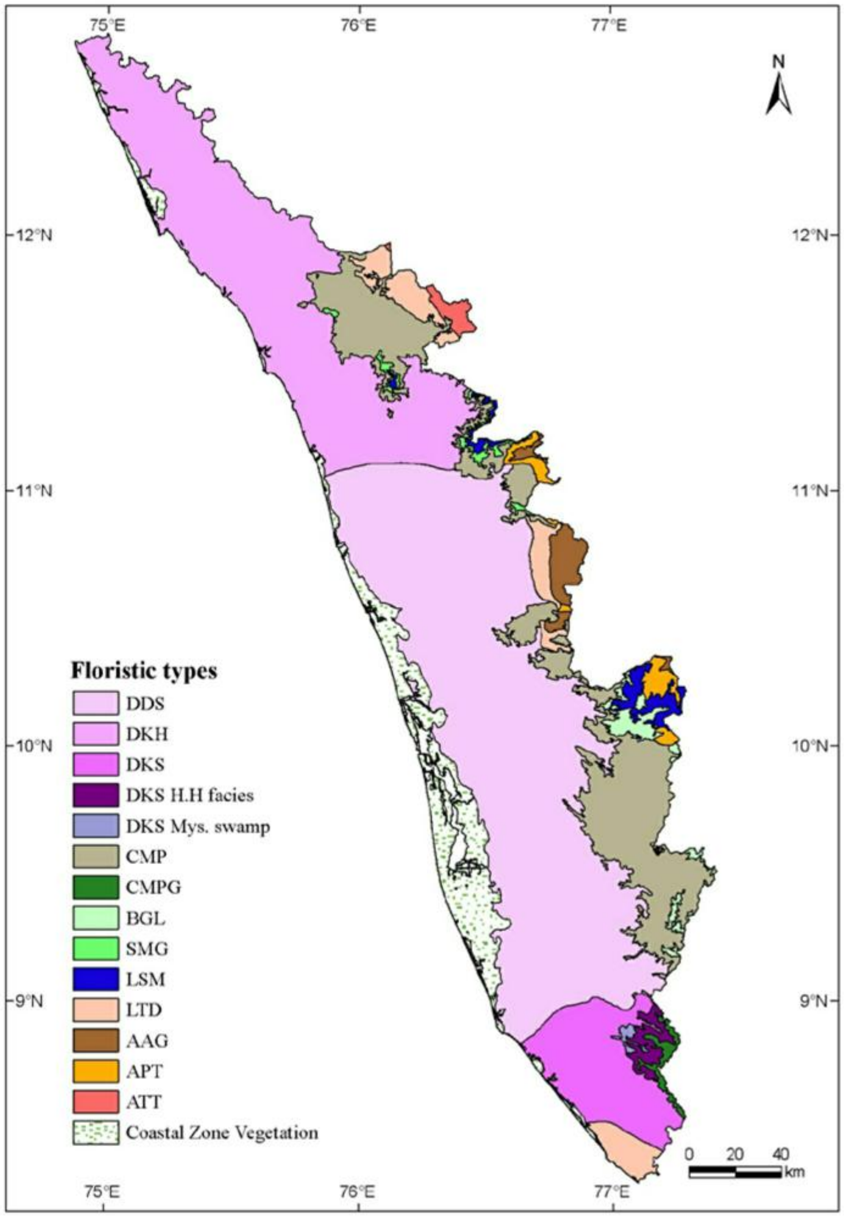

Figure 5: Vegetation type in Kerala (Source: (Ramesh & Gurukkal, 2007))

Kochi can also boast of having coastal zonal vegetation which contains mostly evergreen vegetation. This would give a negligible impact due to tree cover with respect to seasons as there will not be much change in tree cover that may contribute to the LST variation across the year (Figure 5).

4. Methodology

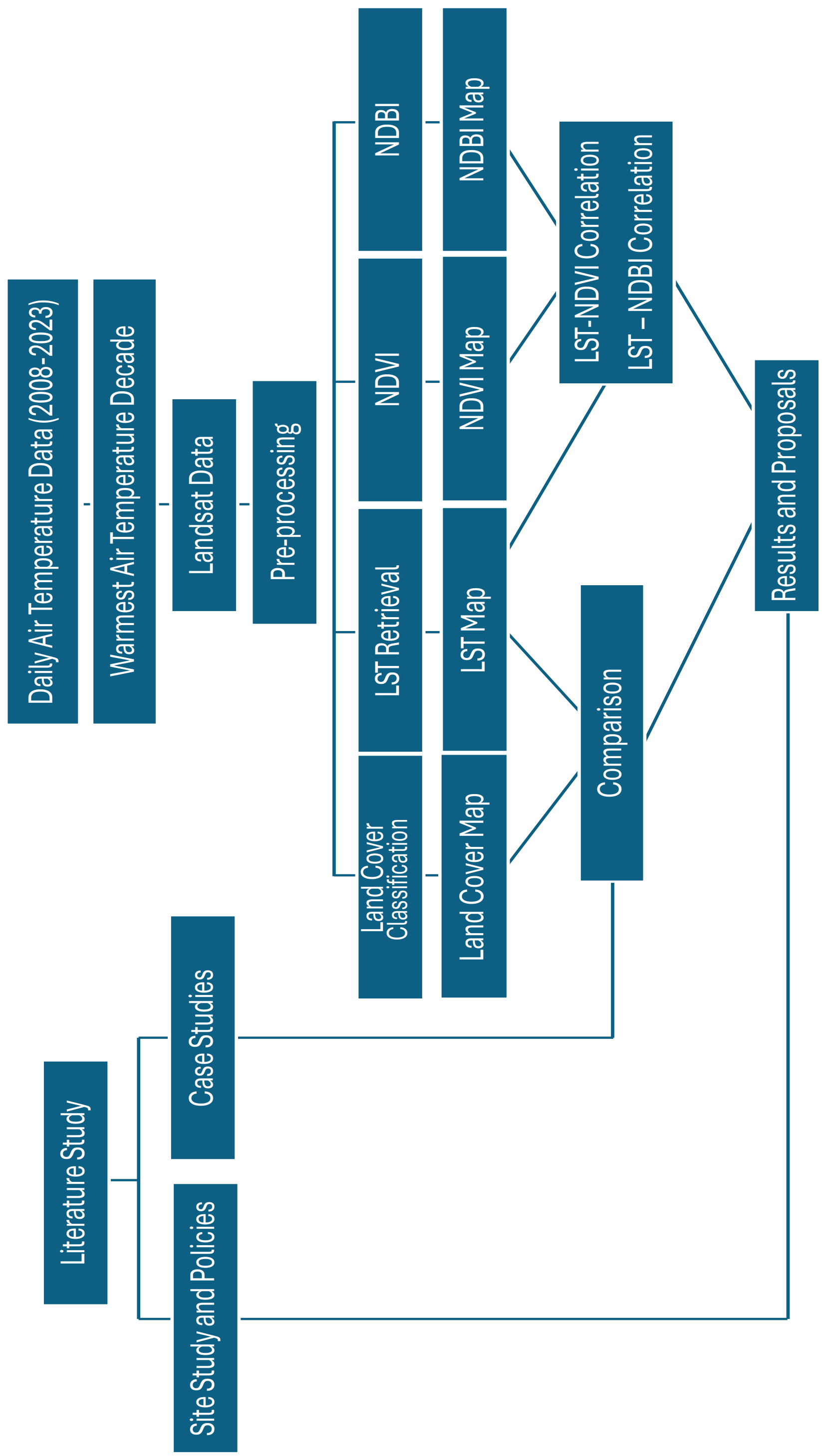

Figure 6: Flow chart of the Methodology (Source: Author)

4.1. Identification of Warmest Decade of the Month

It is essential to figure out the warmest decade of the warmest month of the year to carry out the study of the LST. The Landsat image acquired from the above-mentioned period can give a more accurate and highest value of LST observed in the site.

- The daily air temperature data of Kochi from the past 15 years (1^{st} January 2008 – 31^{st} March 2023) was obtained from the Data Supply Portal ((Climate Research & Services)) which included the daily average, daily maximum as well as the daily minimum temperature.
- The data was processed in MS Excel to get the monthly average temperature of the past 15 years and graphs were plotted between months and monthly average maximum and minimum temperature to obtain the warmest month of the year.
- Now to shortlist the warmest decade of the month, the air temperature data was processed in MS Excel to obtain the average temperature of 3 decades of each month of the past 15 years, and 3 separate graphs were plotted between months and average maximum and minimum temperature of 3 decades of each month to obtain the warmest decade of the year (which is decade of the year with highest average maximum temperature of past 15 years data).

(**N.B.:** March 11-20 was found to be the warmest decade of the year in KMC)

4.2. LST Maps

An LST map provides spatially detailed temperature data, highlighting areas with elevated heat levels within urban environments. This information is crucial for identifying heat distribution patterns, assessing the impact of urbanization, and developing mitigation strategies. (Guha et al., 2020)

4.2.1. LST map using daytime data

- For obtaining the LST maps Landsat 8 images for date in the warmest (one with the highest air temperature) decade range shortlisted (March 08.03.2023 – 05:11 am UTC – 10:41 am Local Time) with less than 10% cloud cover were downloaded from USGS Earth Explorer ((ESRI, n.d.)).

  (File link: https://earthexplorer.usgs.gov/scene/metadata/full/5e81f14f59432a27/LC81440532023067LGN00/)

  (**N.B.**: The Landsat images in the warmest decade of year figured out, i.e., March 11-20; of the year 2023 didn't have cloud coverage less than 10%. So, data from the nearest date to that date range with cloud coverage less than 10% was retrieved)

- Imported the Bands 4, 5 and 10 into ArcMap.

  Digital number in remote sensing systems, a variable assigned to a pixel, usually in the form of a binary integer in the range of 0–255 in case of 8-bit resolution (i.e. a byte). The range of energies examined in a remote sensing system is broken into 256 bins. But Landsat 8 OLI sensor stores these data as DNS with a range from 0 to 65536. ((Government, Landsat Missions, n.d.))

  The MTL (Metadata) file included along with the Landsat images downloaded from EarthExplorer contains detailed information about the satellite image, such as acquisition date, sensor type, calibration coefficients, and geographic coordinates, essential for processing and analyzing the data (Schowengerdt, 2012) (Ramey, Rose, & Tyerman, 1995).

- Conversion to TOA Radiance
  - Landsat 8 Level-1 data can be converted to TOA spectral radiance using the radiance rescaling factors in the MTL file:

$$L_\lambda = M_L{*}Q_{cal} + A_L$$

where:

- L_λ = TOA spectral radiance (Watts/(m2 * srad * μm))
- ML =Band-specific multiplicative rescaling factor from the metadata (RADIANCE_MULT_BAND_x, where x is the band number)
- AL=Band-specific additive rescaling factor from the metadata (RADIANCE_ADD_BAND_x, where x is the band number)
- Qcal = Quantized and calibrated standard product pixel values (DN)

((Government, Landsat Missions, n.d.))

N.B where:

- M_L = RADIANCE_MULT_BAND_10 = 3.3420E-04 from "LC08_L2SP_144053_20230308_20230316_02_T1_MTL.txt"
- A_L = RADIANCE_ADD_BAND_10 = 0.10000 from "LC08_L2SP_144053_20230308_20230316_02_T1_MTL.txt"

- Conversion to Top of Atmosphere Brightness Temperature
  - Thermal band data can be converted from spectral radiance to top-of-atmosphere brightness temperature using the thermal constants in the MTL file:

$$BT = K2 / \ln((K1/ L_\lambda) + 1) - 273.15$$

where:

- BT = Top of atmosphere brightness temperature (°C)where:
- L_λ = TOA spectral radiance (Watts/(m2 * srad * μm))
- K1 = Band-specific thermal conversion constant from the metadata (K1_CONSTANT_BAND_x, where x is the thermal band number)
- K2 =Band-specific thermal conversion constant from the metadata (K2_CONSTANT_BAND_x, where x is the thermal band number)

((Government, Landsat Missions, n.d.))

N.B where:

- K1 = K1_CONSTANT_BAND_10 = 774.8853 from "LC08_L2SP_144053_20230308_20230316_02_T1_MTL.txt"
- K2 = K2_CONSTANT_BAND_10 = 1321.0789 from "LC08_L2SP_144053_20230308_20230316_02_T1_MTL.txt"

- The proportion of vegetation Pv is calculated using the formula:

$$Pv = Square\ ((NDVI - NDVImin) / (NDVImax - NDVImin))$$

  - The minimum and maximum values of the NDVI image were displayed directly in the image (both in ArcGIS, QGIS, ENVI, Erdas Imagine).
  - NDVImin = -0.142
  - NDVImax = 0.802

((Giscrack, 2024))

- Calculation of Emissivity ε

$$\varepsilon = 0.004 * Pv + 0.986$$

  - The formula is used in the raster calculator, the value of 0.986 corresponds to a correction value of the equation.

((Giscrack, 2024))

- Calculation of the Land Surface Temperature

$$LST = (BT / (1 + (0.00115 * BT / 1.4388) * Ln(\varepsilon)))$$

  - Finally, the LST equation is applied to obtain the land surface temperature map.

((Giscrack, 2024))

- The final output file 'LST' is then properly symbolized by changing the symbology to stretched classification with the following color scheme:

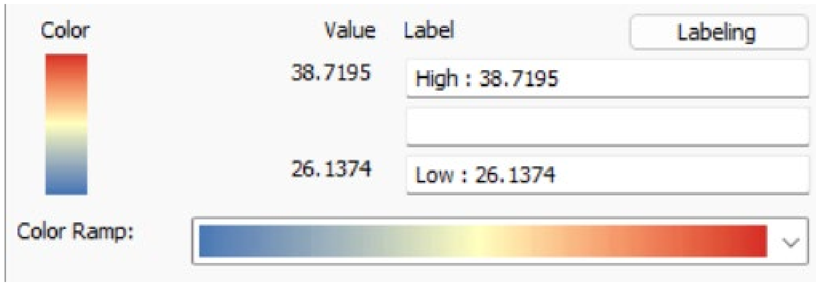

Figure 7: Symbology settings given for LST map (daytime) processed (Source: Author)

- Output map is exported as a jpeg file with proper legends, symbology, and scale.

4.2.2. LST map using nighttime data

LST map analysis of Kochi in nighttime would give an idea about the diurnal variation and LST distribution at the coldest hours of the day in the city. Efforts were made to retrieve Landsat images at nighttime and failed as even Landsat satellites pass over the geographical zone of Kochi only in the daytime (Government, What are the acquisition schedules for the Landsat satellites?, n.d.). Landsat 8 and 9 can acquire nighttime, open ocean, and ascending scenes, but special requests are to be made in order to get this done (Missions, n.d.).

4.2.3. LST map for validation

A validation check is to be done for the LST map to assess its accuracy and credibility. For this another LST map has to be made from Landsat data retrieved from a date close to the previously retrieved data for comparison.

- For obtaining the LST maps for validation, the Landsat 8 images for date (20.02.2023 – 05:11 am UTC – 10:41 am Local Time) closest to the dates of the one used in the previous step (08.03.2023 – 05:11 am UTC – 10:41 am Local Time) with less than 10% cloud cover were downloaded from USGS Earth Explorer ((ESRI, n.d.)).

  (File link: https://earthexplorer.usgs.gov/download/options/landsat_ot_c2_l1/LC81440532023051LGN00/)

  (**N.B.**: The Landsat data for February 20th was used because the rest all the Landsat images nearest to March 8th data either had more than 10% cloud coverage or were Landsat 7 images which had errors and no strip correction as recommended by USGS

  In 2003, a part of the Landsat 7 sensor failed. The result was that the outside margins of all the images had stripes of missing data. A malfunction on Landsat 7 in 2003 resulted in the loss of about 25% of the data from each image (NASA, 2009).

- The steps used in the previous sub-section are followed similarly to get the final output file 'LSTVal' is then properly symbolized by changing the symbology to stretched classification with the following color scheme:

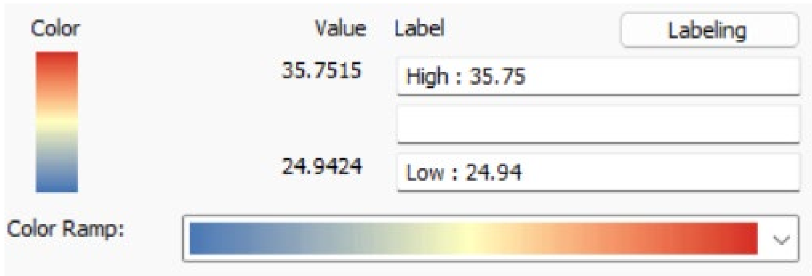

Figure 8: Symbology settings given for Validation LST map processed (Source: Author)

- Output map is exported as a jpeg file with proper legends, symbology, and scale.

4.3. LST - Ward wise comparison

A ward-wise comparison of LST is needed to have a clear understanding of UHI concentration at the ward scale level and to provide proposals at the Municipality level.

- Downloaded Landsat 8 images for date March 08.03.2023 with less than 10% cloud cover from USGS Earth Explorer (ESRI, n.d.)
- The ward boundary shapefile of Kochi Municipality is collected from 'The Greater Cochin Development Authority' (GCDA).
- The already obtained 'LST' shapefile was clipped with a boundary file.
- The Zonal statistics tool is used on the above-mentioned clipped files with the ward boundary file with the 'ward_number' as the zone field.
- The output tables were joined with the 'WardBoundary' file's attribute table with 'ward_number' as the mutual field.
- The 'WardBoundary' file is now given proper symbology for exporting the LST map with the quartile-based classification of the mean values.

4.4. Land Cover Maps

Land cover composition and configuration are used to identify the determinants of the Land Surface Temperature (LST) as they affect heat absorption and retention. (Tran et al., 2017)

Land cover classes used in this study are built-up area, tree cover, water bodies, barren soil, and grass/lawn/agriculture.

- Imported the Band 1-7 tiff files (of Landsat 8 images from date March 08.03.2023) into ArcMap
- Using composite band tool from the data management catalog of the system toolboxes of the toolbox. Selected all 7 bands as input raster and got the output raster as Compositeband.
- Changed its RGB components with the following to get real image colors:
  - Red – Band 4
  - Green – Band 3
  - Blue – Band 2
- Added classification tools to the toolbar.
- Started making samples for the map for LC classes by sampling using drawing polygon.
- For vegetation, water, built-up, and barren soil the following RGB setting was used for better identification:
  - Red – Band 5
  - Green – Band 4
  - Blue – Band 3
- For agricultural/lawn/grass the following RGB setting was used for better identification:
  - Red – Band 4
  - Green – Band 3
  - Blue – Band 2
- A signature file was made with the class samples made using sample manager as 'Classification_classes'.

- Maximum likelihood classification is used on the 'Compositeband' file using the 'Classification_classes' signature file and output file named as 'LULCclasses'.
- Proper symbolling is done on the LULC map.

4.5. Accuracy Check

An accuracy check is necessary for having the user and producer accuracy which will boost the credibility of the study and analysis of the LC maps obtained in the previous step.

- The 'Create Accuracy Assessment Check' tool is used on the 'LULCclasses' shape file with the random sampling strategy and 100 random points.

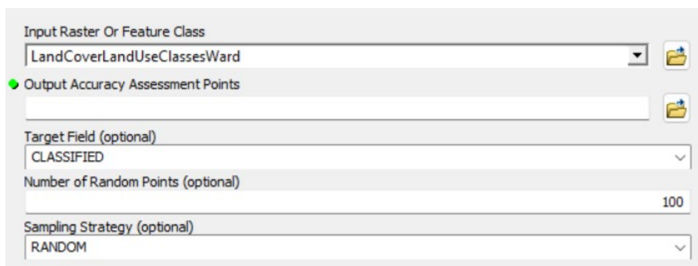

Figure 9: Image of the Settings used for 'Create accuracy assessment check' tool (Souce: Author)

- Each point is then checked with the Google Earth map and the ground truth value is added to the attribute table of the 'accuracy check' file.
- Finally, the confusion matrix (which consists of the user accuracy and producer accuracy) is obtained using the 'compute confusion matrix' tool on the 'accuracy check' file.

4.6. Vegetation Cover

As mentioned before, NDVI is a spectral index for analyzing vegetation cover on the site. Normalized Difference Vegetation Index (NDVI) is essential for analyzing Land Surface Temperature (LST) because NDVI helps assess vegetation cover's cooling effects. They provide a comprehensive understanding of how different land cover types influence LST patterns. (Guha et al., 2018)

Imported the Bands 4 and 5 (of Landsat 8 images from date March 08.03.2023) into ArcMap.

- For Landsat 8:
  - NDVI = (B5-B4)/(B5+B4)
- Raster Calculator (ArcToolBox / Spatial Analysis Tools / Map Algebra / Raster Calculator) tool is used to calculate NDVI.
- The Output file named 'NDVIRasterCalc' is properly symbolized by changing the symbology to stretched classification with the following color scheme:

Figure 10: Symbology settings given for the NDVI maps generated (Source: Author)

- The NDVI for the following classes are as follows:
  - -1 to 0: Non-vegetated surfaces (e.g., water, urban areas, barren land)
  - 0 to 0.2: Sparse vegetation or stressed vegetation
  - 0.2 to 0.5: Moderate vegetation
  - 0.5 to 1: Dense, healthy vegetation

  (Rouse et al., 1974)
- Proper symbology is given for the NDVI output map. The output map is exported as a jpeg file with proper legends, symbology, and scale.

4.7. Built-up (along with barren land) Cover

As mentioned before, NDBI is a spectral index for analyzing the Built-up cover as well as the Barren land cover. Difference Built-up Index (NDBI) is essential for analyzing Land Surface Temperature (LST) because NDBI identifies urban areas that typically exhibit higher temperatures. They provide a comprehensive understanding of how different land cover types influence LST patterns (Guha et al., 2018).

Imported the Bands 5 and 6 (of Landsat 8 images from date March 08.03.2023) into ArcMap.

- For Landsat 8:
    - NDBI = (B6-B5)/(B6+B5)
- Raster Calculator (ArcToolBox / Spatial Analysis Tools / Map Algebra / Raster Calculator) tool is used to calculate NDBI.
- The Output file named 'NDBIRasterCalc' is properly symbolized by changing the symbology to stretched classification with the following color scheme:

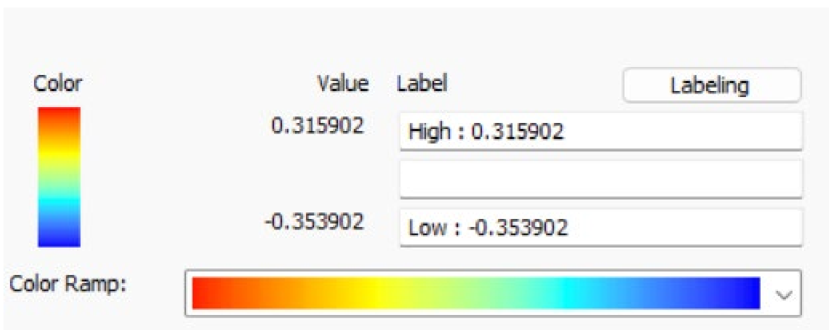

Figure 11: Symbology settings given for the NDBI maps generated (Source: Author)

- The NDBI for the following classes are as follows:
    - -1 – -0.5: Turbid Water
    - -0.5 – -0.01: Clean Water
    - -0.1 – 0.49: Soil/Vegetation/Minor Built-up
    - 0.49 – 1: Major Built-up

  (Zha et al., 2003)

- Proper symbology is given for the NDBI output map. The output map is exported as a jpeg file with proper legends, symbology, and scale.

4.8. LST drivers - Ward-wise comparison

A ward-wise comparison of land cover, built-up cover, and vegetation are needed to analyze the correlation with LST at the ward scale level.

- Downloaded the Landsat 8 images for date March 08.03.2023 with less than 10% cloud cover from USGS Earth Explorer (ESRI, n.d.)
- Ward boundary shapefile of Kochi Municipality is collected from the Greater Cochin Development Authority (GCDA).
- The already obtained 'LULCclasses', 'NDBI', and 'NDVI' shapefiles were clipped with boundary file.
- The Zonal statistics tool is used on each of the above clipped files with the ward boundary file with the 'ward_number' as the zone field.
- The output tables were joined with the 'WardBoundary' file's attribute table with 'ward_number' as the mutual field.
- The 'WardBoundary' file is now given proper symbology for exporting each NDVI, and NDBI maps with quartile-based classification of the mean values.

A ward-wise comparison of built-up area and vegetation cover percentage was done from the land cover maps using Excel:

- The scatterplot graph and Pearsons' correlation co-efficient (r) (using Pearsons' value function) are obtained for each of the LST drivers (NDBI, NDVI) with the corresponding LST values.
- The scatterplot graph and Pearsons' correlation co-efficient (r) (using Pearsons' value function) are obtained for each of the LST drivers (Mean ward NDBI, Mean ward NDVI, Ward wise percentage of Built-up cover, Ward wise percentage of Tree cover, Ward wise percentage of Green cover, Ward wise percentage of Water Bodies) with the corresponding LST mean values.

  N.B. The Pearson co-efficient (r), one of the most common correlation co-efficient, measures the strength and direction of a linear relationship between 2 variables. Its values range from -1 to 1. Negative values indicate a negative correlation between variables and positive values indicate a positive correlation. The further the coefficient is from zero, whether it is positive or negative, the better the fit and the greater the correlation. Values at or close to zero imply a weak correlation.

Pearson value's magnitude of:

- 0 - 0.3 indicates poor/weak correlation
- 0.3 - 0.59 indicates fair correlation
- 0.6 - 0.79 indicates moderately strong correlation
- 0.8 - 1 indicates very strong correlation

(FERNANDO, 2024) (Berman, 2016)

4.9. Ward-wise Road Density Map

Roads can be possible LST drivers. Hence an analysis of the ward-wise road density map; that is the road length per unit area; can be used to find the relation between road density and LST.

- After importing the 'WardBoundary' shapefile to ArcMap, the quickOSM plug-in is used to extract the highways and streets into a vector file.
- The sum line length tool is used with the Boundary file to the highway file to get the total road length in each ward.
- Field calculator is used to calculate the road density of each ward in a new field 'RoadDensity' using the formula:

Road density(km/sq.km) = Total Road length of ward/ Total area of the ward

- The road density file is then properly symbolized using the Road density field as a classification field with quartile classification.

5. Results

Recalling the research objectives:

- To analyze spatial variations in land surface temperatures (LST) across different wards and identify LST hotspots within a Tropical monsoon city on the warmest days of the year.
- To figure out the LST drivers in Cochin city.

5.1. Warmest Decade of the Warmest Month

From Figure 12 and Annexure 1, March was found to be the warmest month of the year in Kochi. From Figure 13, Figure 14, Figure 15, Annexure 2, Annexure 3 and Annexure 4, it is evident that during March, the hottest average daytime air temperature (35°C) occurs in the second decade of the month (March 11-20 in particular).

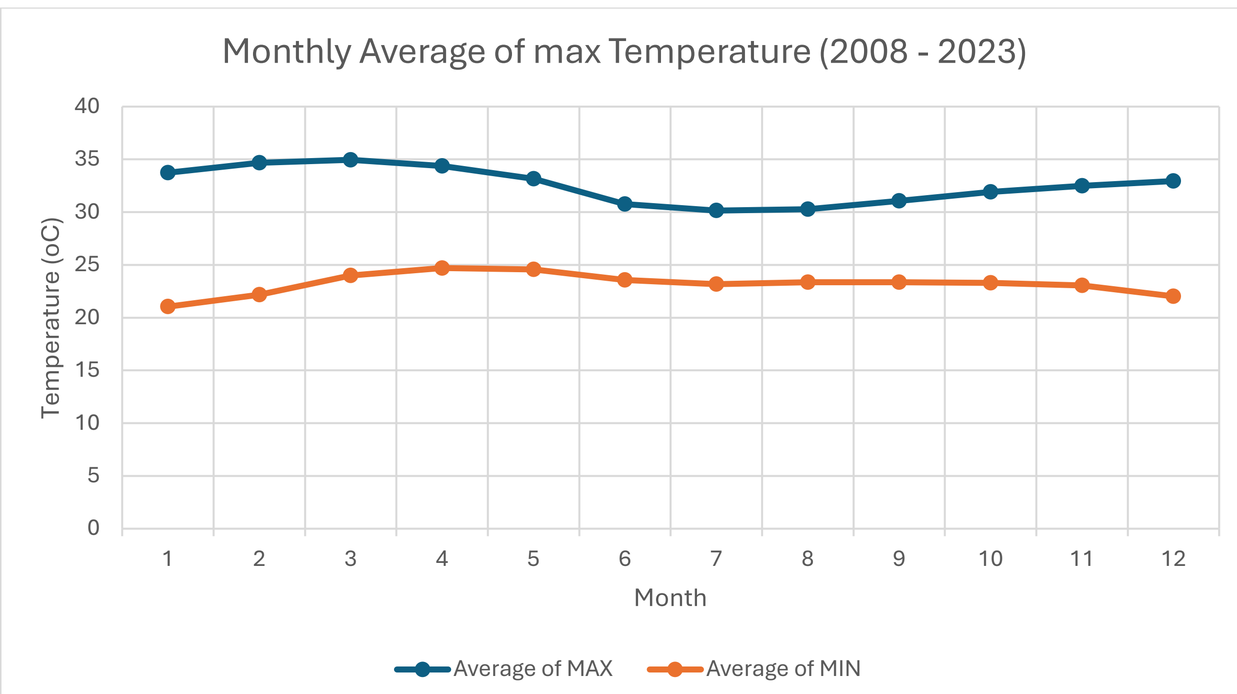

Figure 12: Chart showing the average of daily maximum temperature(°C) from 15 years' data (2008-2023) of each month (Source: Author; Data Source: DSP https://dsp.imdpune.gov.in/)

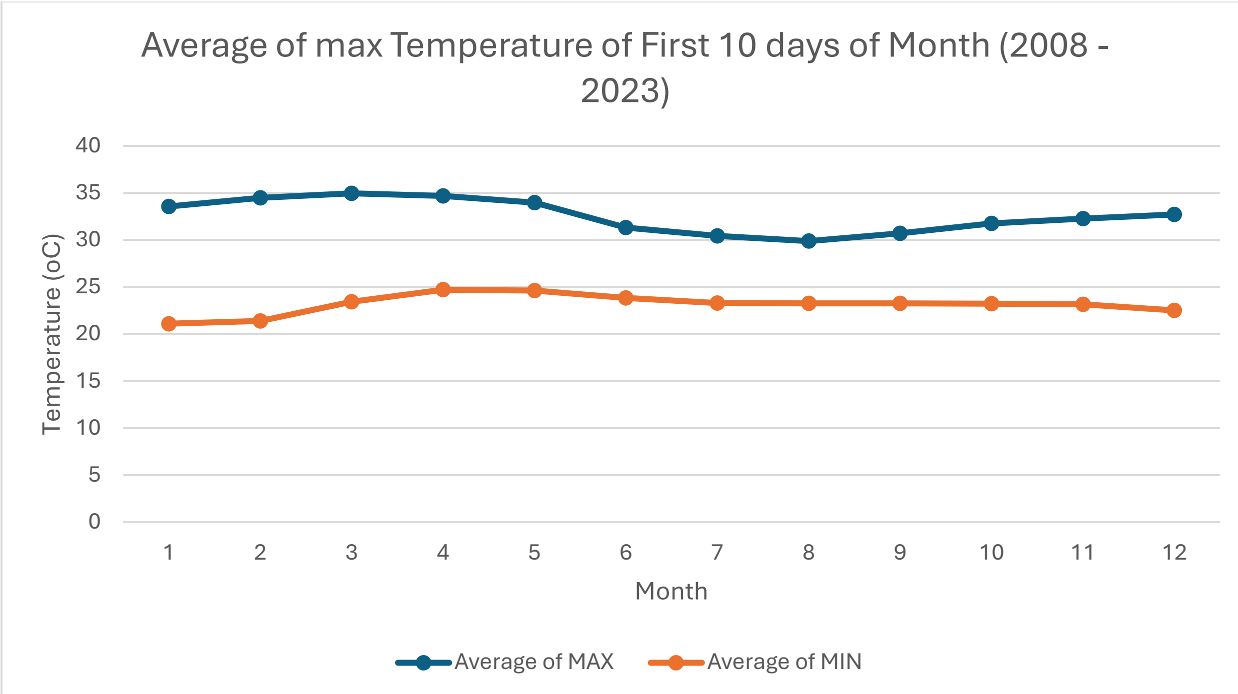

Figure 13: Chart showing the average of daily maximum temperature(°C) from 15 years' data (2008-2023) of the first 10 days each month (Source: Author; Data Source: DSP https://dsp.imdpune.gov.in/)

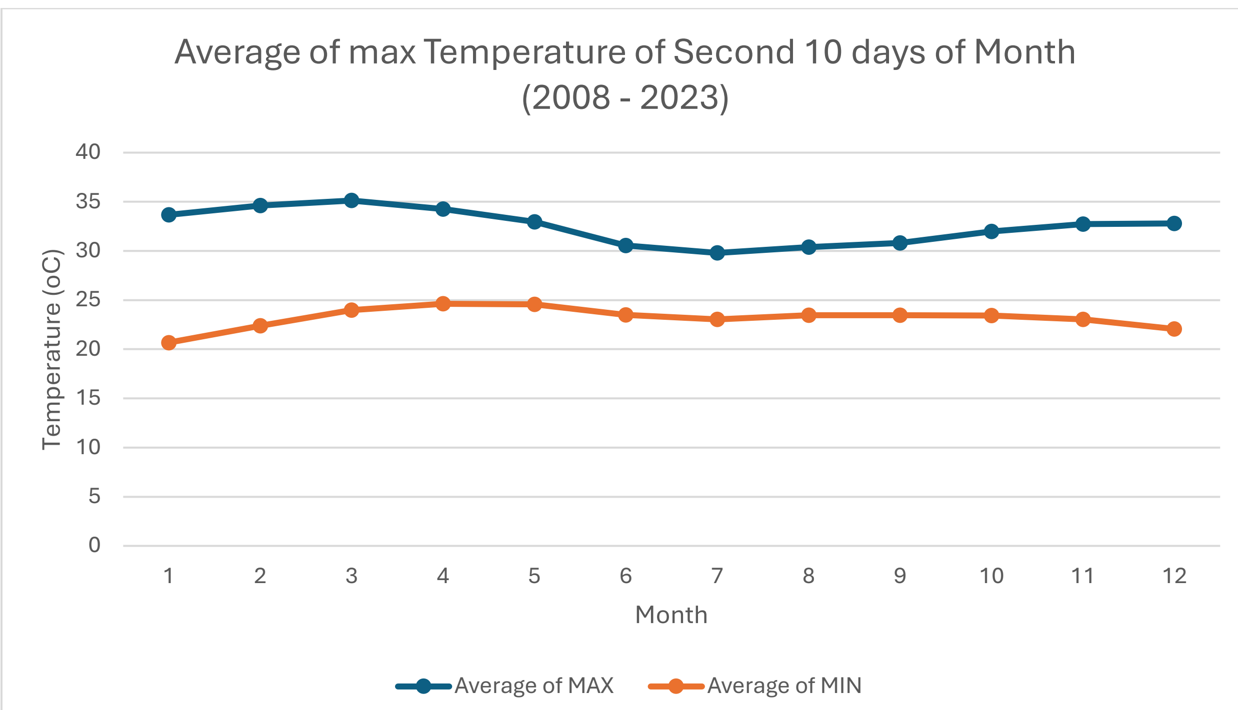

Figure 14: Chart showing the average of daily maximum temperature(°C) from 15 years' data (2008-2023) of the second 10 days each month (Source: Author; Data Source: DSP https://dsp.imdpune.gov.in/)

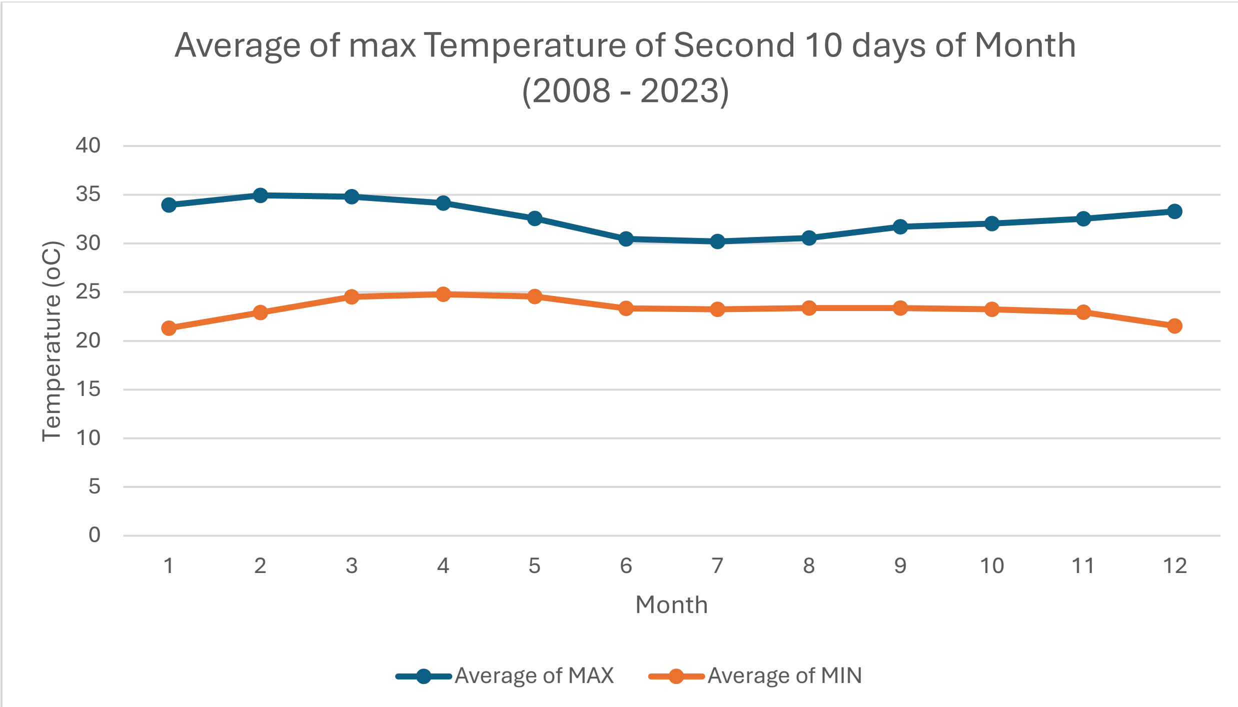

Figure 15: Chart showing the average of daily maximum temperature(°C) from 15 years' data (2008-2023) of the last 10-11 days each month (Source: Author; Data Source: DSP https://dsp.imdpune.gov.in/)

5.2. LST

The Landsat image available in the warmest decade (March 11-20) of the year had high cloud coverage over the study area, i.e.: KMC. Hence a Landsat image from the closest date to the warmest decade of the year with the least cloud cover (less than 10%) was used for analysis which was from March 8^{th}, 2023. According to the Landsat 8 data retrieved on March 8th, 2023 (05:12 am UTC/ 10:42 am Local Time), Kochi exhibits a range of daytime Land Surface Temperature (LST) values spanning from 26.14°C to 38.72°C (12.58°C range) (Figure 16). The maximum LST concentration in daytime is observed in ward 29 which is the Northern part of Willington Island and Wards 61, 37, 65, 66, 67, 3, 5, 6, and 9 (Figure 16). The minimum LST concentration in the daytime is observed in wards 16, 30, and 68.

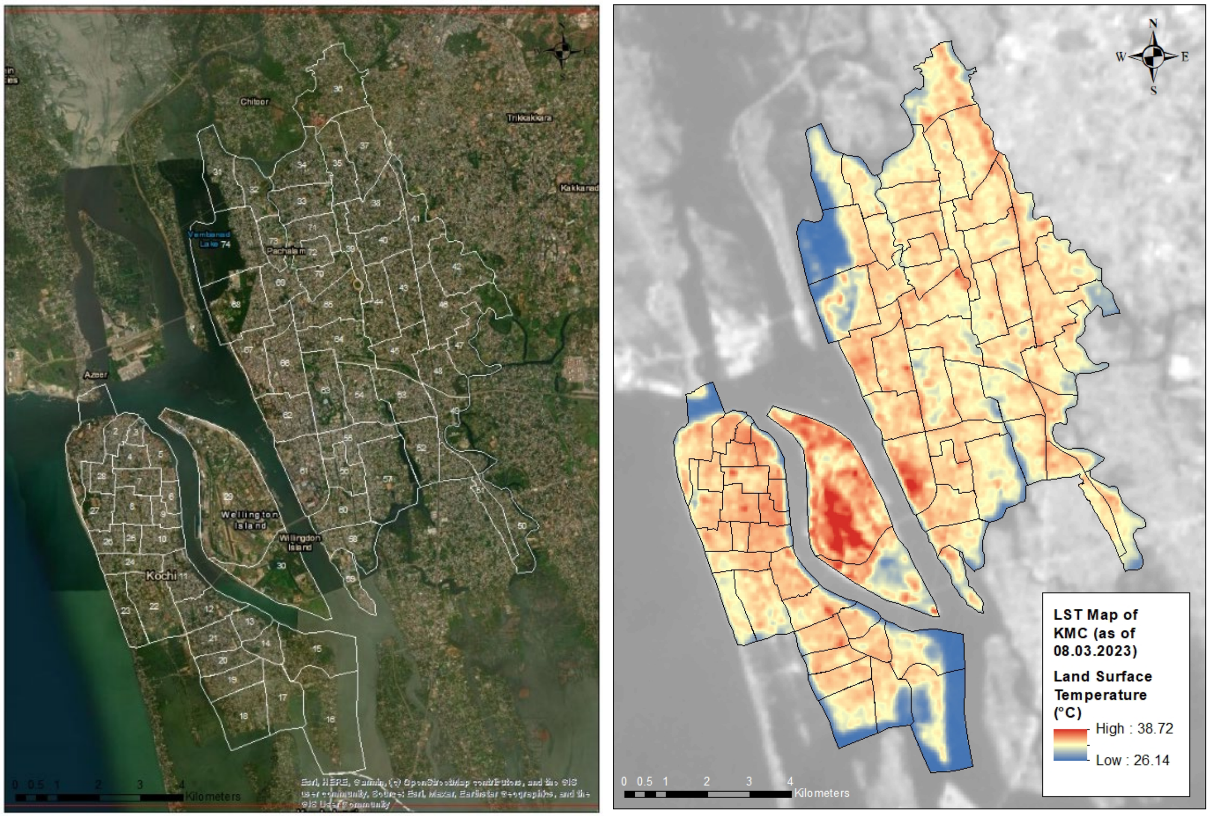

Figure 16: (On the left) Administrative boundary of KMC. (On the right) Daytime Land Surface Temperature map of KMC as of 08.03.2023 (10:42 am Local Time). (Source: Author)

The LST pattern in both the March 8th sample Landsat 8 image and the February 20th sample Landsat 8 image is similar in comparison (Figure 17). The range of LST value of KMC of March 8th data is from 26.14°C to 38.72°C whereas, for Feb 20th data, it is from 24.94°C to 35.75°C.

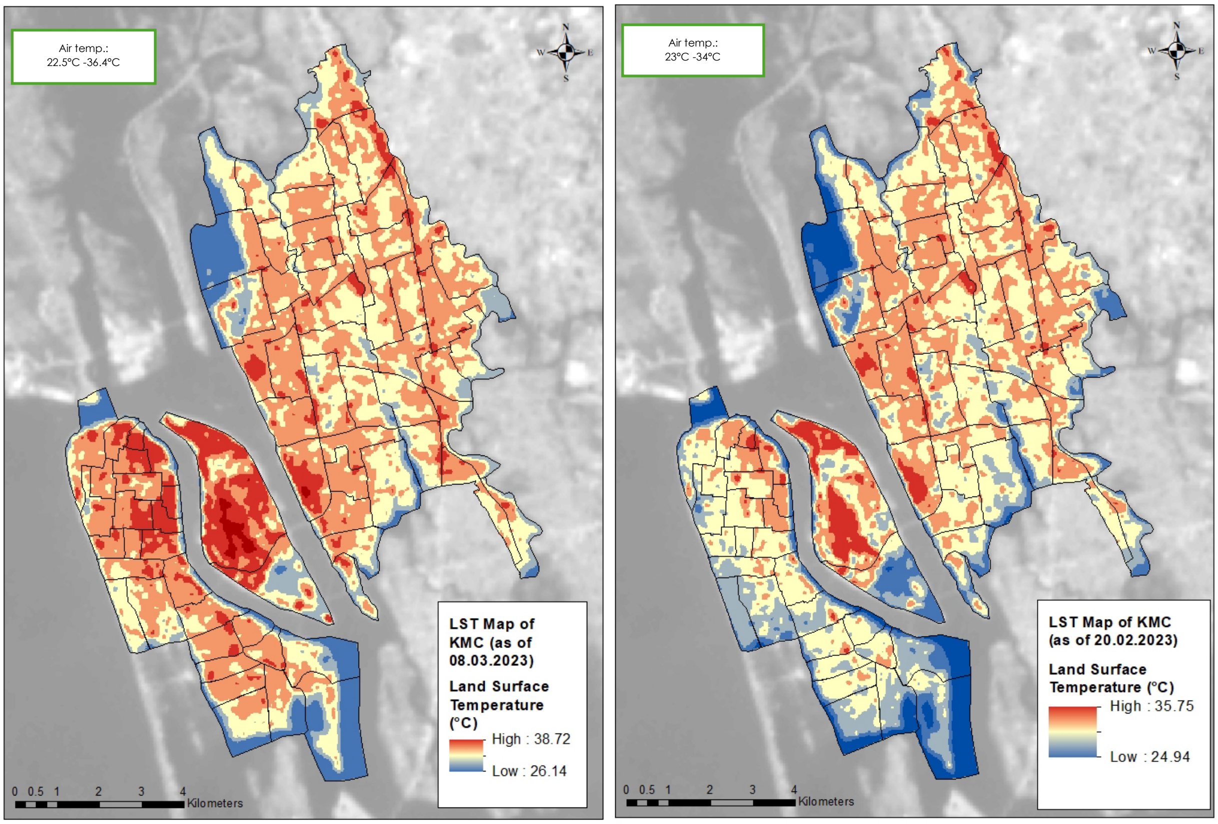

Figure 17: (On the left) Daytime Land Surface Temperature map of KMC as of 08.03.2023 (10:42 am Local Time). (On the right) Daytime Land Surface Temperature map of KMC as of 20.02.2023 for a comparative validation (10:42 am Local Time). (Source: Author)

Table 7: Comparison of Maximum, Minimum and Range of LST of KMC observed with the literature study articles (Source: Author)

City	**LST Minimum Value**	**LST Maximum Value**	**LST Range**	**Date & time of observation**
Trivandrum, India	19.01	39.49	20,48	25th February 2022
Kurunegala, Sri Lanka	23	32.0	9	2019 (10:23 am LT)
Chittagong, Bangladesh	21.49	31.87	10,38	24 April 2020
Hat Yai, Thailand	15.79	33.69	17,9	05 March 2010
Manila, Philippines	17.13	42.64	25,51	02 April 2019 (10:09 am LT)
Mumbai, India	18	46	28	02 June 2015 (10:32 am LT)

Pune, India	12.8	50.5	37,7	03 January 2019 (05:27 am LT)
Kolhapur, India	24.09	44.64	20,55	22 March 2009 (10:44 am LT)
Kochi, India	**26.13**	**38.71**	**12.58**	**08 March 2023 (10:41 am)**

5.3. LST – Ward wise comparison

The mean LST of 74 wards of wards has a range of 4.81°C with an average of 31.55°C. Ward 29 exhibits the highest mean LST of 33.30°C and ward 16 exhibits the lowest mean LST of 28.49°C (Table 8). The warmest wards are 2, 3, 4, 6, 7, 8, 9, 10, 11, 21, 24, 25, 26, 28, 29, 61, 66, and 67. The coolest wards are 1, 13, 15, 16, 17, 18, 23, 30, 31, 32, 34, 47, 50, 52, 57, 58, 59, 68, and 74 (Figure 18, Annexure 5).

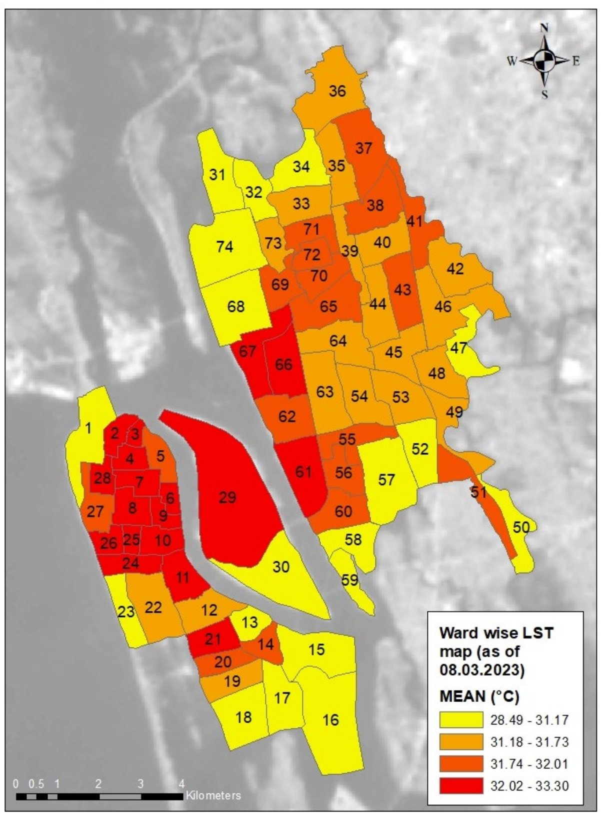

Figure 18: Land Surface Temperature map of KMC showing mean LST of each Wards as of 08.03.2023 (Source: Author)

Table 8: Table showing the Quartile classification of the Mean LST of each ward as of 08.03.2023 (Source: Author)

Quartile classification of Mean LST of each ward	
LST Min	28.49°C
LST 1st Quartile	31.15°C
LST 2nd Quartile	31.73°C
LST 3rd Quartile	32.02°C
LST Max	33.30°C

5.4. Land Cover Maps

Approximately 65% (5,265,900 Sq.m.) of the Cochin Municipality comprises built-up areas. This substantial proportion underscores the rapid urban growth and development taking place in Cochin, highlighting the unique challenges and opportunities associated with managing urbanization and mitigating urban heat island effects in this region (Table 9, Figure 20).

The green area, encompassing both tree cover, grasslands, and agricultural cover, constitutes only 25% of the entire study area in Cochin. This relatively low percentage of green cover highlights a potential contributing factor to the observed rise in temperature within the city. The tree cover solely contributes only 6% of the total land cover of KMC (Figure 19,Figure 20).

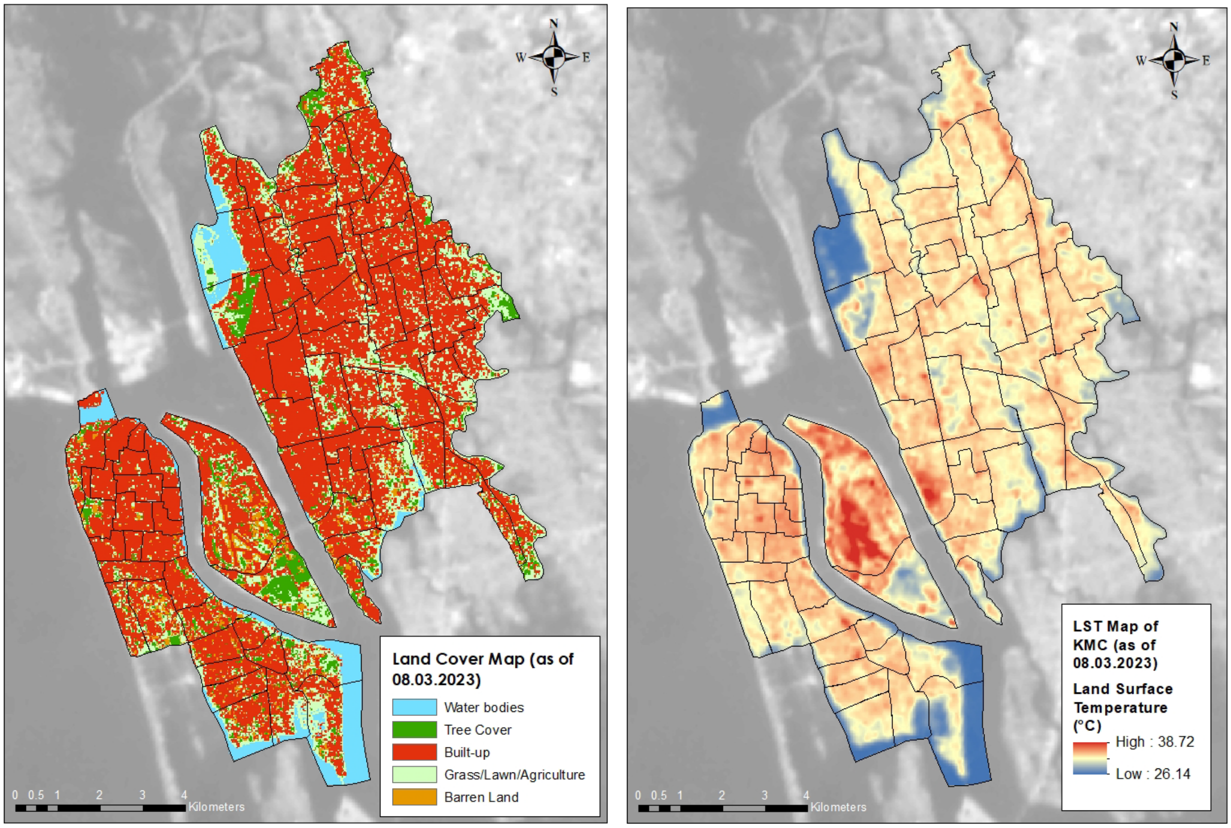

Figure 19: (On the left) Land Cover Map of KMC as of 08.03.2023. (On the right) Land Surface Temperature map of KMC as of 08.03.2023 (Source: Author)

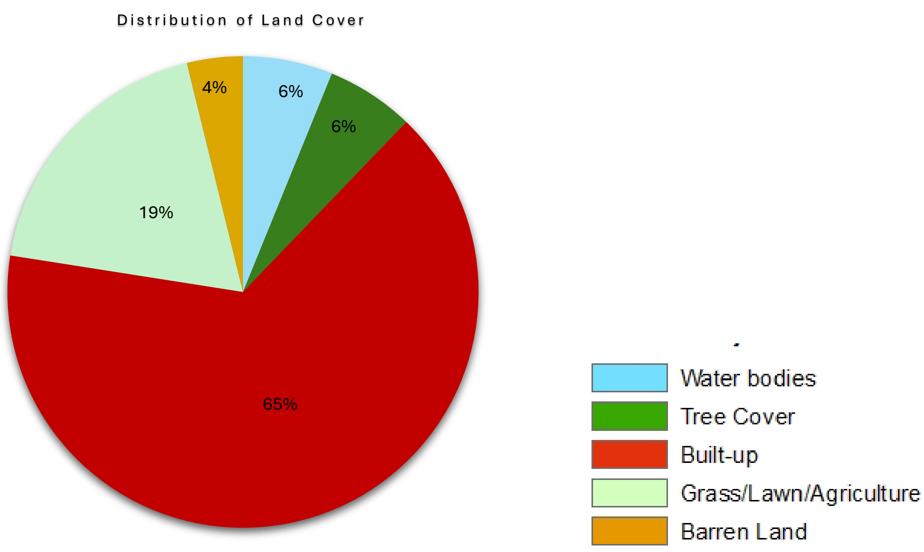

Figure 20: Pie Chart of distribution of Land Cover classification in KMC (Source: Author).

Table 9: Distribution of Land Cover of KMC as of 08.03.2023 (Source: Author)

Land Cover	Area (Sq.m.)	Percentage
Water Bodies	5,265,900	6
Tree cover	5,157,000	6
Built-up(Urban/Impervious)	55,808,100	65
Grass/Lawn/Agriculture	15,975,900	19
Barren Soil	3,276,900	4

5.5. Accuracy Check

From the accuracy matrix of the land cover (Table 10), it is clear that the overall accuracy of LC map of Cochin is 69% and the Kappa value is 0.47 which is considered as moderate to good. User's accuracy of LC map ranges from 44% (for grass/lawn class which is low) to 100%, while considering producer's accuracy barren land (14%) and grass/lawn (29%) showed least accuracy and rest of the classes showed acceptable accuracies. The commision error of the LC map ranged from 0 to 0.26 and the omission error ranged from 0.08 to 0.86.

Table 10: The Accuracy matrix of the Land Cover Map generated of KMC as of 08.03.2023 (Source: Author)

ClassValue	Water Body	Tree Cover	Built-up	Grass/ Lawn	Barren Land	Total	User Accuracy	Kappa	Error: Commission
Water Body	5.00	0.00	0.00	0.00	0.00	5.00	1.00	0.00	0.00
Tree Cover	0.00	7.00	0.00	0.00	0.00	7.00	1.00	0.00	0.00
Built-up	1.00	12.00	49.00	3.00	6.00	71.00	0.69	0.00	0.31
Grass/ Lawn	0.00	5.00	4.00	7.00	0.00	16.00	0.44	0.00	0.56
Barren Land	0.00	0.00	0.00	0.00	1.00	1.00	1.00	0.00	0.00
Total	6.00	24.00	53.00	10.00	7.00	100.00	0.00	0.00	-
Producer Accuracy	0.83	0.29	0.92	0.70	0.14	0.00	0.69	0.00	-
Kappa	0.00	0.00	0.00	0.00	0.00	0.00	0.00	0.47	-
Error: Omission	0.17	0.71	0.08	0.30	0.86	-	-	-	

5.6. Built-up and Vegetative cover

As of March 8th, 2023, the Normalized Difference Built-up Index (NDBI) of Cochin municipality falls within the range of -0.35 to 0.31 and the Normalized Difference Vegetation Index (NDVI) of Cochin municipality falls within the range of -0.095 to 0.50 (Figure 21).

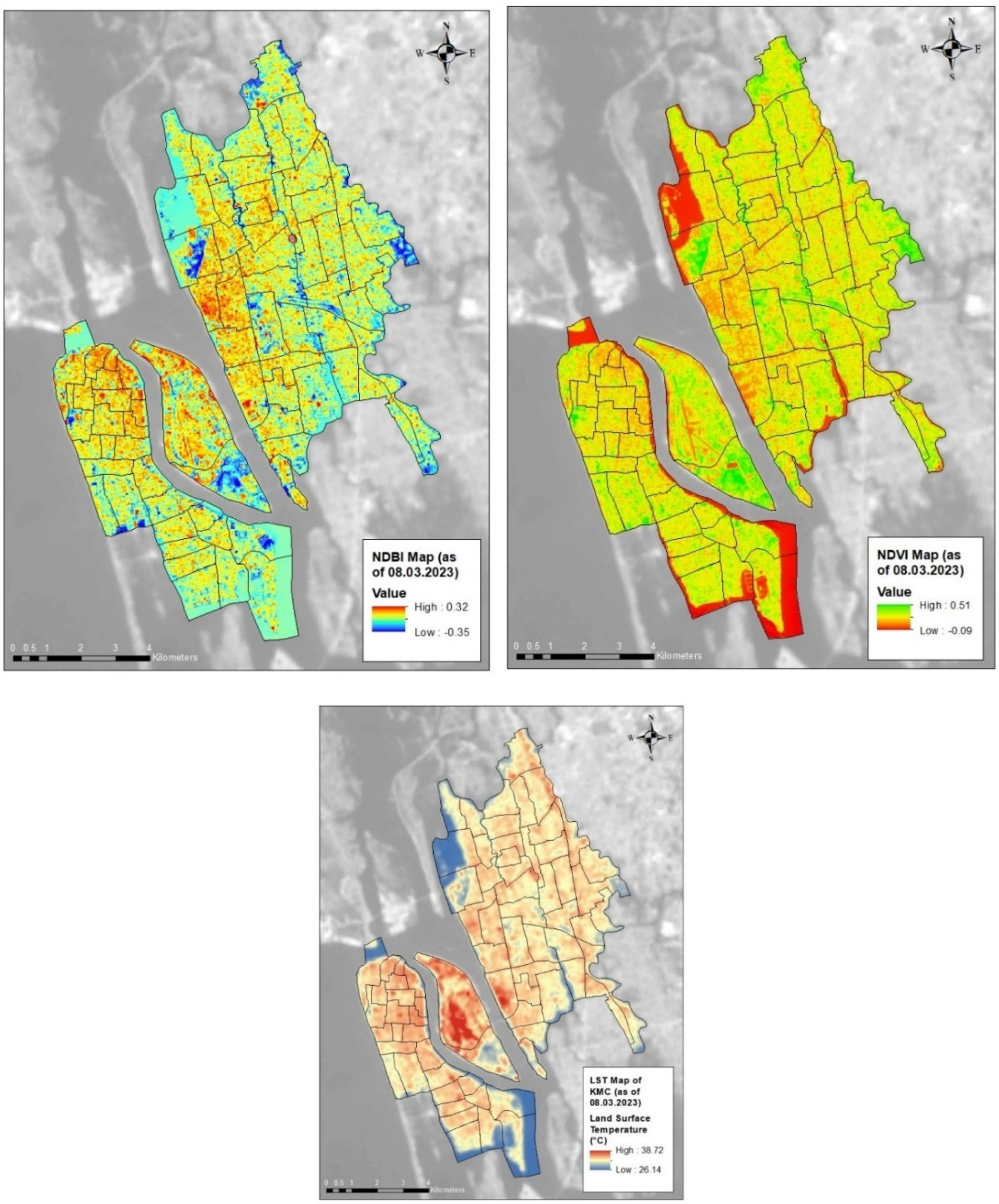

Figure 21: (On the top left) NDBI Map of KMC. (On the top right) NDBI Map of KMC. (On the bottom) Land Surface Temperature map of KMC as of 08.03.2023 for comparison (Source: Author)

5.7. LST Drivers - Ward-wise comparison

On ward-wise comparison, mean ward LST is positively correlated with mean ward NDBI (with a Pearsons' correlation co-efficient r of 0.53) and very weakly correlated with mean ward NDVI (with a Pearsons' correlation co-efficient r of 0.21) with an exception for Ward 29 (Figure 22). An analysis of mean Normalized Difference Vegetation Index (NDVI), Normalized Difference Built-up Index (NDBI), and Land Surface Temperature (LST) on a ward-wise basis reveals distinct patterns on the Willington Island. Specifically, the northern ward of the Willington Island exhibits high LST and NDBI values, indicating elevated temperatures and significant built-up or impervious surfaces characteristic of industrial areas. Conversely, the southern part of the island showcases high NDVI values, suggesting abundant vegetation cover and greenery. This spatial distribution aligns with the observed trait of the island, where the northern ward is dominated by industrial infrastructure, while the southern part boasts dense green spaces.

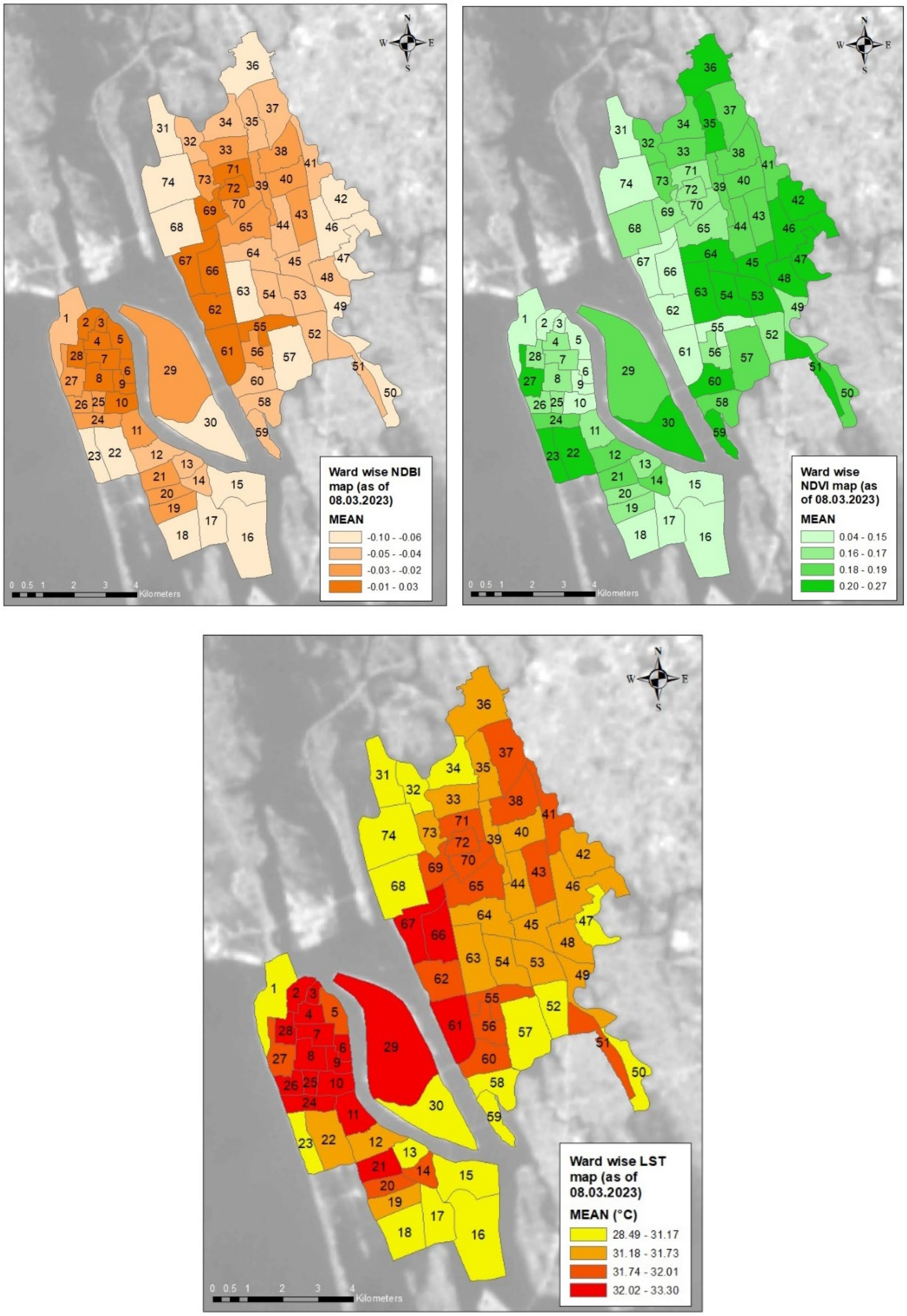

Figure 22: (On the top left) NDBI Map showing mean NDBI of each ward of KMC. (On the top right) NDVI Map showing mean NDVI of each ward of KMC. (On the bottom) LST map showing mean LST of each ward of KMC as of 08.03.2023for comparison (Source: Author)

Ward 30(south part of the Willington Island) has the lowest built-up percentage of 24.51% and Ward 3 has the highest built-up percentage of 96.2% with KMC having an average of 71.4% built-up area per ward. Wards 3, 9, and 66 have the lowest tree cover percentage of 0% and Ward 30 has the highest tree cover percentage of 39.15% with KMC having an average of 4.72% tree cover area per ward which is a low value. Ward 9 has the lowest green area percentage of 0.99% and Ward 30 has the highest green area percentage of 65.26% with KMC having an average of 21.14% green area per ward (Annexure 6, Figure 24).

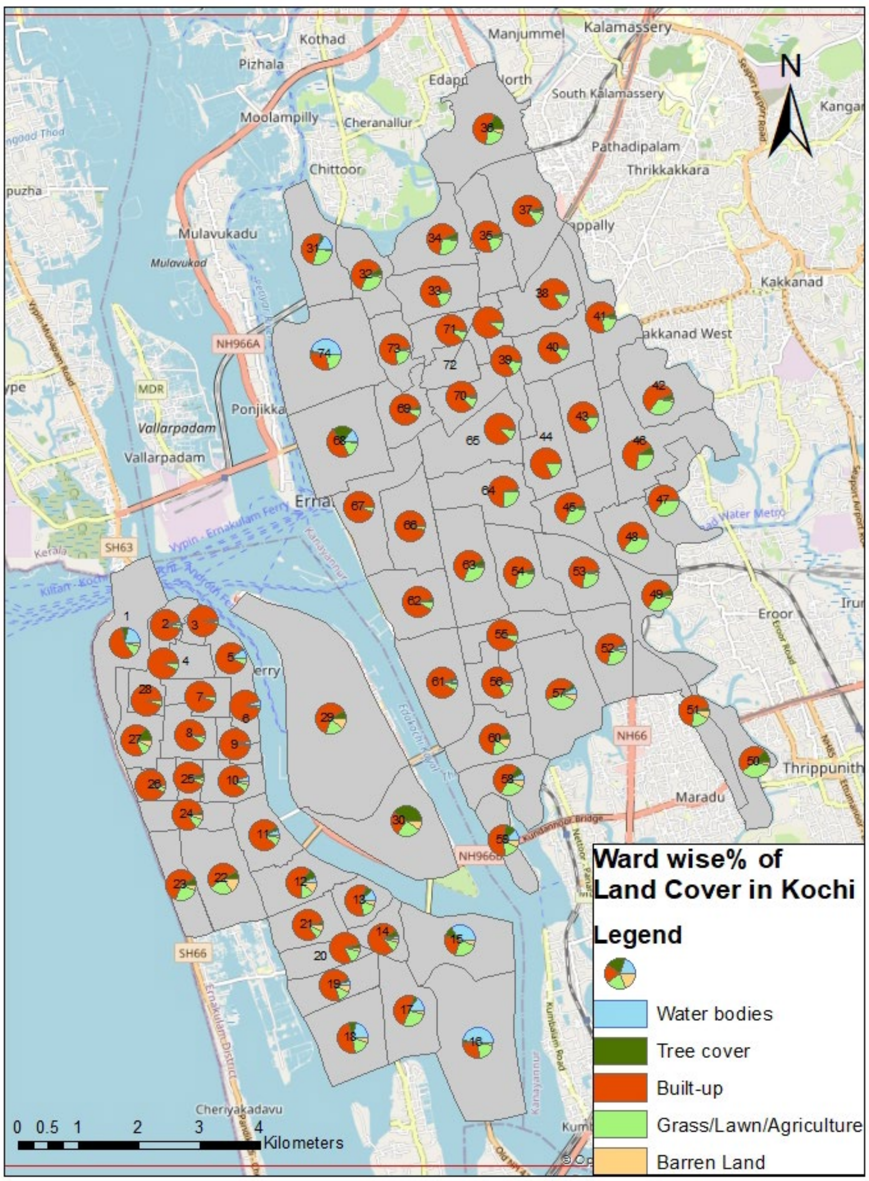

Figure 23: Map showing percentage land cover of each ward of KMC. (Source: Author)

Table 11: Table showing the Quartile classification of the Built-up percentage, Green Area (Tree cover + Grass/Lawn/Agriculture) percentage, Tree Cover percentage & Mean LST of each ward as of 08.03.2023 (Source: Author)

Built-up % Min	**Green Area % Min**	**Tree Cover % Min**	**LST Min**
24.51	0.99	0	28,48804219680
Built-up % 1st Quartile	**Green Area % 1st Quartile**	**Tree Cover % 1st Quartile**	**LST 1st Quartile**
60.57	10.62	1.28	31,15029564
Built-up % 2nd Quartile	**Green Area % 2nd Quartile**	**Tree Cover % 2nd Quartile**	**LST 2nd Quartile**
76.16	20.28	3.10	31,73298811
Built-up % 3rd Quartile	**Green Area % 3rd Quartile**	**Tree Cover % 3rd Quartile**	**LST 3rd Quartile**
86.54	31.22	6.21	32,0229009
Built-up % Max	**Green Area % Max**	**Tree Cover % Max**	**LST Max**
96.20	65.26	39.14	33,29799472540
Built-up % Mean	**Green Area % Mean**	**Tree Cover % Mean**	**LST Mean**
71.39	**21.14**	**4.72**	**29.29**

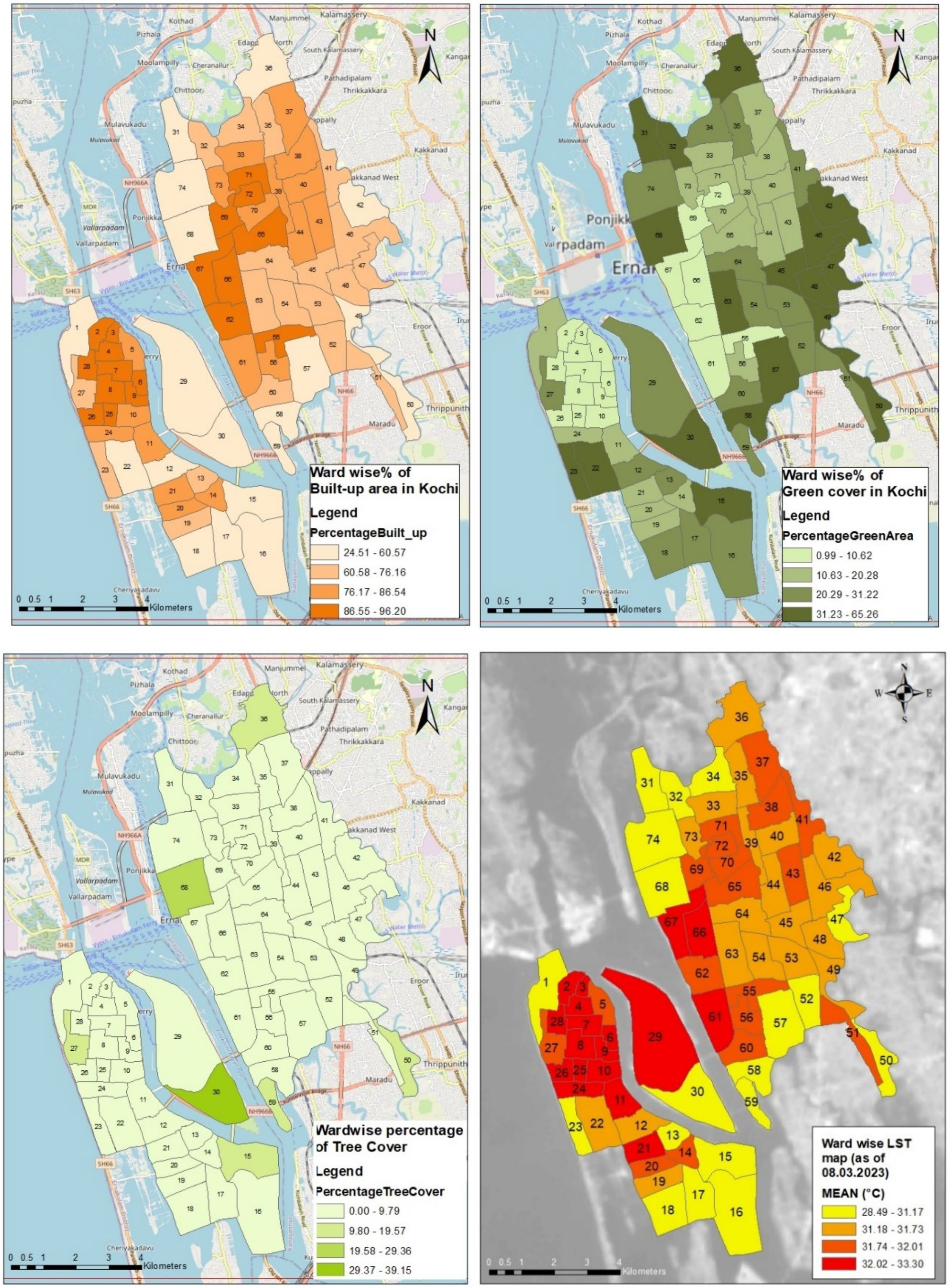

Figure 24:(On the top left) Map showing percentage Built-up of each ward of KMC. (On the top right) Map showing percentage Green Area of each ward of KMC. (On the bottom left) Map showing percentage Tree Cover of each ward of KMC. (On the bottom right) LST map showing mean LST of each ward of KMC as of 08.03.2023 for comparison (Source: Author)

From Figure 25, it is evident that Wards 1, 15, 16, 17, 18, 31, 68, and 74 has more than 12% of water bodies included in the ward bodies.

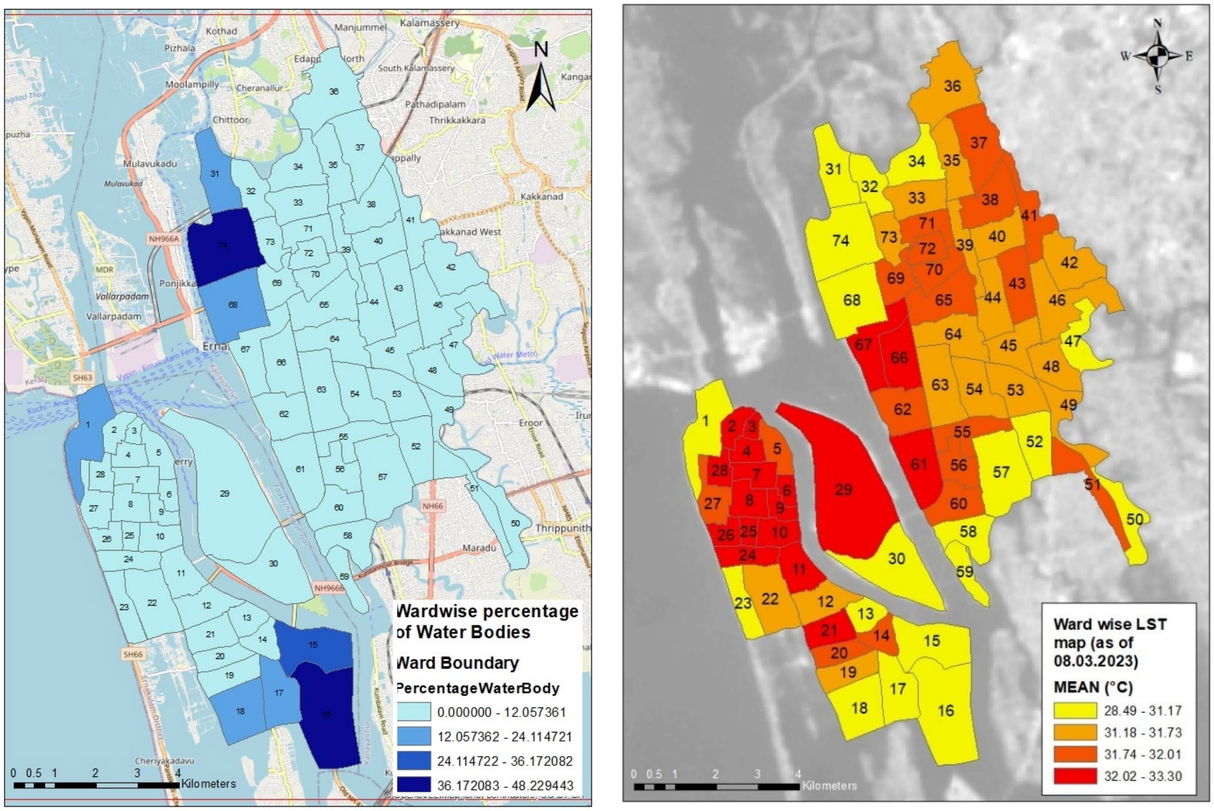

Figure 25: (On the left) Map showing percentage Water Bodies Cover of each ward of KMC. (On the right) LST map showing mean LST of each ward of KMC as of 08.03.2023 for comparison (Source: Author)

Table 12: Comparison of Land Cover of KMC observed with the literature study articles (N.B: The green cover is considered as all the vegetation added grass/agricultural land and lawns if not specifically classified as tree cover in the table) (Source: Author)

City	**% of Built-up area**	**% of Tree Cover**	**% of green area**	**% of Water Bodies**	**% of Barren Land /others**
Trivandrum, India	42.23		53.79	1.48	2.5
Kurunegala, Sri Lanka	10.8		54.1	0.7	34.3
Chittagong, Bangladesh	17.50	27.94	38.96	11.83	3.77
Hat Yai, Thailand					
Manila, Philippines	79.7		15.81	2.94	1.55

Mumbai, India	70.9	11.3	4.1	6.8	7.0
Pune, India	48	18	25	3	6
Kolhapur, India	-	-	-	-	-
Kochi, India	**65**	**6**	**19**	**6**	**4**

5.8. Correlation of LST with NDBI, NDVI, Built-up cover percentage, Tree Cover percentage and green cover percentage.

Upon the correlation between Land Surface Temperature (LST) and Normalized Difference Built-up Index (NDBI) through a scatterplot graph, a moderate positive correlation emerges with an R^2 value of 0.1678 and correlation coefficient (r - Pearsons's value) of 0.4059 (Figure 26).

The scatterplot analysis depicting the relationship between Land Surface Temperature (LST) and Normalized Difference Vegetation Index (NDVI) revealed a moderate negative correlation of 0.1924 (R^2), and correlation co-efficient of -0.4406 (r – Pearsons's value) (Figure 26).

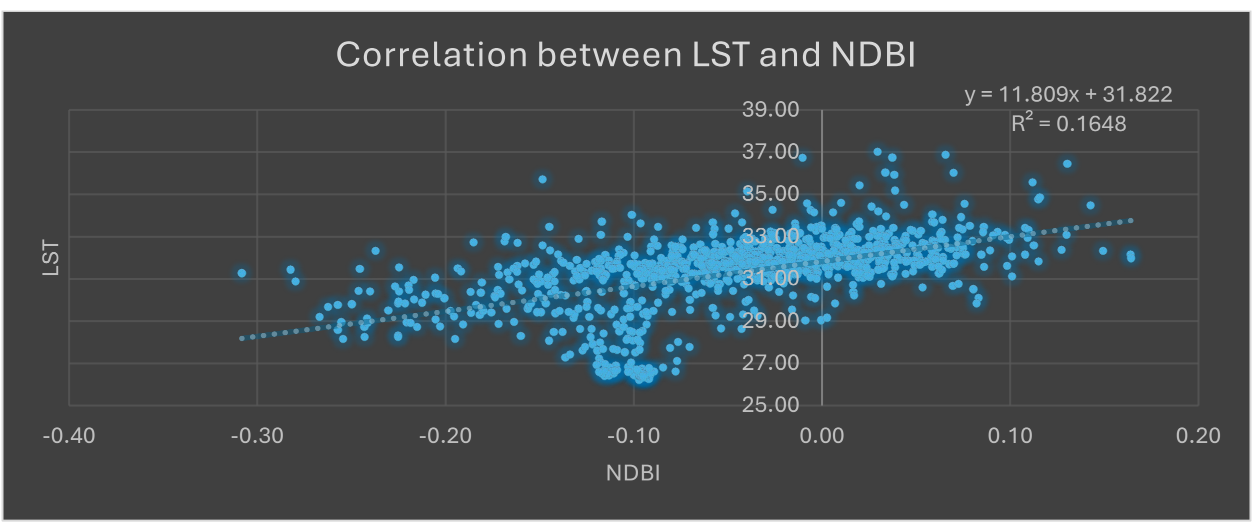

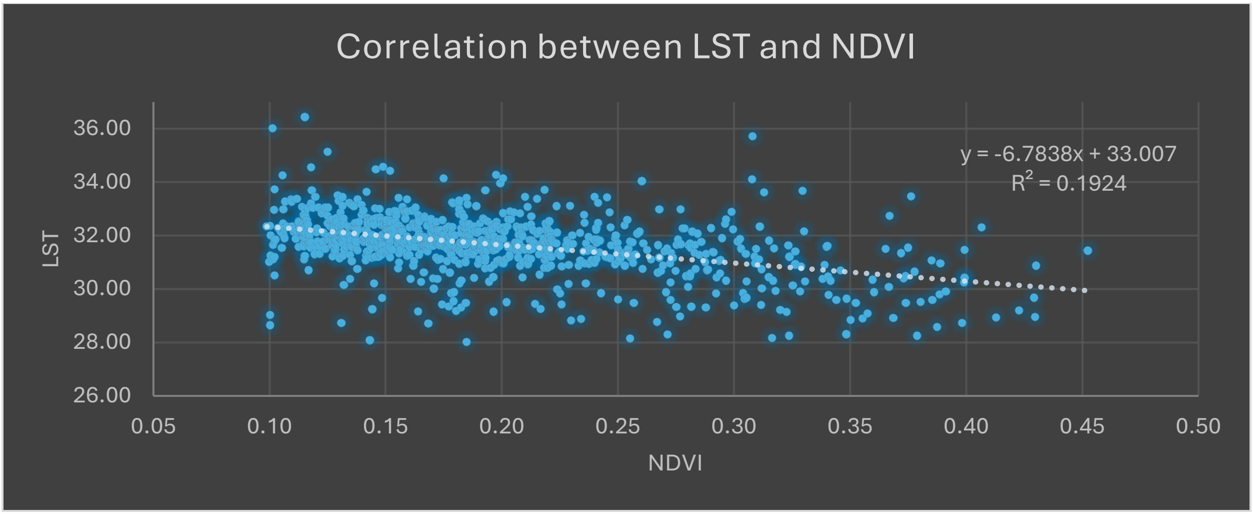

Figure 26: (Top) Scatterplot graph between LST and NDBI of KMC as of 08.03.2023. generated. (Bottom) Scatterplot graph between LST and NDVI of KMC as of 08.03.2023. (Source: Author)

From the scatterplot graphs in Figure 27 it is evident Built-up cover shows a strong positive correlation with LST with a correlation co-efficient (r-value) of 0.826 and R^2 value of 0.6823. The tree cover shows a weak negative correlation with LST with a correlation co-efficient (r-value) of -0.307 and an R^2 value of 0.0947. The green cover shows a moderate negative correlation with LST with a correlation co-efficient (r-value) of -0.563 and an R^2 value of 0.3169.

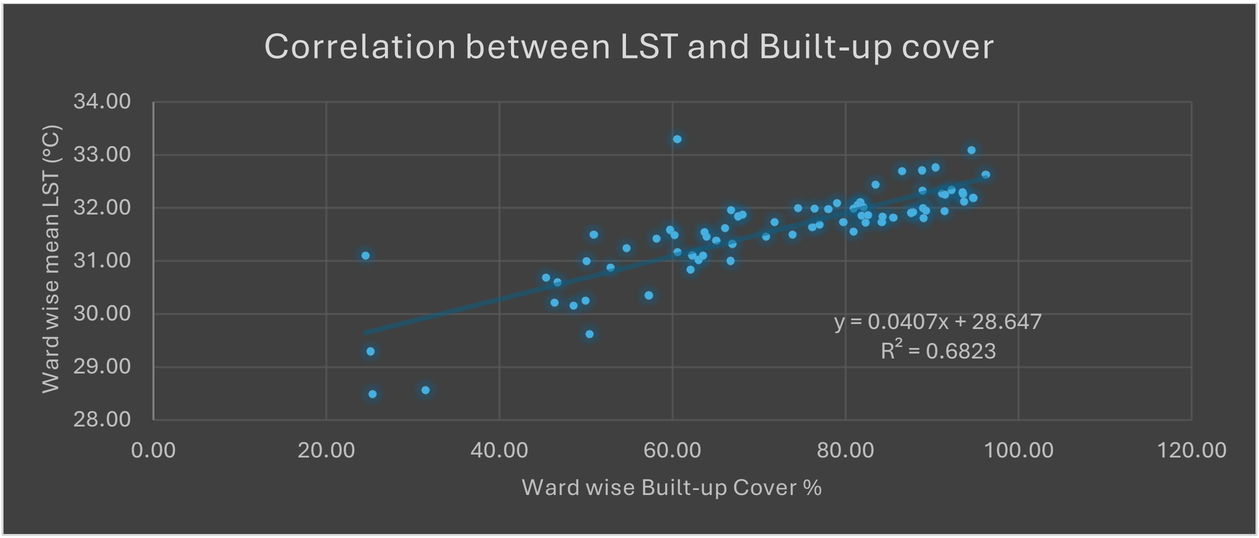

Figure 27: (Top)Scatterplot graph between ward-wise LST and ward-wise Built-up cover percentage of KMC as of 08.03. 2023.. (Middle)Scatterplot graph between ward-wise LST and ward-wise tree cover percentage

of KMC as of 08.03. 2023.. (Bottom)Scatterplot graph between ward-wise LST and ward-wise Green cover percentage of KMC as of 08.03.2023 (Source: Author)

The water body cover shows a fairly strong negative correlation with LST with a correlation co-efficient (r-value) of -0.79 and an R^2 value of 0.625. The barren soil cover shows a very weak negative correlation with LST with a correlation co-efficient (r-value) of -0.08 and an R^2 value of 0.0068 (Figure 28).

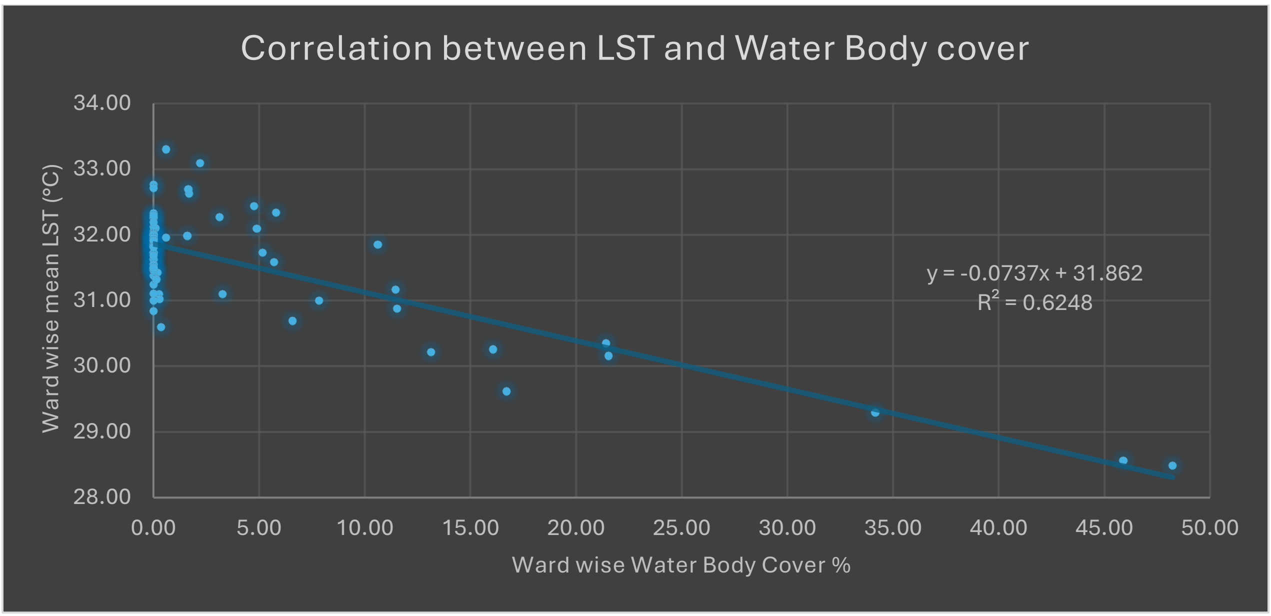

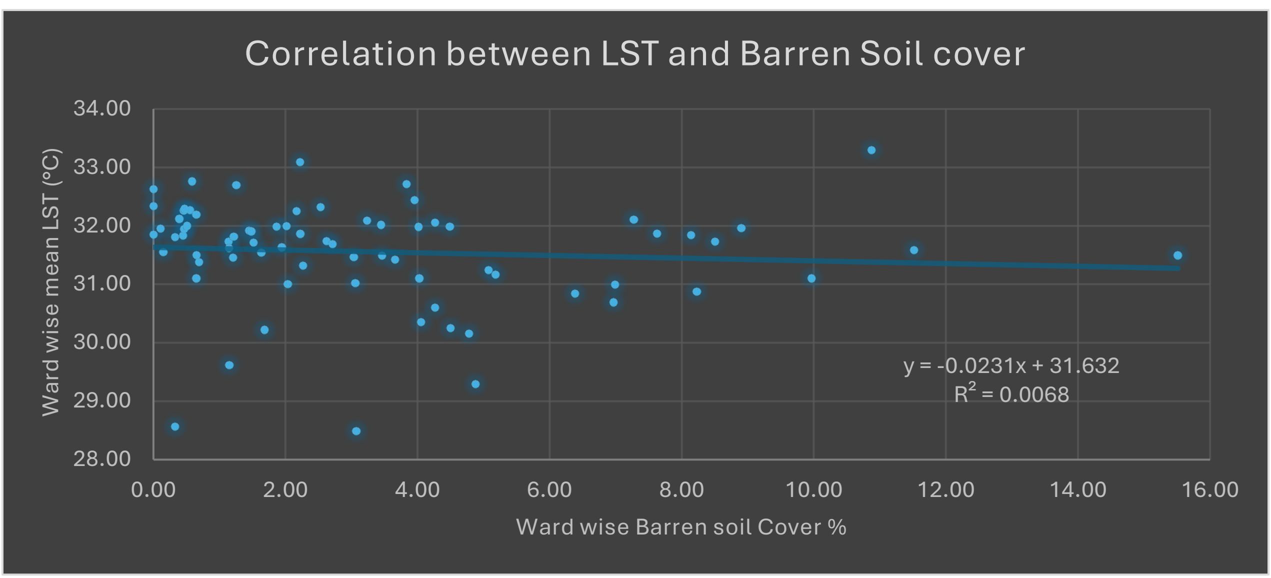

Figure 28: (Top)Scatterplot graph between ward-wise LST and ward-wise Water Body cover percentage of KMC as of 08.03. 2023.. (Bottom)Scatterplot graph between ward-wise LST and ward-wise Barren Soil cover percentage of KMC as of 08.03.2023 (Source: Author)

Table 13: Comparison of correlation co-efficient of LST with various LST drivers (Source: Author).

LST Drivers	**Method (Spatial Division)**	**Correlation co-efficient (R-Value) observed with LST**
NDBI	Fishnet	0.4059
NDVI	Fishnet	-0.4406
Built-up cover	Ward-wise	0.826
Tree Cover	Ward-wise	-0.307
Green cover (Tree Cover + Grass)	Ward-wise	-0.563
Water Bodies cover	Ward-wise	-0.79
Barren Soil cover	Ward-wise	-0.08

5.9. Impact of roads and activities on LST

Upon overlaying the main road networks from OSM over the LST maps showed an observation of higher LST aligning with the major roads like NH66, MG road (in wards 61, 62, and 66), and Banerji Road (wards 65 and 66) (Figure 29). On comparison between ward-wise road density and ward-wise mean LST map didn't showcase any considerable correlation between road density and LST (Figure 30).

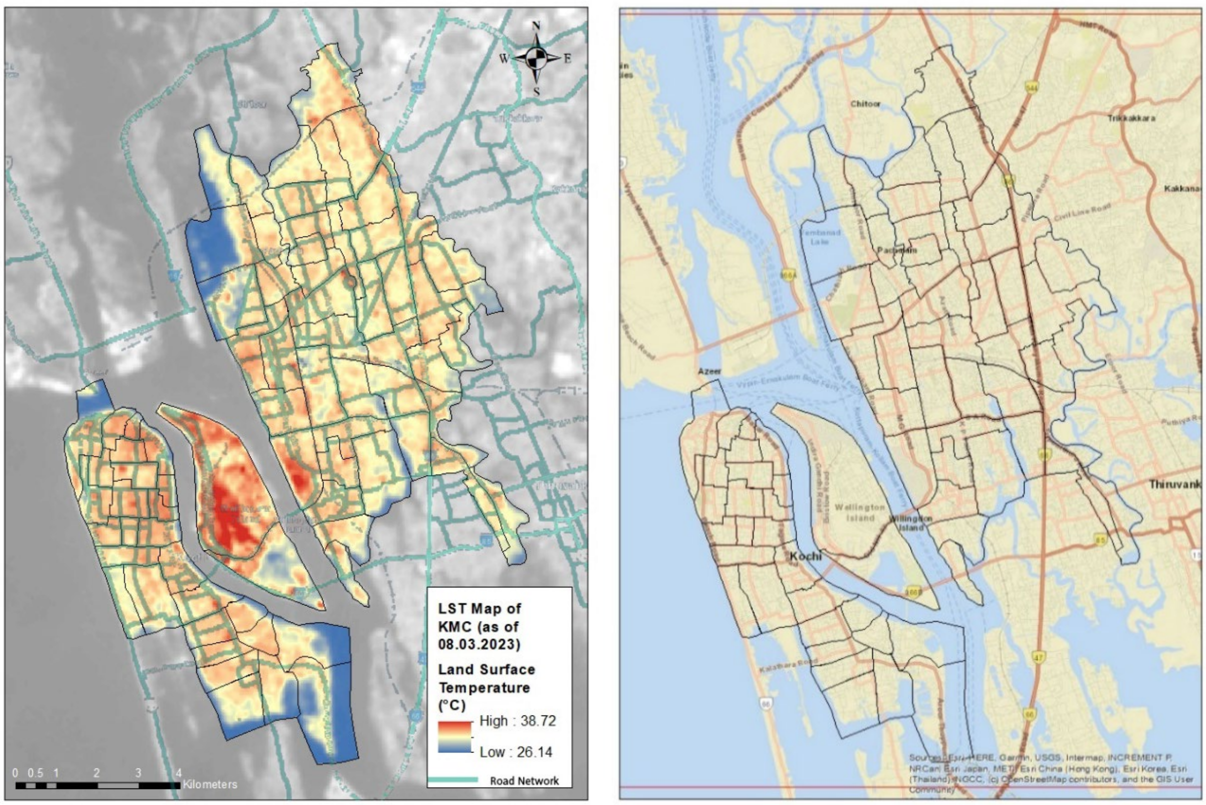

Figure 29: (On the left) Daytime Land Surface Temperature map of KMC overlayed with main road networks of Kochi as of 08.03.2023 (10:42 am Local Time). (On the right) Open Street map overlayed with municipal boundaries of Kochi for reference (Source: Author)

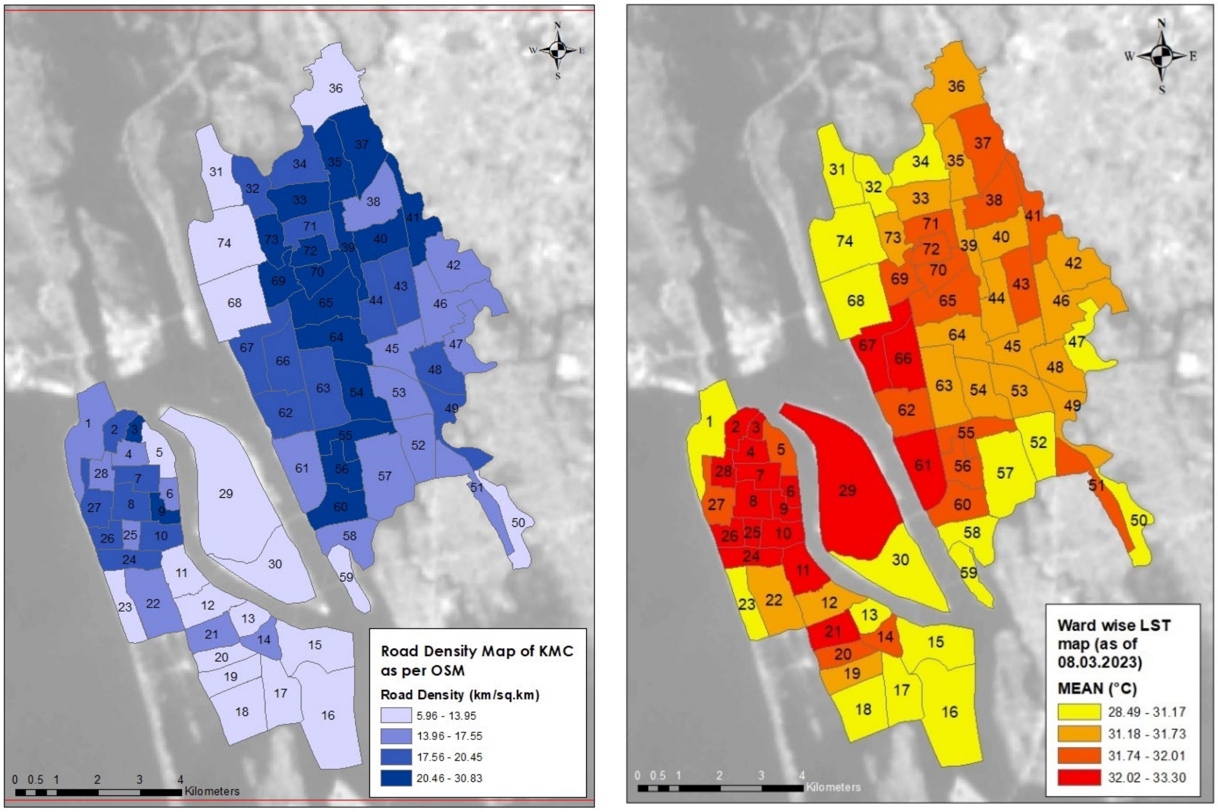

Figure 30: (On the left) Map showing Road density (km/sq.km.) of each ward of KMC. (On the right) LST map showing mean LST of each ward of KMC as of 08.03.2023 for comparison (Source: Author)

6. Discussion

The literature on LST in tropical monsoon cities has shown a gap in proposing specific actions for specific sites for LST-Reduction. The outcome and recommendations of those have been very general without spatially specific which would make the decision-making for planners difficult.

Also, the studies haven't been specific about the date and time at which the Landsat images have been retrieved thus reducing the possibility of analyzing an LST map of a city with its peak values.

This study has tried to overcome these limitations by statistically figuring out the warmest date range of the year and analyzing the data from those specific times.

Ward-wise analysis helps us to study Kochi by dividing it into geographical sub-units based on its homogenous land-use division. Also, this could make the outcome more usable and user-friendly for the planners and decision-makers to work on.

Figure 31: Map showing the Administrative boundary of KMC with 74 wards (Source: Author).

6.1. Findings 1 – Narrow Range of LST in Kochi

Kochi's Land Surface Temperature (LST) as determined by the study ranges from 26.13°C to 38.71°C, giving a total variation of 12.58°C. This range of variation aligns closely with the LST values observed in the case study of Kurunegala and Chittagong, while the rest of the case studies variation range was between 17.9°C - 37°C. This narrow range of LST for KMC (26.13°C-38.72°C) as of 08.03.2023. data generated by the analysis can be attributed to the following reasons:

- The time of acquisition of the Landsat 8 data (10:42 am Local time) is not the peak temperature hour of day which is between 12:00 pm and 15:00 pm in India (Climate Research & Services)
- Cochin has a more homogenous urban fabric when compared to other cities in the case study articles (Voogt & Oke, 2003).
- Errors or inaccuracies in the data processing steps.

6.2. Findings 2 – Green cover as an LST driver

KMC had a total green cover of 25% including tree cover (6%) and other vegetative covers (19%). The weak negative correlation between LST and NDVI (r-value: -0.4406) observed in the study of KMC didn't align with the results of literature case studies articles (Trivandrum: -0.503, Kurunegala: -0.91, Hat Yai: -0.505, Kolhapur: -0.954). The reason for this can be:

- The abundant impervious surfaces like concrete and asphalt have lower solar radiation reflectance(Voogt & Oke, 2003).
- The presence of water bodies (Arabian Sea and Vembanadu Lake) can produce a cooling effect (when included in the ward area) which can influence LST and affect its correlation between LST and NDVI.(Srivastava et al., 2012)

- Humidity and moisture content can affect the accuracy of NDVI and LST measurements.
- The lower spatial resolution (100m) of Landsat 8 may limit the detection of the sparse vegetation of Kochi and hence may not capture its impact in LST (Karnieli et al., 2010).

The percentage of Tree Cover in Kochi (6%) is very low in comparison with Pune, Mumbai and Chittagong case studies which may be due to a higher error of omission (0.71) in the LC map. This can be the reason for the really weak correlation between Mean Tree Cover percentage and Mean Ward LST (Pearsons's value: -0.307) as lower tree cover may not impact LST.

The ward-wise comparison between Mean Green Cover percentage (Percentage of tree cover and other vegetative cover in each ward) and Mean Ward LST showed a more acceptable correlation (with a moderate negative correlation of Pearsons' value: -0.563) in comparison to Trivandrum and Hat Yai case studies. However, it isn't a strong correlation, the main reason for this can attributed to the very low green cover of Cochin (25%) which is lower in comparison to the majority of the case studies except that of Mumbai (15.4%) and Manila (15.81%).

This can be easily understood from the tree cover and green cover maps and its classification (Figure 24). Except wards 15, 27, 30, 36, 50, 59, and 68, every other ward had a tree cover percentage of less than 19.57%. This low tree cover may not be enough to impact the LST in those wards. Norton et al. (2015) found that urban areas with at least 30% tree cover tend to experience noticeable cooling effects suggesting that a threshold of around 30% tree cover might be necessary for considerable temperature reductions (Norton et al., 2015).

Another study by Bowler et al. (2010) reviewed various urban green spaces and found that parks and areas with significant tree cover (around 20-40%) consistently showed lower LST compared to surrounding urban areas (Bowler et al., 2010).

The ward 30, despite being close to the industrial hub in Willington Island features 1st quartile mean LST values within Cochin Municipality. This can be attributed to the presence of dense green spaces (Tree cover of 39% and total green cover of 65% of the ward) on the southern part of the island, which contributes to local cooling effects and temperature moderation. The concentration of green cover in this area highlights the potential of vegetation in mitigating land surface temperature rise and enhancing environmental quality in urban settings.

From these observations, increasing the percentage of tree cover or green space above 20% can be used as an LST reduction technique for high mean LST class wards. Some Nature Based Solutions Strategies for achieving this can be:

- Parks and Green space restoration: Beninde J. et al. (2015) suggested restoring degraded parks and natural areas within cities can increase the quality and quantity of green spaces (Beninde et al., 2015).
- Green Corridors: Colding, J. (2007) proposed developing green corridors along transportation routes such as railways and highways can connect discrete green spaces and provide a continuous green cover (Colding, 2007).
- Green roofs and green walls: Oberndorfer, E, et al. (2007) suggested installing green roofs on buildings can create additional green spaces and contribute to urban biodiversity (Oberndorfer et al., 2007).
- Community Gardens and Urban Agriculture: Orsini, F., et al. (2013) opined encouraging urban agriculture on rooftops, in backyards, and community plots can increase the green cover along with producing local food (Orsini et al., 2013).

6.3. Findings 3 – Water bodies as an LST driver

The lowest LST is observed in the vicinity of Vembanadu Lake (Wards 16, 74, 15, 31, 18, 68, 17, 1), which traverses through the city, suggesting the moderating influence of water bodies on local temperature conditions. On further ward-wise analysis, a strong negative correlation of water body cover percentage and LST with a correlation co-efficient (r-value) of -0.79 reconfirms this observation. From (Figure 25), it is evident that wards with more than 12% water bodies showcased very low LST (in the 1st quartile LST).

A study by Li et al. (2013) found that urban water bodies have a considerable cooling effect on LST up to 200 meters from the source. They confirmed that even small water bodies constituting even 5% of the urban area can impact the LST (Li et al., 2009).

Sun and Chen (2012) also analyzed a similar observation that lakes covering even 5% of the urban area have a cooling effect of 2-3°C LST reduction within 200 meters extent (Sun & Chen, 2012).

From this we can conclude Increasing water body cover to 5-12% can be used as a LST reduction technique. Some Nature Based Solutions Strategies for achieving this can be:

- Stormwater Ponds and Retention Basins: Fletcher, T. et al. (2015) suggested creating stormwater ponds to manage runoff, reduce flooding, and provide urban water bodies that enhance local microclimates (Fletcher et al., 2015).
- Blue-green corridors: Mell, I. C. (2013) proposed integrating blue-green corridors that combine water spaces which enhance connectivity and ecological benefits (Mell, 2013).
- Urban Lakes and Ponds: Sun, R., et al. (2012) suggested creating new urban ponds in parks and residential areas to provide recreational opportunities and improve microclimate.

6.4. Findings 4 – External factors affecting LST

Another interesting finding was that the highest LST values are recorded in the industrial area situated on Willington Island (Ward 29), adjacent to the naval base and near the Port area in Kochi. The ward is surrounded by water bodies and the percentage of tree-cover and green cover of the ward are 9% and 28% respectively (Annexure 6) which are considerable fractions of land cover, suggesting that these LST drivers have a minimal impact specifically in the case of this ward. This can be due to external factors like industrial activities.

Voogt et al. (2003) suggested that industrial heat generation, high thermal conductive infrastructure material, and release of pollutants including greenhouse gases like CO2 can contribute to local warming affecting local climate and LST (Voogt & Oke, 2003).

High LST and NDBI alongside low LST with high NDVI in Willington Island's wards reveal varying land use: industrial activity in the north (ward 29) increases temperatures and decreases vegetation, whereas the greener south (ward 30) mitigates heat effects. Recognizing these differences is vital for land management, urban planning, and creating green infrastructure to improve environmental sustainability in Willington Island and Cochin Municipality.

Some Nature Based Solutions Strategies for LST reduction in industrial areas where neither green space nor water bodies can be implemented can be:

- Cool roofs and cool pavements: Akbari, H., et al. (2008) suggested using reflective materials for roofs will reflect more sunlight and absorb less heat. Applying permeable or reflective materials as pavements will reduce heat absorption (Akbari & Levinson, 2012).
- Permeable surfaces: Ferguson, B. K. (2005) recommended using permeable materials for sidewalks, parking lots and other paved areas will enhance water infiltration and reduce heat (Ferguson, 2006).

6.5. Findings 5 – Built-up cover as an LST driver

The high built-up area of Kochi (65%) indicates a significantly higher urbanization rate compared to other cities in Kerala (For comparison, Thiruvananthapuram, the capital city of Kerala has a 42.23% Urban area)(Anupriya & Rubeena, 2023).

The correlation between ward-wise built-up cover percentage and ward-wise mean LST has been observed as a strong positive one (with Pearsons's coefficient r: 0.826) (Table 13) indicating that built-up cover can increase the LST.

The observation that all the wards in the peak LST class except ward 29 (industrial/port area) has a minimum built-up cover of 80% (Annexure 6); reassures this finding.

Zhou, W., et al. (2011) have suggested that increased built-up areas are associated with higher LST due to materials used in construction and the reduction of vegetative cover, which provides the cooling effect through evapotranspiration (Zhou et al., 2011).

The minimum values of NDBI align closely with the findings of previous literature case studies.

However, notable disparities arise when comparing the maximum NDBI values. While the literature case studies report maximum NDBI values ranging from 0.47 to 0.8, indicating higher impervious surface coverage in case study areas, Cochin exhibits lower maximum NDBI values. This could mean that Cochin's maximum impervious area is less dense than those in the case studies. The reason for Kochi's maximum LST (38.71°C) being lower than the values observed in the literature case study of Indian cities (39.47°C – 50.5°C) can be due to this less dense Built-up area.

NBS strategies like cool roofs, cool pavements, and impervious pavements integrated into Built-up cover can be impactful in LST-reduction. Vertical development can also be a suitable guideline for future development to reduce the built-up coverage.

6.6. Findings 6 – Observed advantage of the Study Methodology

Cochin Municipality stands out for its highest minimum Land Surface Temperature (LST) when compared with case study areas (Trivandrum, Kurunegala, Chittagong, Hat Yai, Manila, Mumbai, Pune, Kolhapur), with values ranging from 19°C to 24°C. This indicates that even the lowest daytime temperature recorded in Cochin is relatively higher than the minimum temperatures observed in the areas examined in the case studies.

Conversely, the maximum LST values observed in Cochin fall within the range of results derived from the case study regions, suggesting similarities in the highest temperature extremes experienced across these areas.

These observations in comparison between the case studies (minimum and maximum LST) can be due to several factors:

- The time and date of Landsat data used in case studies may not be from the warmest (highest air temperature) decade of the year which is likely to exhibit peak LST values.
  In comparison to the case study articles, only the Kolhapur study has a minimum LST (24.06°C) close to Kochi's study (26.13°C). It is interesting to note that Kolhapur study's Landsat data was retrieved on 22 March 2009 (10:44 am Local Time) which is close to the peak temperature hours (12 pm -3 pm) in summer (Table 7). So, this observation can support the methodology used in Kochi's study to pinpoint the warmest decade of the year to study the peak LST conditions.
- Homogeneity of the urban fabric: Kochi may have a more homogenous urban fabric than the cities used in the case studies which will decrease the range of LST throughout Kochi. Zhou et sl. (2019) suggested that the homogeneous land cover types lead to less variability in surface temperatures (Zhou et al., 2011).

This finding suggests that studying the LST on the warmest day of the year can analyze the peak LST conditions in a city rather than retrieving the input data from a random day of the season. The day and time of retrieving the data is important for an LST study. However, there exists a limitation for Landsat data as the Landsat satellite offers an image of a city with a 16-day interval and at the same time always, which may not be the peak temperature hour of the day. This is due to the orbiting nature of Landsat satellites hovering over a specific zone and reaching the same zone after 16 days (Government, What are the acquisition schedules for the Landsat satellites?, n.d.).

6.7. Impacts of roads on LST

While overlaying the main road network with the LST map of Kochi, higher LST along NH66 as well as main roads like MG road (in wards 61, 62 and 66) and Banerji Road (wards 65 and 66) can be observed. This implies that roads may also impact the LST and increase urban heat with it.

But on a more detailed ward-wise road density analysis which included all the road networks in KMC and its comparison with LST couldn't generate a good correlation between them. Several other factors like road width, road materials, and traffic density can affect these results (From the first observation it was clear that it was the main roads with high traffic density that showcased higher LSTs).

6.8. Operational Implications

The operational implications of our findings are the following:

- The wards are 2, 3, 4, 6, 7, 8, 9, 10, 11, 21, 24, 25, 26, 28, 29, 61, 66, and 67 should be given the highest priority in the climate planning policy of KMC as their Mean LST lie over the 3rd quartile in LST analysis made.
- The wards 2,3,5,6,9,10,11,21,24,25,26, and 29 falls in the touristic zone, hence the heat rise here may impact the thermal comfort, thereby affecting the tourism economy.
- Ward 29 was analyzed with max mean LST among all the wards, these would be mainly due to the industrial and port activities happening on Willington Island. Cool roofs and reflective cool paints can be fruitful recommendations for mitigating the LST effects in industrial areas.
- Wards 61,66, and 67 are mainly commercial areas. The traffic density and activities are really high in these areas. This can be a reason for the high LST observed here.

- Most wards adjacent to Vembanadu Lake show low green cover and high built-up cover values due to lakefront development for tourism (lakefront's development) and port activities. This urban infrastructure that reduces vegetation cover, can be recommended to integrate green roofs to mitigate this effect.

If the strategic guidelines proposed are specific for each ward, then decision-making will be easier as local governance is one of the main reasons for the ward division in India. The following table (Table 14) shows the strategic guideline for each ward in the peak LST class to reduce the LST impacts:

Table 14: Table of Strategic recommendations for wards in the Peak LST class to achieve LST-Reduction. (Source: Author)

Ward No:	Major Land use	% Green Cover	% Water body	Recommended Strategies for LST-Reduction
2	Residential	5.17	3.14	• Increase Green Cover to 20% • Vertical development
3	Residential	2.11	1.69	• Increase Green Cover to 20% • Vertical development
4	Residential	9.00	0.00	• Increase Green Cover to 20% • Increase water body cover to 3-5% • Vertical development

6	Residential/ Educational	1.93	5.80	• Increase Green Cover to 20% • Vertical development
7	Residential/ Govt. Property	5.97	0.00	• Increase Green Cover to 20% • Vertical development
8	Residential/ Educational	7.30	0.00	• Increase Green Cover to 20% • Increase water body cover to 3-5% • Vertical development
9	Residential	0.99	2.22	• Increase Green Cover to 20% • Vertical development
10	Residential	7.78	4.77	• Increase Green Cover to 20% • Cool roofs and permeable pavements • Vertical development
11	Residential/ Commercial	12.84	4.90	• Increase Green Cover to 20% • Cool roofs and permeable pavements • Vertical development

21	Residential	10.92	0.11	• Increase Green Cover to 20% • Increase water body cover to 3-5% • Vertical development
24	Residential	14.34	0.00	• Increase water body cover to 3-5% • Cool roofs and permeable pavements • Vertical development
25	Residential	8.54	0.00	• Increase Green Cover to 20% • Increase water body cover to 3-5% • Vertical development
26	Residential	6.31	0.00	• Increase Green Cover to 20% • Increase water body cover to 3-5% • Vertical development
28	Residential/ Educational	5.89	0.00	• Increase Green Cover to 20% • Increase water body cover to 3-5% Vertical development

29	Industrial/ Transportation/ Govt. Property	27.95	0.60	• Increase water body cover to 3-5% • Cool roofs and permeable pavements • Vertical development
61	Govt. Property/ Commercial/ Residential	10.55	1.65	• Increase Green Cover to 20% • Cool roofs and permeable pavements • Vertical development
66	Commercial	4.57	0.00	• Increase Green Cover to 20% • Cool roofs and permeable pavements • Vertical development
67	Commercial	5.99	0.00	• Increase Green Cover to 20% • Cool roofs and permeable pavements • Vertical development

6.8.1. Proposals as per Kochi Master Plans aligning with operational implications

Transit-oriented development: TOD along the Metro route is proposed with the consideration of creating recreational green spaces (Figure 32) (Corporation, City Development Plan (CDP), 2023). This aligns with the operational implications we suggested for wards 61, 66 and 67 (Table 12). This also aligns with preliminary findings observed in road impact on LST.

Sponge city concept: Urban areas in KMC are proposed to be designed like giant sponges with considerations of creating engineered depressions, ponds etc. as NBS (Figure 32) (Corporation, City Development Plan (CDP), 2023). This aligns with the operational implications recommended for wards 21, 67 (Table 14).

Vertical Development: Setbacks from water bodies and wetlands on the site limit low-rise construction, necessitating high-rise buildings. Vertical development is favored to mitigate flood risks. Open spaces with nature-based solutions are essential to manage excess water flow (Corporation, City Development Plan (CDP), 2023). Hence vertical development (attaining minimum coverage and maximum FAR) is proposed in wards with high built-up area to mitigate its future effects which aligns with our operational implications (6.5).

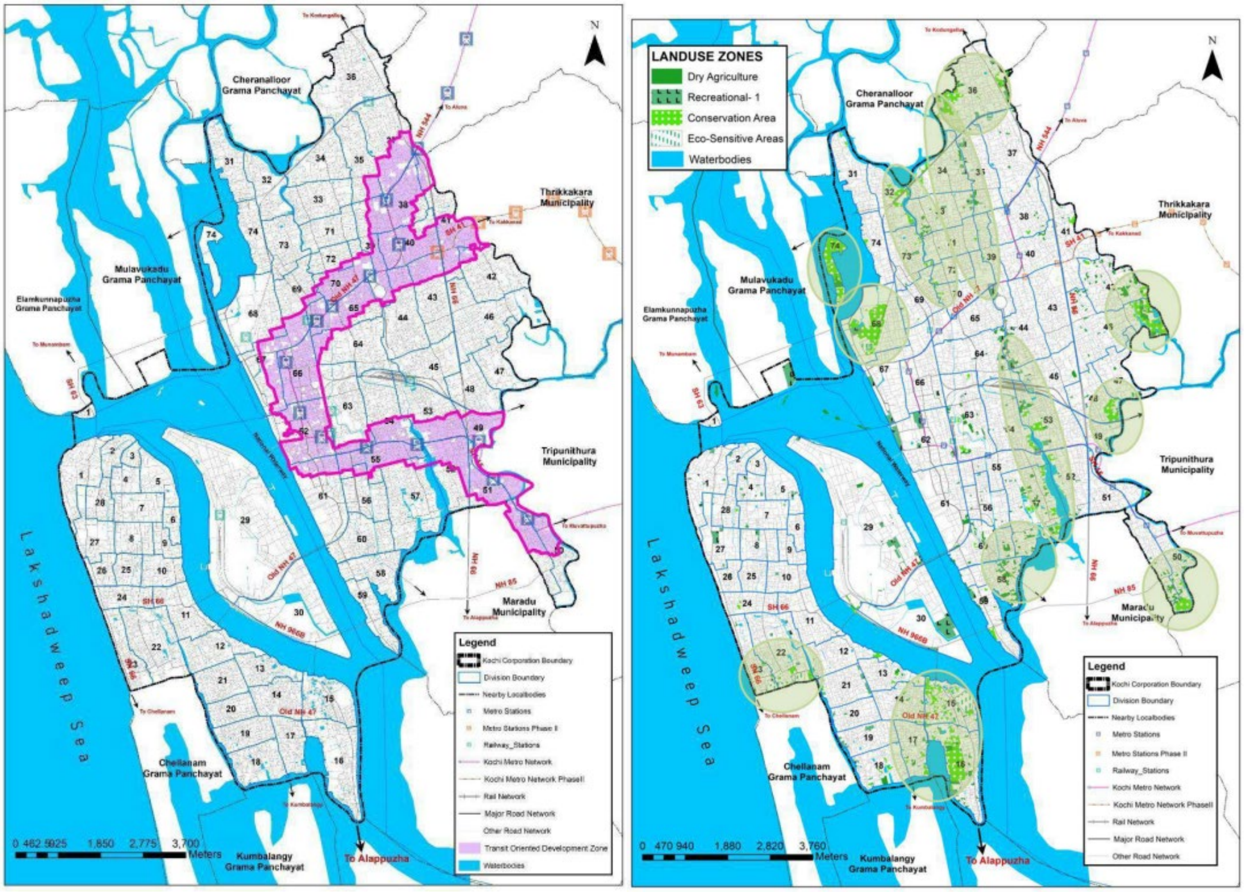

Figure 32: (On the left) Proposed Transit Oriented Development Corridor as per Kochi Master Plan. (On the right) Sponge city concept proposal spots as per Kochi Master Plan (Source: (Corporation, City Development Plan (CDP), 2023))

Other Guidelines ((Corporation, City Development Plan (CDP), 2023)):

- RESIDENTIAL USE ZONE: **Wells** and **irrigation ponds** incidental to community needs. **Plant nurseries**, pump houses, Urban agricultural facilitation centers, **Urban forestry** & **organic farming**, smoke houses or similar uses for agriculture value addition attached to a residential building, poultry farms, dairy, and kennels.
- COMMERCIAL USE ZONE: **Plant nursery,** storage of agricultural produces and seeds pump house, **wells,** and **irrigation ponds**. Dairy farm, Poultry farm. **Urban forestry & organic farming**, Urban agricultural facilitation center. Tot lots/**parks**/playgrounds.
- INDUSTRIAL USE ZONE: All industrial activities and modernization of existing industries with or without changing the built-up area to reduce heat production. **Parks** and Playgrounds attached to incidental residential use. **Urban forestry & organic farming.**

- TRANSPORTATION USE ZONE: **Parks and open spaces**, **Urban forestry & organic farming.**
- Ground coverage: The **maximum ground coverage** requirement for all plots and projects within the TOD influence zone shall be **60%** and a minimum 30% so as to ensure the urban form desirable for TOD.
- WATER BODIES: All existing water bodies shall be conserved.
- BUFFER (WATER BODIES): **Green patches, green belts, parks, open spaces, biodiversity gardens, bird sanctuaries, orchards, social forestry, beautification, landscaping** etc.
- For all new constructions, if pavements are provided on-site, **at least 50% of the total open space shall be left unpaved** or **paved with suitable materials enabling percolation of rainwater**.

6.9. Limitation of the study

The study used the Landsat data thereby limiting the time of analysis of LST to only late morning time (which excluded the peak temperature hour of the day) at which Landsat passes over the geographical zone of Kochi. This also limited the diurnal LST variation analysis in Kochi. The frequency of Landsat passing over the site is limited to 16 days and the Landsat data of the warmest day wasn't included in the Landsat inventory due to this 16-day interval limitation. The spatial resolution of Landsat 8 being limited to 100m for thermal image and 30m for spectral images also affected the accuracy of LST, LST-drivers, spectral indices and land cover used in the study. Although the study utilized municipal wards as spatial units, the size of these units varied and had unique characteristics that could impact LST. Several other factors like road width, roof materials, and road materials that could affect the LST were not considered as parameters.

In the context of changing climatic conditions, such as delayed onset of hot days (for example, in Torino, summer is typically expected from June 20 to September 22, but this year hot days haven't been observed until mid-July), the findings of the hottest decade require additional validation methods.

7. Conclusion

The studies on LST in tropical monsoon cities have analyzed the city as a whole single unit without considering any geographical sub-units. Hence the study results and recommendations proposed by them were too generic instead of being localized. These can be seen as a gap in research. Moreover, the time and date of retrieval of the satellite images were random from a season. Due to this, the results and solutions suggested by the studies may not be for the peak LST conditions faced by the city. This gap was also observed to be used as an area for research.

To address the above-mentioned gaps, a tropical monsoon city, Kochi on the southwestern coast of India was selected as the site for a research study of LST. Kochi, being one of the most urbanized cities in the state of Kerala, was an apt option for the study as there was an increasing need for addressing the heat rise in the city and how it affects the population there. A constant need for an LST reduction to mitigate the impacts of heat was observed in Cochin.

The study objective was to:

- To analyze spatial variations in land surface temperatures (LST) across different urban wards and identify LST hotspots within a Tropical monsoon city on the warmest days of the year.
- To figure out the LST drivers in the urban city.

This study started by pinpointing the warmest day of the year in Kochi statistically from the past 15 years' (2008-2023) air temperature data. After this, efforts were put to retrieve the Landsat image acquired during the warmest decade of the year (which was observed to be in the range of March 11- March 20) which didn't give fruitful results due to the limitations of the Landsat satellite. Hence, the data acquired during the closest date (08th March 2023) to the warmest decade was retrieved. After this, GIS was used to generate the LST maps, Spectral indices (NDVI, NDBI) maps, and other ward-wise LST drivers (Built-up cover, Tree cover, green cover, Water Body cover, Barren soil) maps of Kochi using the satellite images and were analyzed. Here wards were used as the minimum spatial unit of analysis as ward division had an administrative as well as land-use influence.

The findings indicated that the range of LST variation of KMC was very narrow compared to the literature case studies referred to, which can be due to the more homogeneous spatial nature or unique geographical character of KMC or due to the inaccuracies of the Landsat data. The green cover, built-up cover, and water bodies were the major LST drivers in KMC with just the industrial zone being an exception. Wards with at least 20% green cover showcased lower mean LST indicating the LST reduction nature of vegetative cover. Wards with more than 5% water bodies were observed to exhibit lower mean LST values which points out that water bodies can reduce LST. Wards with the highest mean LST values were found to have more than 79% built-up area, which indicates the built-up area is an essential contributor to LST.

Operational implications for the warmest wards suggested:

- Increasing the green cover by over 20% (green roofs, green walls, urban agriculture, green corridors, parks and green space restoration).
- Increasing the water body cover by over 3-5% (urban ponds, blue-green corridors, stormwater ponds and retention basins).
- Implementation of vertical development, cool roofs, and permeable and reflective pavements.

The minimum LST value observed in KMC was higher than that of the cities in the literature case study. This may be due to the selection criteria used in this study of retrieving the satellite image acquired on the warmest day of the year instead of a random day. The ward-wise analysis of LST drivers provided more fruitful results than using spectral indices like NDVI and NDBI for finding the correlation with LST.

The industrial/port zone (ward 29) showed a result (higher LST) entirely contrasting to the previously mentioned findings which opened to field for future research to increase the parameters studied as LST drivers by including land use, road width, roof materials, pavement materials etc. Also, a more detailed study on road networks as an LST driver considering other parameters like road width, traffic density and road materials can give more fruitful results. To overcome the limitations of Landsat data, other remote sensing sources like ECOSTRESS can be used for more spatial resolution data with higher resolution that can retrieved for any desirable time. These studies can provide a more accurate analysis and results. Given the changing climatic conditions, including delayed onset of hot days (e.g., this year in Torino, summer began unusually late, not until mid-July), the findings of the hottest decade necessitate supplementary validation methods.

As hypothesized, the peak LST conditions in KMC were able to be analyzed when satellite images were retrieved from the warmest day of the year within the limitation of Landsat. Analyzing LST by administrative units (Municipal wards in the case of KMC), rather than the entire city has helped the study provide ward-wise operational implications which will have very good utility in decision-making and urban planning for adapting to warm-spells.

This study emphasizes how crucial localized analysis is to comprehend the dynamics of LST in tropical monsoon towns like Kochi. The results support the use of nature-based remedies in ward-specific interventions to successfully lower LST. Furthermore, by using higher resolution remote sensing methods and examining a wider range of LST affecting factors, the work highlights the potential for more precise future research.

Bibliography

Abdullah, S., Barua, D., Abdullah, S. M. A., & Rabby, Y. W. (2022). Investigating the Impact of Land Use/Land Cover Change on Present and Future Land Surface Temperature (LST) of Chittagong, Bangladesh. *Earth Systems and Environment*, *6*(1). https://doi.org/10.1007/s41748-021-00291-w

Akbari, H., & Levinson, R. (2012). Evolution of cool-roof standards in the US. In *Advances in Building Energy Research: Volume 3*. https://doi.org/10.3763/aber.2008.0201

Almadrones-Reyes, K. J., & Dagamac, N. H. A. (2023). Land-use/land cover change and land surface temperature in Metropolitan Manila, Philippines using landsat imagery. *GeoJournal*, *88*(2). https://doi.org/10.1007/s10708-022-10701-9

Anupriya, R. S., & Rubeena, T. A. (2023). Spatio-temporal urban land surface temperature variations and heat stress vulnerability index in Thiruvananthapuram city of Kerala, India. *Geology, Ecology, and Landscapes*. https://doi.org/10.1080/24749508.2023.2182088

Arnfield, A. J. (2003). Two decades of urban climate research: A review of turbulence, exchanges of energy and water, and the urban heat island. *International Journal of Climatology*, *23*(1). https://doi.org/10.1002/joc.859

Beck, H. E., Zimmermann, N. E., McVicar, T. R., Vergopolan, N., Berg, A., & Wood, E. F. (2020). Present and future Koppen-Geiger climate classification maps at 1-km resolution (vol 5, 180214, 2018). *SCIENTIFIC DATA*, *7*(1).

Beninde, J., Veith, M., & Hochkirch, A. (2015). Biodiversity in cities needs space: A meta-analysis of factors determining intra-urban biodiversity variation. In *Ecology Letters* (Vol. 18, Issue 6). https://doi.org/10.1111/ele.12427

Bowler, D. E., Buyung-Ali, L., Knight, T. M., & Pullin, A. S. (2010). Urban greening to cool towns and cities: A systematic review of the empirical evidence. In *Landscape and Urban Planning* (Vol. 97, Issue 3). https://doi.org/10.1016/j.landurbplan.2010.05.006

Colding, J. (2007). "Ecological land-use complementation" for building resilience in urban ecosystems. *Landscape and Urban Planning*, *81*(1–2). https://doi.org/10.1016/j.landurbplan.2006.10.016

Dousset, B., & Gourmelon, F. (2003). Satellite multi-sensor data analysis of urban surface temperatures and landcover. *ISPRS Journal of Photogrammetry and Remote Sensing*, *58*(1–2). https://doi.org/10.1016/S0924-2716(03)00016-9

Ferguson, B. K. (2006). Porous Pavements : the Making of Progress in Technology and Design. *International Conference on Concrete Block Paving*.

Fletcher, T. D., Shuster, W., Hunt, W. F., Ashley, R., Butler, D., Arthur, S., Trowsdale, S., Barraud, S., Semadeni-Davies, A., Bertrand-Krajewski, J. L., Mikkelsen, P. S., Rivard, G., Uhl, M., Dagenais, D., & Viklander, M. (2015). SUDS, LID, BMPs, WSUD and more – The evolution and application of terminology surrounding urban drainage. *Urban Water Journal*, *12*(7). https://doi.org/10.1080/1573062X.2014.916314

Gohain, K. J., Mohammad, P., & Goswami, A. (2021). Assessing the impact of land use land cover changes on land surface temperature over Pune city, India. *Quaternary International*, *575–576*. https://doi.org/10.1016/j.quaint.2020.04.052

Government of Kerala., & StatePlanningBoard. (2017). Economic Review 2017 | State Planning Board, Thiruvananthapuram, Kerala, India. In *Economics review,*.

Guha, S., Govil, H., Dey, A., & Gill, N. (2018). Analytical study of land surface temperature with NDVI and NDBI using Landsat 8 OLI and TIRS data in Florence and Naples city, Italy. *European Journal of Remote Sensing*, *51*(1). https://doi.org/10.1080/22797254.2018.1474494

Guha, S., Govil, H., Gill, N., & Dey, A. (2020). Analytical study on the relationship between land surface temperature and land use/land cover indices. *Annals of GIS*, *26*(2). https://doi.org/10.1080/19475683.2020.1754291

IPCC. (2014). IPCC Climate Change 2014: Fifth Assessment Report. In *Intergovernmental Panel on Climate Change*.

Irons, J. R., Dwyer, J. L., & Barsi, J. A. (2012). The next Landsat satellite: The Landsat Data Continuity Mission. *Remote Sensing of Environment*, *122*. https://doi.org/10.1016/j.rse.2011.08.026

Jensen, J. R. (2009). Remote Sensing of the Environment: An Earth Resource Perspective, 2nd Ed. *Prentice Hall, Upper Saddle River, NJ*.

Karnieli, A., Agam, N., Pinker, R. T., Anderson, M., Imhoff, M. L., Gutman, G. G., Panov, N., & Goldberg, A. (2010). Use of NDVI and land surface temperature for drought assessment: Merits and limitations. *Journal of Climate*, *23*(3). https://doi.org/10.1175/2009JCLI2900.1

Li, J. juan, Wang, X. rong, Wang, X. jun, Ma, W. chun, & Zhang, H. (2009). Remote sensing evaluation of urban heat island and its spatial pattern of the Shanghai metropolitan area, China. *Ecological Complexity*, *6*(4). https://doi.org/10.1016/j.ecocom.2009.02.002

Mell, I. C. (2013). Can you tell a green field from a cold steel rail? Examining the "green" of Green Infrastructure development. *Local Environment*, *18*(2). https://doi.org/10.1080/13549839.2012.719019

Menon, S., Akbari, H., Mahanama, S. ., Sednev, I., & Levinson, R. (2010). Radiative forcing and temperature response to changes in urban albedos and associated CO2 offsets. *Environmental Research Letters*, *5*(1).

Nandi, N., & Dede, M. (2022). Urban Heat Island Assessment using Remote Sensing Data in West Java, Indonesia: From Literature Review to Experiments and Analyses. *Indonesian Journal of Science and Technology*, *7*(1). https://doi.org/10.17509/ijost.v7i1.44146

Norton, B. A., Coutts, A. M., Livesley, S. J., Harris, R. J., Hunter, A. M., & Williams, N. S. G. (2015). Planning for cooler cities: A framework to prioritise green infrastructure to mitigate high temperatures in urban landscapes. *Landscape and Urban Planning*, *134*. https://doi.org/10.1016/j.landurbplan.2014.10.018

Oberndorfer, E., Lundholm, J., Bass, B., Coffman, R. R., Doshi, H., Dunnett, N., Gaffin, S., Köhler, M., Liu, K. K. Y., & Rowe, B. (2007). Green roofs as urban ecosystems:

Ecological structures, functions, and services. In *BioScience* (Vol. 57, Issue 10). https://doi.org/10.1641/B571005

Orsini, F., Kahane, R., Nono-Womdim, R., & Gianquinto, G. (2013). Urban agriculture in the developing world: A review. In *Agronomy for Sustainable Development* (Vol. 33, Issue 4). https://doi.org/10.1007/s13593-013-0143-z

Peel, M. C., Finlayson, B. L., & McMahon, T. A. (2007). Updated world map of the Köppen-Geiger climate classification. *Hydrology and Earth System Sciences*, *11*(5). https://doi.org/10.5194/hess-11-1633-2007

Ramesh, B., & Gurukkal, R. (2007). Forest landscapes of the southern western Ghats, India. *Https://Doi.Org/10.4000/Books.Ifp.6846*, *1-*.

Ranagalage, M., Ratnayake, S. S., Dissanayake, D. M. S. L. B., Kumar, L., Wickremasinghe, H., Vidanagama, J., Cho, H., Udagedara, S., Jha, K. K., Simwanda, M., Phiri, D., Perera, E. N. C., & Muthunayake, P. (2020). Spatiotemporal variation of urban heat islands for implementing nature-based solutions: A case study of kurunegala, Sri Lanka. *ISPRS International Journal of Geo-Information*, *9*(7). https://doi.org/10.3390/ijgi9070461

Ruthirako, P., Darnsawasdi, R., & Chatupote, W. (2015). Intensity and pattern of land surface temperature in Hat Yai City, Thailand. *Walailak Journal of Science and Technology*, *12*(1).

Sahana, M., Dutta, S., & Sajjad, H. (2019). Assessing land transformation and its relation with land surface temperature in Mumbai city, India using geospatial techniques. *International Journal of Urban Sciences*, *23*(2). https://doi.org/10.1080/12265934.2018.1488604

Srivastava, A. K., Tripathi, S. N., Dey, S., Kanawade, V. P., & Tiwari, S. (2012). Inferring aerosol types over the Indo-Gangetic Basin from ground based sunphotometer measurements. *Atmospheric Research*, *109–110*. https://doi.org/10.1016/j.atmosres.2012.02.010

Sun, R., & Chen, L. (2012). How can urban water bodies be designed for climate adaptation? *Landscape and Urban Planning*, *105*(1–2). https://doi.org/10.1016/j.landurbplan.2011.11.018

Tanaji, P. P., Ajit, C. V., & Vishnu, D. S. (2021). Urban weather assessment using LST, NDBI and NDVI of Kolhapur city, Maharashtra. *Disaster Advances*, *14*(4).

Tiepolo, M., Galligari, A., Tonolo, F. G., Moretto, E., & Stefani, S. (2023). LST-R: A method for assessing land surface temperature reduction in urban, hot and semi-arid Global South. *MethodsX*, *10*. https://doi.org/10.1016/j.mex.2022.101977

Tran, D. X., Pla, F., Latorre-Carmona, P., Myint, S. W., Caetano, M., & Kieu, H. V. (2017). Characterizing the relationship between land use land cover change and land surface temperature. *ISPRS Journal of Photogrammetry and Remote Sensing*, *124*. https://doi.org/10.1016/j.isprsjprs.2017.01.001

US EPA. (2013). Reducing Urban Heat Islands: Compendium of Strategies | Heat Island Effect | US EPA. *Us Epa*.

Voogt, J. A., & Oke, T. R. (2003). Thermal remote sensing of urban climates. *Remote Sensing of Environment*, *86*(3). https://doi.org/10.1016/S0034-4257(03)00079-8

Weng, Q., Rajasekar, U., & Hu, X. (2011). Modeling urban heat islands and their relationship with impervious surface and vegetation abundance by using ASTER images. *IEEE Transactions on Geoscience and Remote Sensing*, *49*(10 PART 2). https://doi.org/10.1109/TGRS.2011.2128874

Xu, H. (2006). Modification of normalised difference water index (NDWI) to enhance open water features in remotely sensed imagery. *International Journal of Remote Sensing*, *27*(14). https://doi.org/10.1080/01431160600589179

Zha, Y., Gao, J., & Ni, S. (2003). Use of normalized difference built-up index in automatically mapping urban areas from TM imagery. *International Journal of Remote Sensing*, *24*(3). https://doi.org/10.1080/01431160304987

Zhang, X., Friedl, M. A., Schaaf, C. B., Strahler, A. H., Hodges, J. C. F., Gao, F., Reed, B. C., & Huete, A. (2003). Monitoring vegetation phenology using MODIS. *Remote Sensing of Environment*, *84*(3). https://doi.org/10.1016/S0034-4257(02)00135-9

Zhou, W., Huang, G., & Cadenasso, M. L. (2011). Does spatial configuration matter? Understanding the effects of land cover pattern on land surface temperature in urban landscapes. *Landscape and Urban Planning*, *102*(1). https://doi.org/10.1016/j.landurbplan.2011.03.009

Berman, J. J. (2016). *Pearson Correlation*. Retrieved from ScienceDirect: https://www.sciencedirect.com/topics/computer-science/pearson-correlation

Britannica, T. E. (2024). *Kochi, India*. Retrieved from www.britannica.com: https://www.britannica.com/place/Kochi-India

Climate Research & Services, I. M. (n.d.). *DATA SUPPLY PORTAL.* Retrieved from https://dsp.imdpune.gov.in/: https://dsp.imdpune.gov.in/

Corporation, K. M. (2022, February). *Kochi Municipal Corporation Annual Report 2018-2019.* Retrieved from kochicorporation.lsgkerala.gov.in: https://kochicorporation.lsgkerala.gov.in/system/files/2022-02/KMC_annual_Report_2018-19.pdf

Corporation, K. M. (2023). *City Development Plan (CDP)*. Retrieved from c-hed.org: https://c-hed.org/city-development-plan-cdp/

Editor, T. N. (2024, February 20). *experts call for caution as mercury level soars in Kochi*. Retrieved from newindianexpress.com: https://www.newindianexpress.com/states/kerala/2024/Feb/20/experts-call-for-caution-as-mercury-level-soars-in-kochi

ESRI. (n.d.). *EarthExplorer*. Retrieved from USGS: https://earthexplorer.usgs.gov/

FERNANDO, J. (2024, February 07). *The Correlation Coefficient: What It Is and What It Tells Investors*. Retrieved from Investopedia: https://www.investopedia.com/terms/c/correlationcoefficient.asp

Geodiode. (2011, September 12). *Tropical monsoon and tropical savannah*. Retrieved from geodiode.com: https://geodiode.com/climate/tropical-monsoon-and-tropical-savannah/

Giscrack. (2024). *Geographic Information Systems (GIS)*. Retrieved from giscrack: https://giscrack.com/

Government, U. S. (n.d.). *Landsat Missions*. Retrieved from USGS: https://www.usgs.gov/landsat-missions

Government, U. S. (n.d.). *What are the acquisition schedules for the Landsat satellites?* Retrieved from USGS: https://www.usgs.gov/faqs/what-are-acquisition-schedules-landsat-satellites#:~:text=Each%20satellite%20makes%20a%20complete,scene%20area%20on%20the%20globe.

Kochi Municipal Corporation, G. o. (2024). *History*. Retrieved from kochicorporation.lsgkerala.gov.in: https://kochicorporation.lsgkerala.gov.in/en/history/8

koeppen-geiger. (n.d.). *Koppen 1936*. Retrieved from koeppen-geiger.vu-wien.ac.at: https://koeppen-geiger.vu-wien.ac.at/pdf/Koppen_1936.pdf

Maxwell, R. (2013, April 17). *Landsat 8*. Retrieved from geographyrealm.com: https://www.geographyrealm.com/landsat-8/#:~:text=The%20satellite%20has%20sensors%20that,at%2060%20meter%20spatial%20resolution.

Ministry of Earth Sciences, N. D. (n.d.). *Radar - Kochi*. Retrieved from mausam.imd.gov.in: https://mausam.imd.gov.in/imd_latest/contents/index_radar.php?id=Kochi

Missions, L. (n.d.). *Landsat Acquisitions*. Retrieved from usgs.gov: https://www.usgs.gov/landsat-missions/landsat-acquisitions#:~:text=Nighttime%2C%20open%20ocean%2C%20and%20ascending,are%20approved%20and%20are%20acquired

NASA. (2009, November 18). *The Sorting Problem*. Retrieved from Earth Observatory: https://earthobservatory.nasa.gov/features/GlobalLandSurvey/page2.php#:~:text=In%202003%2C%20a%20part%20of,the%20data%20from%20each%20image.

Ramey, D., Rose, L., & Tyerman, L. (1995). *Alias/WaveFront Material (.mtl) File Format*. Retrieved from fileformat.info: https://www.fileformat.info/format/material

S, A. (2024, May 8). *Kerala's heat waves a sign of climate change's unequal impact*. Retrieved from policycircle.org: https://www.policycircle.org/environment/severe-heat-wave-kerala/

School, W. S. (2018, June 18). *Evapotranspiration and the Water Cycle*. Retrieved from https://www.usgs.gov/: https://www.usgs.gov/special-topics/water-science-school/science/evapotranspiration-and-water-cycle#:~:text=Evapotranspiration%20is%20the%20sum%20of,atmosphere%20via%20evaporation%20and%20transpiration.

State Election Commission, K. (n.d.). *Delimitation*. Retrieved from www.sec.kerala.gov.in: https://www.sec.kerala.gov.in/portal/kc/delimit

State Election Commission, K. (n.d.). *https://www.sec.kerala.gov.in.* Retrieved from www.sec.kerala.gov.in`: https://www.sec.kerala.gov.in/portal/resources/downloadAttachment/ea78b52a-d647-4d8b-8d01-c741f350943c

Annexure

Annexure A

Annexure 1: Table showing the average of daily maximum and minimum temperature(°C) from 15 years data (2008-2023) of each month (Source: Author; Data Source: DSP https://dsp.imdpune.gov.in/)

Month	Average of Temp. MAX	Average of Temp. MIN
January	33,73	21,04
February	34,67	22,19
March	34,96	23,99
April	34,36	24,70
May	33,15	24,57
June	30,77	23,56
July	30,15	23,19
August	30,28	23,36
September	31,07	23,36
October	31,93	23,30
November	32,50	23,05
December	32,94	22,02
Average	**32,56**	**23,20**

Annexure 2: Table showing the average of daily maximum and minimum temperature(°C) from 15 years data (2008-2023) of first 10 days each month (Source: Author; Data Source: DSP https://dsp.imdpune.gov.in/)

Average of 1st Decade of each Months		
Month	**Average of Temp. MAX**	**Average of Temp. MIN**
January	33,56	21,10
February	34,49	21,40
March	34,96	23,43
April	34,67	24,71
May	33,96	24,62
June	31,30	23,85

July	30,44	23,28
August	29,88	23,25
September	30,70	23,26
October	31,77	23,24
November	32,25	23,15
December	32,71	22,53
Average	**32,58**	**23,15**

Annexure 3: Table showing the average of daily maximum and minimum temperature(°C) from 15 years data (2008-2023) of second 10 days each month (Source: Author; Data Source: DSP https://dsp.imdpune.gov.in/)

Average of 2nd Decade of each Months		
Month	**Average of Temp. MAX**	**Average of Temp. MIN**
January	33,67	20,68
February	34,63	22,38
March	35,12	23,97
April	34,27	24,62
May	32,97	24,56
June	30,55	23,50
July	29,80	23,03
August	30,38	23,47
September	30,81	23,46
October	31,97	23,44
November	32,72	23,05
December	32,81	22,06
Average	**32,51**	**23,19**

Annexure 4: Table showing the average of daily maximum and minimum temperature(°C) from 15 years data (2008-2023) of last 10-11 days each month (Source: Author; Data Source: DSP https://dsp.imdpune.gov.in/)

Average of 3rd Decade of each Months		
Month	**Average of Temp. MAX**	**Average of Temp. MIN**
January	33,95	21,31
February	34,94	22,90
March	34,81	24,52
April	34,14	24,78
May	32,57	24,53
June	30,47	23,32
July	30,20	23,25
August	30,56	23,35
September	31,71	23,37
October	32,03	23,23
November	32,54	22,95
December	33,28	21,51
Average	**32,59**	**23,26**

Annexure B

Annexure 5: Table showing Mean, minimum and maximum values of each wards of KMC as of 08.03.2023 (Source: Author).

Ward_numbe	NDBI_MIN	NDBI_MAX	NDBI_MEAN	NDVI_MIN	NDVI_MAX	NDVI_MEAN	LST_MIN	LST_MAX	LST_MEAN
1	-0,2528	0,1649	-0,0400	-0,0768	0,4286	0,1169	26,4813	33,7867	30,3487
2	-0,2584	0,1460	0,0141	-0,0752	0,4269	0,1198	27,1404	33,4431	32,2661
3	-0,1350	0,1804	0,0287	-0,0756	0,3236	0,0906	27,6656	34,2076	32,6276
4	-0,2158	0,2011	0,0127	0,0646	0,3773	0,1469	31,6089	34,2649	32,7620
5	-0,2225	0,1939	0,0023	-0,0747	0,3784	0,1010	26,8008	34,3554	31,8493
6	-0,1423	0,1775	0,0134	-0,0720	0,2609	0,0911	27,5701	34,2561	32,3390
7	-0,1772	0,1505	0,0073	0,0677	0,3433	0,1533	31,3313	34,9499	32,2606
8	-0,2123	0,1945	-0,0066	0,0385	0,3821	0,1581	31,4579	35,0638	32,7096
9	-0,1541	0,1378	0,0158	-0,0686	0,2959	0,1083	27,8658	34,3002	33,0900
10	-0,2372	0,1224	-0,0144	-0,0788	0,4066	0,1410	27,3812	34,1169	32,4360
11	-0,2674	0,1955	-0,0302	-0,0830	0,4437	0,1538	27,3695	34,1590	32,0898
12	-0,3132	0,1446	-0,0573	-0,0844	0,4985	0,1859	27,0094	35,2308	31,5846
13	-0,2843	0,1595	-0,0573	-0,0806	0,4423	0,1499	27,0070	33,2649	31,1666
14	-0,3179	0,1251	-0,0427	-0,0728	0,4057	0,1837	27,0187	33,1981	31,9856
15	-0,3167	0,1031	-0,0978	-0,0921	0,4577	0,1100	26,3141	33,2472	29,2912
16	-0,2619	0,1747	-0,0807	-0,0954	0,3998	0,0474	26,1374	32,6871	28,4880
17	-0,2437	0,0890	-0,0637	-0,0812	0,3684	0,1266	26,3613	33,0291	30,2542
18	-0,2475	0,1564	-0,0675	-0,0927	0,3751	0,1384	26,1492	33,1512	30,1559
19	-0,2402	0,1016	-0,0376	-0,0694	0,3881	0,1687	27,0375	33,0982	31,7321
20	-0,2373	0,1366	-0,0371	-0,0546	0,4193	0,1706	27,7285	34,0152	31,9809
21	-0,2431	0,1454	-0,0321	-0,0718	0,3622	0,1765	27,7145	34,7720	32,1036
22	-0,3120	0,1740	-0,0677	-0,0247	0,4736	0,2115	27,9489	33,1999	31,4951
23	-0,3292	0,1078	-0,0728	-0,0391	0,4495	0,2073	28,0632	31,9514	30,8380
24	-0,3094	0,1073	-0,0353	0,0239	0,4391	0,1805	28,5358	33,6160	32,0530
25	-0,2610	0,0752	-0,0214	0,0796	0,4152	0,1698	31,1454	33,3874	32,3239
26	-0,2533	0,0761	-0,0184	-0,0248	0,4402	0,1637	28,9629	33,5096	32,2506
27	-0,2847	0,1581	-0,0390	0,0665	0,4696	0,2033	28,7884	33,8352	31,8683
28	-0,1776	0,1668	-0,0026	0,0628	0,3512	0,1546	31,0825	33,1826	32,1206
29	-0,2725	0,3159	-0,0183	-0,0850	0,4558	0,1798	27,7145	38,7195	33,2980

30	-0,3539	0,1676	-0,0985	-0,0603	0,4741	0,2683	27,4278	35,6705	31,0983
31	-0,2101	0,1011	-0,0701	-0,0940	0,3609	0,1309	26,5213	32,0707	29,6197
32	-0,3395	0,1567	-0,0461	-0,0420	0,5086	0,1757	27,0140	32,7317	31,0184
33	-0,2812	0,1751	-0,0334	-0,0476	0,4508	0,1759	29,0666	32,9151	31,7338
34	-0,2559	0,1479	-0,0523	-0,0530	0,4018	0,1829	27,2620	32,8637	31,0031
35	-0,3043	0,1258	-0,0462	0,0663	0,4402	0,1995	29,9003	32,9795	31,6347
36	-0,2785	0,2173	-0,0753	-0,0086	0,4598	0,2238	27,8284	34,4989	31,2416
37	-0,2743	0,1261	-0,0400	0,0298	0,4234	0,1821	30,0560	34,2408	31,9875
38	-0,1974	0,1804	-0,0333	0,0381	0,3493	0,1782	30,8484	33,8336	31,8621
39	-0,1926	0,1194	-0,0320	0,0647	0,3816	0,1794	30,7489	33,4230	31,7165
40	-0,2248	0,1483	-0,0352	0,0449	0,3693	0,1741	30,1709	33,6740	31,7309
41	-0,3286	0,1443	-0,0477	0,0231	0,4958	0,1802	28,3658	33,7491	31,9953
42	-0,3098	0,1485	-0,0687	0,0728	0,4613	0,2197	28,9900	32,6066	31,4870
43	-0,2213	0,1388	-0,0314	0,0541	0,3843	0,1725	30,5646	33,2248	31,8350
44	-0,2643	0,1445	-0,0420	0,0416	0,3983	0,1813	30,4461	33,3629	31,5493
45	-0,2954	0,1146	-0,0589	0,0652	0,4574	0,2074	29,1477	33,1359	31,6194
46	-0,3243	0,1278	-0,0726	0,0295	0,4709	0,2142	27,4128	33,7671	31,3807
47	-0,2745	0,1080	-0,0708	-0,0191	0,3847	0,2021	28,6814	33,0845	31,1015
48	-0,2679	0,0982	-0,0614	-0,0470	0,4332	0,1861	28,7276	33,5008	31,4584
49	-0,2840	0,1367	-0,0637	-0,0499	0,4023	0,1649	28,2998	33,4898	31,4250
50	-0,2915	0,1274	-0,0868	-0,0465	0,4110	0,1790	27,2293	33,4586	30,5945
51	-0,2075	0,1164	-0,0517	-0,0084	0,4123	0,1942	30,4004	33,7022	31,8408
52	-0,2553	0,1453	-0,0552	-0,0457	0,3790	0,1619	27,1965	33,8115	31,0996
53	-0,2721	0,1303	-0,0488	-0,0413	0,4144	0,1910	28,3739	33,1157	31,4617
54	-0,2836	0,1312	-0,0579	-0,0450	0,4453	0,1921	27,6027	33,2714	31,3226
55	-0,2220	0,1923	-0,0152	-0,0310	0,3550	0,1464	28,4989	33,7094	31,9414
56	-0,2897	0,1196	-0,0325	0,0356	0,4353	0,1653	31,1204	34,0437	32,0129
57	-0,2931	0,1641	-0,0732	-0,0590	0,4171	0,1714	26,9625	33,0221	30,6887
58	-0,2824	0,1600	-0,0597	-0,0656	0,4280	0,1745	27,2386	33,4199	30,9948
59	-0,3109	0,1565	-0,0498	-0,0676	0,4596	0,1881	27,5374	33,6581	30,8719
60	-0,2971	0,1139	-0,0449	-0,0734	0,4649	0,1918	27,4862	33,2136	31,9578
61	-0,2823	0,1854	-0,0124	-0,0772	0,4523	0,1245	27,6656	37,5724	32,6924
62	-0,2036	0,1981	0,0019	-0,0056	0,3412	0,1416	28,6275	33,9068	31,9992
63	-0,3313	0,1643	-0,0623	0,0404	0,4701	0,2092	28,6823	33,8426	31,5421
64	-0,3059	0,1478	-0,0557	0,0337	0,4513	0,1964	29,2559	33,1314	31,4985

65	-0,2495	0,1927	-0,0179	0,0269	0,4533	0,1565	30,2135	35,2769	31,9180
66	-0,2058	0,1568	0,0192	0,0113	0,3673	0,1198	30,7130	35,2656	32,1879
67	-0,1907	0,2809	0,0203	0,0264	0,3485	0,1208	29,4572	34,2784	32,2910
68	-0,3094	0,1298	-0,0742	-0,0704	0,4822	0,1703	26,5307	33,5564	30,2187
69	-0,2878	0,1417	-0,0128	0,0408	0,4329	0,1664	29,4997	33,1425	31,9484
70	-0,2743	0,1399	-0,0194	0,0364	0,4478	0,1655	29,9047	33,1672	31,8172
71	-0,3138	0,1368	-0,0144	0,0528	0,4809	0,1661	29,7825	33,1583	31,9048
72	-0,2920	0,1376	-0,0138	0,0662	0,4564	0,1642	29,4948	32,9375	31,8071
73	-0,3059	0,1558	-0,0352	0,0655	0,4756	0,1847	29,5028	32,9418	31,6844
74	-0,3271	0,1469	-0,0797	-0,0780	0,3835	0,0384	26,3189	33,1650	28,5660

Annexure C

Annexure 6: Table showing different land cover percentage of each wards of KMC as of 08.03.2023 (Source: Author).

WARD_NUMBE	Ward Name	Water Bodies %	Tree Cover %	Urban %	Grass/Lawn %	Barren %
1	FORT KOCHI	21,42	6,42	57,26	10,84	4,05
2	KALVATHY	3,14	1,66	91,14	3,51	0,55
3	EARAVELI	1,69	0,00	96,20	2,11	0,00
4	KARIPPALAM	0,00	1,57	90,41	7,44	0,59
5	MATTANCHERRY	10,61	1,68	81,84	5,87	0,00
6	KOCHANGADI	5,80	0,28	92,27	1,66	0,00
7	CHERALAYI	0,00	0,31	93,57	5,67	0,46
8	PANAYAPPILLI	0,00	0,50	88,86	6,81	3,84
9	CHAKKAMADAM	2,22	0,00	94,57	0,99	2,22
10	KARUVELIPPADY	4,77	0,82	83,49	6,96	3,96
11	THOPPUMPADY	4,90	4,12	79,02	8,73	3,24
12	THAREBHAGAM	5,71	9,59	59,72	13,46	11,52
13	KADEBHAGAM	11,46	6,44	60,60	16,33	5,18
14	THAZHAPPU	1,60	7,69	76,44	9,78	4,49
15	EDAKOCHI NORTH	34,17	10,84	25,13	24,97	4,88
16	EDAKOCHI SOUTH	48,23	2,87	25,34	20,49	3,07
17	PERUMPADAPPU	16,07	3,50	49,93	26,00	4,50
18	KONAM	21,54	7,14	48,58	17,97	4,78
19	PALLURUTHY-KACHERIPPADY	5,17	2,91	71,80	11,63	8,50
20	NAMBYAPURAM	0,00	3,71	78,01	14,26	4,01
21	PULLARDESOM	0,11	2,98	81,70	7,94	7,28
22	MUNDAMVELI	0,00	8,54	50,90	25,04	15,51
23	MANASSERY	0,00	7,38	62,11	24,12	6,39
24	MOOLAMKUZHI	0,00	3,10	81,40	11,24	4,26
25	CHULLIKKAL	0,00	3,48	88,92	5,06	2,53
26	NASRATH	0,00	0,79	91,52	5,52	2,17
27	FORT KOCHI VELI	0,00	13,76	68,09	10,52	7,63
28	AMARAVATHY	0,00	0,39	93,71	5,50	0,39
29	ISLAND NORTH	0,60	9,18	60,57	18,76	10,88
30	ISLAND SOUTH	0,26	39,15	24,51	26,11	9,97
31	VADUTHALA WEST	16,71	4,19	50,41	27,54	1,15
32	VADUTHALA EAST	0,30	6,21	63,02	27,42	3,06

33	ELAMAKKARA NORTH	0,00	1,56	79,77	16,05	2,62
34	PUTHUKKALAVATTOM	0,00	5,81	66,74	25,41	2,04
35	PONEKKARA	0,00	4,14	76,16	17,76	1,95
36	KUNNUMPURAM	0,00	17,46	54,71	22,75	5,08
37	EDAPPALLI	0,00	4,06	80,95	13,12	1,87
38	DEVANKULANGARA	0,00	1,28	82,59	13,90	2,23
39	KARUKAPPILLI	0,00	0,63	82,30	15,55	1,52
40	MAMANGALAM	0,00	1,49	84,18	13,18	1,14
41	PADIVATTOM	0,00	5,17	74,50	18,32	2,02
42	VENNALA	0,00	4,49	60,27	31,77	3,47
43	PALARIVATTOM	0,00	1,05	84,29	14,21	0,45
44	KARANAKODAM	0,00	0,99	80,93	17,93	0,15
45	THAMMANAM	0,00	3,92	66,07	28,86	1,14
46	CHAKKARAPPARAMBU	0,00	8,99	65,05	25,27	0,69
47	CHALIKKAVATTOM	0,00	1,59	62,31	35,45	0,65
48	PONNURUNNI EAST	0,00	0,86	63,93	33,99	1,21
49	VYTTILA	0,19	6,19	58,16	31,80	3,66
50	CHAMBAKKARA	0,36	13,43	46,73	35,21	4,26
51	POONITHURA	0,00	4,85	67,60	19,41	8,14
52	VYTILLA JANATHA	3,27	3,80	63,50	25,40	4,03
53	PONNURUNNI EAST	0,00	3,03	70,81	23,12	3,03
54	ELAMKULAM	0,15	3,36	66,91	27,32	2,26
55	GIRINAGAR	0,00	0,46	91,45	7,62	0,46
56	PANAMPILLY NAGAR	0,00	2,07	82,09	12,40	3,44
57	KADAVANTHRA	6,59	4,32	45,38	36,73	6,97
58	KONTHURUTHY	7,83	7,91	50,08	27,19	6,99
59	THEVARA	11,52	11,52	52,81	15,91	8,23
60	PERUMANOOR	0,61	6,81	66,75	16,93	8,90
61	RAVIPURAM	1,65	2,80	86,54	7,76	1,25
62	ERNAKULAM SOUTH	0,00	2,25	88,96	8,28	0,51
63	GANDHI NAGAR	0,00	5,75	63,70	28,92	1,63
64	KATHRUKADAVU	0,00	1,84	73,87	23,64	0,66
65	KALOOR SOUTH	0,00	0,18	87,81	10,56	1,45
66	ERNAKULAM CENTRAL	0,00	0,00	94,78	4,57	0,65
67	ERNAKULAM NORTH	0,00	0,81	93,54	5,19	0,47
68	AYYAPPANKAVU	13,15	22,72	46,37	16,08	1,68
69	THRIKKANARVATTOM	0,00	2,38	89,29	8,23	0,11
70	KALOOR NORTH	0,00	2,31	85,51	10,96	1,22
71	ELAMAKKARA SOUTH	0,00	0,91	87,57	10,03	1,48
72	POTTAKKUZHI	0,00	1,14	89,05	9,48	0,33
73	PACHALAM	0,00	1,29	77,00	18,99	2,71
74	THATTAZHAM	45,90	2,39	31,45	19,93	0,33